In compliance with the
Canadian Privacy Legislation
some supporting forms
may have been removed from
this dissertation.

While these forms may be included
in the document page count,
their removal does not represent
any loss of content from the dissertation.

University of Alberta

Antibody-targeted liposomal anticancer drugs for the treatment of B-cell malignancies

By

Puja Sapra

A thesis submitted to the Faculty of Graduate Studies and Research in partial fulfillment of the requirements for the degree of Doctor of Philosophy

Department of Pharmacology

Edmonton, Alberta
Fall 2003

National Library of Canada
Acquisitions and Bibliographic Services
395 Wellington Street
Ottawa ON K1A 0N4
Canada

Bibliothèque nationale du Canada
Acquisisitons et services bibliographiques
395, rue Wellington
Ottawa ON K1A 0N4
Canada

Your file Votre référence
ISBN: 0-612-88043-5
Our file Notre référence
ISBN: 0-612-88043-5

The author has granted a non-exclusive licence allowing the National Library of Canada to reproduce, loan, distribute or sell copies of this thesis in microform, paper or electronic formats.

L'auteur a accordé une licence non exclusive permettant à la Bibliothèque nationale du Canada de reproduire, prêter, distribuer ou vendre des copies de cette thèse sous la forme de microfiche/film, de reproduction sur papier ou sur format électronique.

The author retains ownership of the copyright in this thesis. Neither the thesis nor substantial extracts from it may be printed or otherwise reproduced without the author's permission.

L'auteur conserve la propriété du droit d'auteur qui protège cette thèse. Ni la thèse ni des extraits substantiels de celle-ci ne doivent être imprimés ou aturement reproduits sans son autorisation.

Canada

University of Alberta

Library Release Form

Name of Author: Puja Sapra

Title of Thesis: Antibody-targeted liposomal anticancer drugs for the treatment of B-cell malignancies

Degree: Doctor of Philosophy

Year this Degree Granted: 2003

Permission is hereby granted to the University of Alberta Library to reproduce single copies of this thesis and to lend or sell such copies for private, scholarly or scientific research purposes only.

The author reserves all other publication and other rights in association with the copyright in the thesis, and except as herein provided, neither the thesis nor any substantial portion thereof may be printed, or otherwise reproduced an any material form whatever without the author's prior written permission.

Date: 23/07/03

University of Alberta

Faculty of Graduate Studies and Research

The undersigned certify that they have read, and recommend to the Faculty of Graduate Studies and Research for acceptance, a thesis entitled **Antibody-targeted liposomal anticancer drugs for the treatment of B-cell malignancies** submitted by Puja Sapra in partial fulfillment of the requirements for the degree of Doctor of Philosophy.

July 23, 2003

Dr. P.S. Low, External Examiner

Dedicated to my beloved parents

ABSTRACT

Cancer chemotherapy is limited by the poor selective toxicity of anticancer drugs. Selective targeting of antibody-targeted liposomal anticancer drugs to surface antigens on malignant cells is a recognized strategy for increasing the therapeutic effectiveness of chemotherapeutic drugs. Research in this thesis is aimed at studying factors that will help in optimization of antibody-targeted liposomal formulations of anticancer drugs for use in the treatment of B-cell malignancies. Liposomal doxorubicin (DXR) or liposomal vincristine (VCR) were targeted to human B-lymphoma (Namalwa) cells via whole monoclonal antibodies (mAbs) or their Fab' fragments (Fab') against the internalizing CD19 or CD22 epitopes or the non-internalizing CD20 epitope.

All targeted liposomal formulations (immunoliposomes) of DXR or VCR had increased association with, and cytotoxicity against, Namalwa cells relative to non-targeted liposomes. The therapeutic effectiveness of immunoliposomal DXR was improved by using Fab' fragments vs. whole mAbs or by targeting to CD19 (internalizing) vs. CD20 (non-internalizing). Targeting immunoliposomal DXR to CD22 was less effective than targeting to CD19. Immunoliposomal VCR was equally effective whether targeted to either CD19 or CD20, via either whole mAbs or Fab'. Immunoliposomal VCR was superior to immunoliposomal DXR, independent of the target epitope. Targeting immunoliposomal VCR, but not immunoliposomal DXR, to two epitopes (CD19 and CD20) further improved the therapeutic results. Untargeted liposomal formulations of DXR had synergistic cytotoxic effects with anti-CD19 and untargeted liposomal formulations of VCR had synergistic cytotoxic responses with anti-CD19 or anti-CD20.

Therapeutic responses seem to be related to a number of factors including internalization of the immunoliposomes, their rate of clearance, drug release rates, density of target epitopes and the properties of the encapsulated drug. For DXR-containing immunoliposomes therapeutic effectiveness was increased by substituting Fab' for whole mAbs, which decreased the clearance rate of the immunoliposomes and allowed more time for the immunoliposomes to bind to the target cells. For these formulations, increasing intracellular drug concentrations by targeting to internalizing epitopes also increased the therapeutic effectiveness. For the high potency, schedule-dependent drug, VCR, where the cytotoxic action of the drug may synergize with signaling antibodies such as anti-CD19 and anti-CD20, therapeutic responses were high and independent of internalization. Combination therapy with immunoliposomal VCR directed against B-cell epitopes is a logical choice for clinical development as a therapy for B-cell malignancies.

ACKNOWLEDGEMENTS

It is good to have an end to journey toward,
but it is the journey that matters in the end.
Ursula LeGuinn

This thesis is a result of almost four years of experience whereby I have been accompanied and supported by my supervisor, committee members, colleagues, family, and friends. It is a pleasant aspect that I now have the opportunity to express my gratitude for all of them.

I am deeply indebted to my supervisor, Dr. Terry Allen. Her enthusiasm for research and her mission for providing high quality work have made a deep impression on me. I owe her lots of gratitude for showing me the way of research. Her guidance throughout my graduate school term especially in preparation of presentations, writing of manuscripts and this thesis is gratefully appreciated.

I would like to thank the other members of my supervisory committee, Dr. A.S. Clanachan and Dr. L.M. Pilarski who monitored my work, offered me helpful suggestions, and took effort in reading and providing me with valuable comments on this thesis. I would also like to thank Dr. Wendy Gati, Graduate Studies Coordinator, for her encouragement and support throughout my graduate program.

I would like to offer my appreciation to all the members of Allen laboratory (from 1999-2003), for their friendship, encouragement and help with lab work: Elaine Moase, Greg Charrois, Wilson Cheng, Debbie Iden, Janny Zhang, Susan Cubitt, Davis Mumbengegwi, Dipankar Das, Fabio Pastorino, Heather Vandertol-Vanier, Kim Laginha, Joao Moreira, Marc Kirchmeier, Tatsuhiro Ishida, Cheryl Santos, Felicity Wang, Amanda Reichert, Manuella Colla, Jessi Dhillon. I thank you all.

A very special thanks to Elaine for her technical help. I would also like to compliment her for the excellent job she has done as lab manager. Susan is gratefully acknowledged for the production of anti-CD19. My gratitude to Dr Jie Ma, for helping me in devising the protocol for anti-CD19 fragmentation.

I would like to acknowledge the expert advice of Inex Pharmaceuticals (Burnaby, B.C) in the preparation of vincristine liposomes and for the provision of radiolabeled vincristine.

Financial support from the University of Alberta, Faculty of Graduate Studies, Alberta Heritage Foundation for Medical Research, and the Canadian Institutes for Health Research (T.M.A. operating grant) is gratefully acknowledged.

The chain of my gratitude would be definitely incomplete if I forget to thank my parents, brother, and other family members who have been instrumental in all of my achievements in life. Whether it was early morning or late at night, their love, support, and encouragement was only a phone call away. I love you mom and dad.

Finally, I wish to give a special thanks to my husband for his endless love, support, and patience, especially during the writing of this thesis.

I think my journey in graduate school has come to an end. However, experience with the people mentioned above is going to stay with me forever. It is everlasting.

TABLE OF CONTENTS

CHAPTER 1

INTRODUCTION, HYPOTHESIS AND OBJECTIVES 1

1.1 Introduction 2

1.2 Liposomal drug delivery systems 3

1.2.1 Classical liposomes 3

1.2.2 Sterically stabilized (Stealth®) liposomes 4

1.2.3 Ligand-targeted liposomes 8

1.3 Methods of liposome preparation 8

1.4 Loading of drugs into liposomes 9

1.5 Techniques for coupling ligands to liposomes 11

1.5.1 Coupling strategies 13

1.5.2 Post-insertion approach 19

1.6 Advantages of ligand-targeted Stealth® liposomes 20

1.7 Choice of target receptor 22

1.7.1 Receptor expression 22

1.7.2 Internalization 23

1.8 Choice of targeting ligand 27

1.8.1 Whole antibody versus antibody fragments versus non-antibody ligands 27

1.8.2 Immunogenicity and new developments in Ab engineering 29

1.8.3 Pharmacokinetics of ligand-targeted liposomes 31

1.8.4 Ligand density and binding affinity 32

1.9 Choice of drug 33

1.9.1 Drug release rates and the concept of bioavailability 33

1.9.2 Mechanism of action of drug 33

1.10 Extravascular vs. vascular targets 34

1.11 Therapeutic applications of ligand-targeted liposomes 35

1.11.1 Antibodies or antibody fragments as targeting moieties 35

1.11.2 Peptides and other receptor ligands as targeting moieties 42

1.12 The Model System 43

1.12.1 Cell surface antigens: CD19, CD20 and CD22 44

1.12.2 Drugs: Doxorubicin and Vincristine 47

1.13 Hypothesis and Objectives 50

CHAPTER 2

Improved therapeutic responses in xenograft models of human B-lymphoma for long-circulating vincristine-loaded liposomes targeted via anti-CD19 IgG_{2a} or Fab' fragments compared to those loaded with doxorubicin. 54

2.1 ABSTRACT 55

2.2 INTRODUCTION 56

2.3 MATERIALS AND METHODS 60

2.3.1 Materials 60

2.3.2 Mice 61

2.3.3 Tumour cell line 62

2.3.4 Preparation of liposomes 62

2.3.5 Preparation of αCD19 antibody and Fab' fragments 64

2.3.6 Coupling of immunoliposomes 65
2.3.7 Binding and uptake of immunoliposomes 66
2.3.8 *In vitro* cytotoxicity 67
2.3.9 *In vitro* leakage 68
2.3.10 Pharmacokinetics and biodistribution 68
2.3.11 *In vivo* survival experiments 70
2.3.12 Statistical analysis 70
2.4 RESULTS 71
2.4.1 Preparation of anti-CD19 Fab' fragments 71
2.4.2 *In vitro* cellular association of immunoliposomes 71
2.4.3 *In vitro* cytotoxicity 76
2.4.4 *In vitro* leakage experiments 79
2.4.5 Pharmacokinetics and tissue distribution 79
2.4.6 *In vivo* survival experiments in xenograft models of human B-lymphoma 89
2.5 DISCUSSION 94

CHAPTER 3

Internalizing antibodies are necessary for improved therapeutic responses of DXR-containing immunoliposomes 104

3.1 ABSTRACT 105
3.2 INTRODUCTION 105
3.3 MATERIALS AND METHODS 107
3.3.1 Materials 107
3.3.2 Animals, antibodies and cell lines 108

3.3.3 Preparation of liposomes 109

3.3.4 *In vitro* binding and cytotoxicity of immunoliposomes 110

3.3.5 *In vivo* survival experiments 111

3.3.6 Statistical analysis 112

3.4 RESULTS AND DISCUSSION 112

3.4.1 Immunophenotyping of Namalwa cells 112

3.4.2 *In vitro* cell association and confocal experiments 113

3.4.3 *In vitro* cytotoxicity studies 120

3.4.4 *In vivo* survival studies 120

CHAPTER 4

Treatment of B-cell lymphoma with combinations of immunoliposomal anticancer drugs targeted to both the CD19 and CD20 epitopes. 126

4.1 ABSTRACT 127

4.2 INTRODUCTION 127

4.3 MATERIALS AND METHODS 130

4.3.1 Materials 130

4.3.2 Animals, antibodies and cell lines 131

4.3.3 Preparation of liposomes 131

4.3.4 Cell association of immunoliposomes 133

4.3.5 *In vivo* survival experiments 133

4.3.6 Statistical analysis 134

4.4 RESULTS AND DISCUSSION 134

4.4.1 *In vitro* cell association 134

4.4.2 *In vivo* survival studies 138

CHAPTER 4A (Addendum to Chapter 4)

Evaluation of a combination regimen of immunoliposomal DXR targeted to two internalizing (CD19 and CD22) epitopes 151

4A.1 Rationale 152

4A.2 Materials and Methods 152

4A.3 Results and Discussion 153

4A.3.1 *In vitro* cell association 153

4A.3.2 *In vivo* survival 155

CHAPTER 5

CONCLUSIONS AND FUTURE DIRECTIONS 160

5.1 Summarizing discussion and future directions 161

5.2 Clinical applications of immunoliposomal anticancer drugs 169

5.2.1 Immunoliposomal anticancer drugs in the treatment of hematological malignancies 169

5.2.2 Immunoliposomal anticancer drugs targeted to solid tumors 172

5.2.3 Combination therapies with immunoliposomal drugs 173

5.2.4 Immunoliposomes in the treatment of multidrug resistance 175

5.3 Barriers and solutions to the clinical approval of immunoliposomes 176

5.4 Future directions in the field of immunoliposomal drugs 177

5.5 Conclusions 178

REFERENCES 180

LIST OF TABLES

Table 1.1 Selected list of ligand-targeted liposomes that have received evaluation *in vitro* or *in vivo* for delivery of anticancer drugs. 39

Table 2.1A Cytotoxicity of free or liposomal VCR formulations against Namalwa cells. 77

Table 2.1B Cytotoxicity of free or liposomal DXR formulations against Namalwa cells. 78

Table 2.2 Comparison of the pharmacokinetic parameters of targeted and non-targeted liposomes. 82

Table 3.1 Cytotoxicity of various treatments against Namalwa cells.....121

Table 3.2 Survival times of SCID mice after immunoliposomal treatments.....124

Table 4.1 Survival times of SCID mice after immunoliposomal DXR treatments. .141

Table 4.2 Statistical comparison of results of the in vivo survival study reported in Table 4.1.....143

Table 4.3 Survival times of SCID mice after immunoliposomal VCR treatments...147

Table 4.4 Statistical comparison of results of the *in vivo* survival study reported in Table 4.3.....148

Table 4A.1 Survival times of SCID mice after immunoliposomal DXR treatments.156

Table 4A.2 Immunophenotyping of Namalwa cell line using single color flow cytometry. 158

LIST OF FIGURES

Figure 1.1 Three generations of liposomes. 7

Figure 1.2 Liposome classification. 10

Figure 1.3 Remote loading of DXR into liposomes using an ammonium suphate gradient across the liposomal bilayer. 12

Figure 1.4 Methods for coupling antibodies to liposomes. 15

Figure 1.5 Coupling methods influence the orientation of Ab molecules on the liposome surface. 17

Figure 1.6 Mechanisms of action of Stealth® immunoliposomes. 25

Figure 1.7 Antibody fragmentation 28

Figure 1.8 Structural formulae of (A) Vincristine and (B) Doxorubicin 48

Figure 2.1 SDS-PAGE gel of αCD19 and its fragments under non-reducing conditions 72

Figure 2.2 *In vitro* cellular association of liposomes to Namalwa cells. 75

Figure 2.3 Blood clearance of targeted versus non-targeted liposomes in naive BALB/c mice. 81

Figure 2.4 Biodistribution of liposomes to liver and spleen in naïve BALB/c mice. 83

Figure 2.5 Blood clearance of targeted versus non-targeted liposomes in SCID mice bearing Namalwa cells. 85

Figure 2.6 Blood clearance of drug-loaded targeted versus non-targeted in naive BALB/c mice. 87

Figure 2.7 Biodistribution of drug-loaded liposomes to liver and spleen in naïve BALB/c mice. 88

Figure 2.8 Therapeutic efficacy of free VCR or liposomal formulations of VCR in SCID mice injected with Namalwa cells. 90

Figure 2.9 Therapeutic efficacy of free VCR or liposomal formulations of VCR in SCID mice injected with Namalwa cells. 91

Figure 2.10 Therapeutic efficacy of free drugs or liposomal formulations of drugs in SCID mice injected with Namalwa cells. 93

Figure 3.1 *In vitro* cellular association of liposomes to Namalwa cells as a function of concentration at 37°C (closed symbols) or 4°C (open symbols). 114

Figure 3.2 Confocal micrographs of Namalwa cells treated with Rh-PE-labeled immunoliposomes at 37°C. 116

Figure 3.3 Confocal micrographs of Namalwa cells treated with Rh-PE-labeled immunoliposomes at 4°C. 118

Figure 3.4 Enlarged confocal micrographs of anti-CD19 (top) vs. anti-CD20 (bottom) HSPC-SIL at 37°C. 119

Figure 4.1 *In vitro* cellular association of liposomes with Namalwa cells as a function of concentration at 37°C (Panels A and C) or 4°C (Panels B and D). 136

Figure 4.2 Specific cell association of immunoliposomes with Namalwa cells as a function of concentration at 37°C (Panels A and C) or 4°C (Panels B and D)..137

Figure 4A.1 *In vitro* cellular association of liposomes with Namalwa cells as a function of concentration at 37°C. 154

LIST OF ABBREVIATIONS

Ab	antibody
ABS	adult bovine serum
ADCC	antibody-dependent cell-mediated cytotoxicity
αCD19	whole monoclonal antibody, anti-CD19
αCD20	whole monoclonal antibody, anti-CD20
αNS	whole isotype-matched, non-specific control antibody, αPK136
ASC	aqueous counting scintillant
AUC	area under the time concentration curve
B_{max}	maximum number of binding sites per cell
CDC	complement-mediated cytotoxicity
Chol	cholesterol
CL	clearance
DMSO	dimethyl sulphoxide
DSPE	distearoylphosphatidylethanolamine
DTT	dithiothreitol
DXR	doxorubicin
DXR-HSPC-SIL[αCD19]	DXR-loaded HSPC-SIL, targeted via αCD19
DXR-HSPC-SIL[Fab'CD19]	DXR-loaded HSPC-SIL, targeted via Fab'CD19
DXR-HSPC-SIL[αCD20]	DXR-loaded HSPC-SIL, targeted via αCD20
DXR-HSPC-SL	DXR-loaded HSPC-SL
Fab'CD19	Fab' fragments of anti-CD19

Fab'NS	Fab' fragments of an isotype-matched, non-specific control antibody, αPK136
FACS	fluorescence activated cell sorting
FBS	fetal bovine serum
h	hour
[^{3}H]-CHE	cholesterol- [1,2-^{3}H-(N)]-hexadecyl ether
HAMA	human anti-mouse antibody
HBS	HEPES-buffered saline, 25 mM 4-(2-hydroxyethyl)-1-piperazine ethanesulphonic acid, 140 mM NaCl, pH 7.4
HL	hodgkin's lymphoma
HSPC	hydrogenated soy phosphatidylcholine
HSPC-SIL	Stealth® immunoliposomes composed of HSPC:Chol:mPEG:Mal PEG at a 2:1:0.08:0.02 molar ratio
HSPC-SIL[αCD19]	HSPC-SIL targeted via αCD19
HSPC-SIL[αCD20]	HSPC-SIL targeted via αCD20
HSPC-SIL[Fab'CD19]	HSPC-SIL targeted via Fab'CD19
HSPC-SIL[αNS]	HSPC-SIL targeted via αNS
HSPC-SIL[Fab'NS]	HSPC-SIL targeted via Fab'NS
HSPC-SL	Stealth® liposomes composed of HSPC:Chol:mPEG at a 2:1:0.10 molar ratio
Hz-PEG-DSPE	hydrazide-derivatized poly(etylenglycol) covalently linked to distearoylphosphatidylethanolamine

IC_{50}	concentration required for 50% inhibition of cell growth
IgG	immunoglobulin
ILS	increased life span
i.v.	intravenous
K_d	dissociation constant
K_e	elimination rate constant
kg	kilogram
LTS	long-term survivors
LTTs	ligand-targeted therapeutics
LTLs	ligand-targeted liposomes
LUV	large unilamellar vesicles
mAb	monoclonal antibody
Mal-PEG	maleimide-derivatized polyethylene glycol (MW 2000)-distearoylphosphatidylethanolamine
MBP	maleimidophenylbutyrate
2-MEA	2-mercaptoethylamine-HCl
μm	micrometer
mM	millimolar
μg	microgram
μmol	micromole
min	minute
MDR	multidrug resistance

mPEG	methoxypolyethylene glycol (MW 2000), covalently linked via a carbamate bond to distearoylphosphatidylethanolamine
MPS	mononuclear phagocyte system
MRT	mean residence time
MTD	maximum tolerated dose
MTT	3-[4,5-dimethylthiazole-2-yl]-2,5-diphenyltetrazolium bromide
MUV	multilamellar vesicles
MW	molecular weight
NHL	non-hodgkin's lymphoma
nm	nanometers
P	probability
pKa	acidobasic constant
PBS	phosphate buffered saline, pH 7.4
PDP	pyridyldithioproprionate
PEG	polyethylene glycol
Pgp	p-glycoprotein
PL	phospholipid
pmoles	picomoles
Rh-PE	rhodamine dihexadecanoyl phosphatidylethanolamine
scFv	single chain antibody fragments
SCID	severe compromised immunodeficient

S.D.	standard deviation
SDS	sodium dodecyl sulphate
SDS-PAGE	SDS-Polyacrylamide gel electrophoresis
SIL	sterically stabilized Stealth® immunoliposomes
SIL[αCD19]	Stealth® immunoliposomes targeted via whole antibody, anti-CD19
SIL[αCD20]	Stealth® immunoliposomes targeted via whole antibody, anti-CD20
SIL[Fab'CD19]	Stealth® immunoliposomes targeted via Fab' fragments of anti-CD19
SL	sterically stabilized Stealth® liposomes
SM	egg sphingomyelin
SM-SIL	Stealth® immunoliposomes composed of SM:Chol:mPEG:Mal PEG, at a 55:40:4:1 molar ratio
SM-SIL[αCD19]	SM-SIL targeted via αCD19
SM-SIL[αCD20]	SM-SIL targeted via αCD20
SM-SIL[Fab'CD19]	SM-SIL targeted via Fab'CD19
SM-SIL[αNS]	SM-SIL targeted via αNS
SM-SIL[Fab'NS]	SM-SIL targeted via Fab'NS
SM-SL	Stealth® liposomes, composed of SM:Chol:PEG at a 55:40:5 molar ratio
SUV	small unilamellar vesicles

$t_{1/2}$	half-life
Tc	phase-transition temperature
TI	tyraminyinulin
v/v	volume/volume
V_d	volume of distribution
VCR	vincristine
VCR-SM-SIL[αCD19]	VCR-loaded SM-SIL, targeted via αCD19
VCR-SM-SIL[αCD20]	VCR-loaded SM-SIL, targeted via αCD20
VCR-SM-SIL[αNS]	VCR-loaded SM-SIL, targeted via αNS
VCR-SM-SIL[Fab'CD19]	VCR-loaded SM-SIL, targeted via Fab'CD19
VCR-SM-SIL[Fab'NS]	VCR-loaded SM-SIL, targeted via Fab'NS
VCR-SM-SL	VCR-loaded SM-SL
w/v	weight/volume
w/w	weight/weight

CHAPTER 1

INTRODUCTION, HYPOTHESIS AND OBJECTIVES

Some sections from the introduction have been published in
Prog. Lipid Res., *42(5)*: 439-462, 2003

1.1 Introduction

Anticancer drug therapy is fraught with systemic toxicities resulting from cytotoxicity to normal cells. Cancer cells share many common features with the normal host cells from which they originate, so finding unique targets against which anticancer drugs can be selectively directed is difficult. Anticancer drugs have marginal selectivity for malignant cells because they target the reproductive apparatus in cells having high proliferation rates. However, drugs having this mechanism of action result in high toxicities against rapidly dividing normal cells, for example, hair follicles, germ cells and hematopoeitic cells, leading to dose-limiting side effects such as bone marrow depression, mucositis, stomatitis, nausea, alopecia and adverse reproductive effects. The side effects associated with chemotherapy limit the acute dose or cumulative doses that can be administered to patients, which can lead to relapse of the tumor and often the development of drug-resistance.

The medical community has sought alternative therapies that improve selective toxicities against cancer cells. An approach that has been extensively researched is the targeted delivery of anticancer drugs to tumor cells mediated via monoclonal antibodies (mAb) or other ligands. In this regard, a number of ligand-targeted therapeutics (LTTs) e.g., immunotoxins, immunoconjugates, radioimmunotherapy and immunoliposomes have been developed (1-3). The premise behind all these approaches is that antibody (Ab)- or ligand-mediated selective targeting of anticancer therapeutics against antigens or receptors, which are either uniquely expressed or overexpressed on the cancer cells, will increase therapeutic

effectiveness and/or decrease toxicity of the anticancer therapeutics. Immunoliposomes represent a successful integration of drug delivery systems (liposomes) and biological therapeutics (mAbs or their fragments) (see section 1.6). However, despite extensive research done in this field over the last couple of decades, to date no immunoliposomal formulation has received clinical approval. Many questions remain regarding the optimization of targeted liposomal formulations and the applications of immunoliposomes. The goal of this thesis was to conduct basic research with the aim of optimizing immunoliposomal anticancer drugs for the treatment of B-cell malignancies. This research also has implications in the treatment of other malignancies with appropriate targeted liposomal systems.

1.2 Liposomal drug delivery systems

1.2.1 Classical liposomes

Most anticancer drugs, following intravenous (i.v.) administration, have large volumes of distribution (V_d) resulting from their rapid uptake into all the tissues of the body (4). One successful approach has been to use drug carriers such as liposomes to alter the pharmacokinetics and biodistribution of anticancer drugs. In general, liposome encapsulation of drugs results in (sometimes dramatic) reductions in their V_d and significant increases in drug accumulation in solid tumors.

Liposomes (phospholipid bilayer vesicles) are the most advanced of the particulate drug carriers and are now considered to be a mainstream drug delivery technology. Classical liposomes, first described by Bangham *et al.*, (5) are made up of amphiphilic phospholipids and cholesterol, which, upon hydration, self-associate to

form bilayers surrounding an aqueous interior (Figure 1.1A). The non-polar hydrocarbon chains of amphiphilic phospholipids, below a characteristic temperature (phase transition temperature, Tc), exist in a rigid gel state with restricted mobility. Above this temperature, due to thermal excitation, the chains are converted into a disordered liquid like state. Hydration of amphiphilic phospholipids hydrates the polar head groups and reorganizes the phospholipids into bilayer structures (liposomes) with the hydrophilic head groups facing the aqueous medium, and the hydrophobic acyl chains forming the interior of the bilayer. In 1971, the first study describing liposomes as carriers of enzymes or drugs was published (6).

1.2.2 Sterically stabilized (Stealth®) liposomes

One of the major drawbacks of classical liposomes was their rapid clearance from blood, due to adsorption of plasma proteins (opsonins) to the 'naked' phospholipid membrane, triggering recognition and uptake of the liposomes by the receptors present in the mononuclear phagocytic system (MPS). A major advance in the field of liposomes came with the development of sterically stabilized (Stealth®) liposomes, which utilize a surface coating of hydrophilic carbohydrates or polymers, usually a lipid derivative of polyethylene glycol (PEG), to help evade MPS recognition (7-9) (Figure 1.1B). PEG attracts a water layer to the liposome surface, thus providing hydrophilic repulsion to opsonin adsorption. The inclusion of PEG or other hydrophilic polymers extends the half-life of liposomes from less than a few minutes (classical liposomes) to several hours (Stealth® liposomes) and changes the

pharmacokinetics of the liposomes from dose-dependent, saturable pharmacokinetics to dose-independent pharmacokinetics (10, 11).

Both classical and Stealth® liposomes rely on 'passive' targeting to increase the localization of anticancer drugs to solid tumors. Solid tumors have discontinuous endothelial lining and leaky vasculature due to tumor angiogenesis (12, 13). The size of fenestrations in tumor capillaries can be up to around 780 nm. Liposomes in the size range of approximately 50-200 nm can extravasate through these fenestrations and localize in the tumor interstitium (14-16). The vascular endothelium of most normal tissues has tight junctions, which prevent leakage of liposomes into these tissues. In addition, solid tumors have elevated interstitial pressure and impaired lymphatics that hinder the diffusion of colloidal particles such as liposomes from the tumor (17). Once inside the tumor interstitium, cytotoxic drugs are released from the liposomes in a sustained manner, killing the neighboring cells. Passive targeting can increase liposomal drug concentrations in solid tumors several-fold relative to those obtained with free drugs (18). Liposomal formulations of the anthracycline anticancer drugs doxorubicin (Doxil®/Caelyx® and Myocet®) and daunorubicin (Daunosome®) have received clinical approval. In addition, many other liposomal anticancer drugs are in clinical trials trials (19-21).

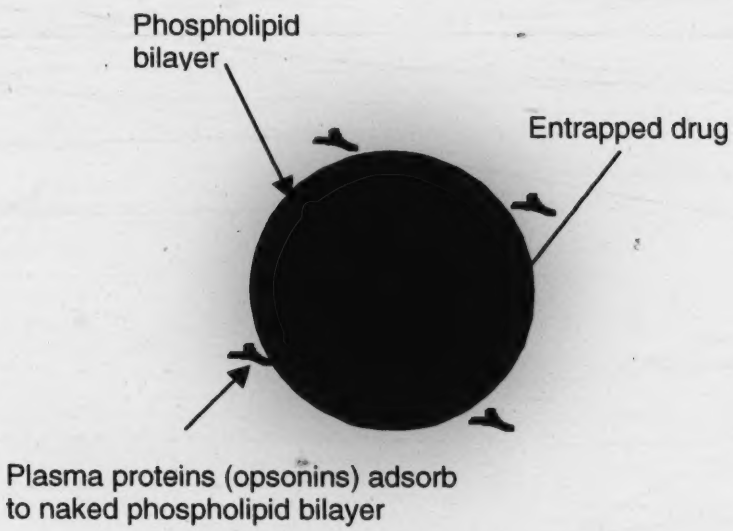

A. Conventional liposome

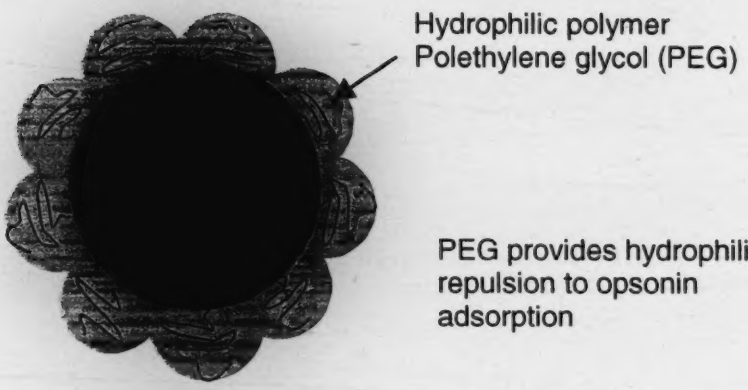

B. Stealth® liposome

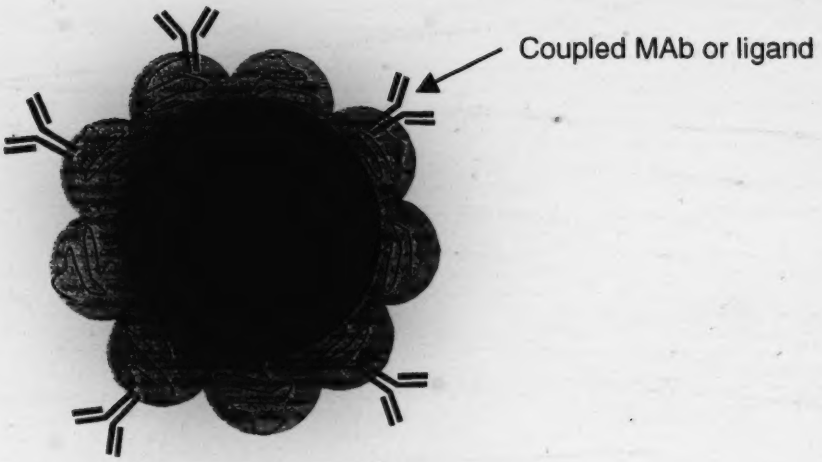

C. Stealth® Immunoliposome

Figure 1.1 Three generations of liposomes.
The naked phospholipid bilayer of classical liposomes (A) attracts plasma proteins (opsonins) to its surface, which promotes recognition of the liposomes by the receptors present in MPS and leads to their fast clearance from the circulation. Stealth® liposomes (B) are sterically stabilized with a coating of surface-grafted hydrophilic polymer (PEG), which provides hydrophilic repulsion to opsonin adsorption, thus increasing the circulation times of the liposomes. Stealth® immunoliposomes (C), i.e., Ab-targeted liposomes, are made by coupling mAbs or Fab'fragments to the PEG-terminus of Stealth® liposomes. (From T.M. Allen)

1.2.3 Ligand-targeted liposomes

In attempts to increase the specificity of interaction of liposomal drugs with target cells and to increase the amount of drug delivered to these cells, recent efforts in the liposome field have focussed on the development of ligand-targeted liposomes (LTLs). These liposomes utilize targeting moieties, coupled to the liposome surface, to deliver selectively the drug-liposome package to the desired site of action (Figure 1.1C). This process is sometimes called active targeting. Targeting moieties may include mAbs, or fragments thereof, and small molecular weight, naturally occurring or synthetic ligands such as peptides, carbohydrates, glycoproteins, or receptor ligands, i.e., essentially any molecule that selectively recognizes and binds to target antigens or receptors that are over-expressed or selectively expressed on cancer cells. To date, liposomes coupled to Abs or Ab fragments, folate or transferrin have been the most extensively researched LTLs (22-32). LTLs formed by coupling whole Ab molecues or their Fab' fragments to the liposomes, termed immunoliposomes were evaluated in this thesis. Most of the principles of immunoliposomes apply to LTLs targeted via other ligands and hence these terms have been used interchangeably in this thesis.

1.3 Methods of liposome preparation

Various methods have been proposed to prepare liposomes. These include hydration of dried lipid films with an aqueous solution (thin film hydration) (5, 33), reverse phase evaporation (34), freeze-thaw (35), detergent dialysis (36) and solvent injection (37). Thin film hydration was employed in this thesis. In this method, a

mixture of lipids is first dissolved in a suitable organic solvent, which is then evaporated using a rotoevaporator to form a thin film on the inside of a glass vessel. Hydration of the dried lipid film, with occasional vortexing, yields liposomes having multiple lamellae (MLVs) (33, 38). MLVs are not preferred as they are heterogenous in size (39) and have low levels of aqueous encapsulation (40) (Figure 1.2).

Many methods exist for fragmenting MLVs into either large or small unilamaeller vesicles (LUVs or SUVs respectively). These include ultrasonication (41), homogenization (42), passage through french press cells (43) and extrusion through membranes with define pore sizes (39, 44). In this thesis, MLVs were extruded through polycarbonate membranes under pressure (< 400 psi) to make LUVs in the size range of 100-130 nm.

1.4 Loading of drugs into liposomes

A variety of drugs having different physicochemical properties can be associated with liposomes. Hydrophilic drugs having low octanol:water partition coefficients (e.g., ara-C) can be entrapped in the aqueous interior of the liposomes (45). Hydrophilic drugs have low release rates from liposomes due to their low membrane permeability, which can limit the amount of bioavailable drug at the tumor site (46). Hydrophobic drugs having high octanol:water partition coefficients (e.g., taxanes) can be associated with the bilayer (45). Although this association can be efficient, hydrophobic drugs can easily redistribute to lipoproteins or other biological membranes (46, 47) and so are readily lost from liposomes *in vivo*. Highly

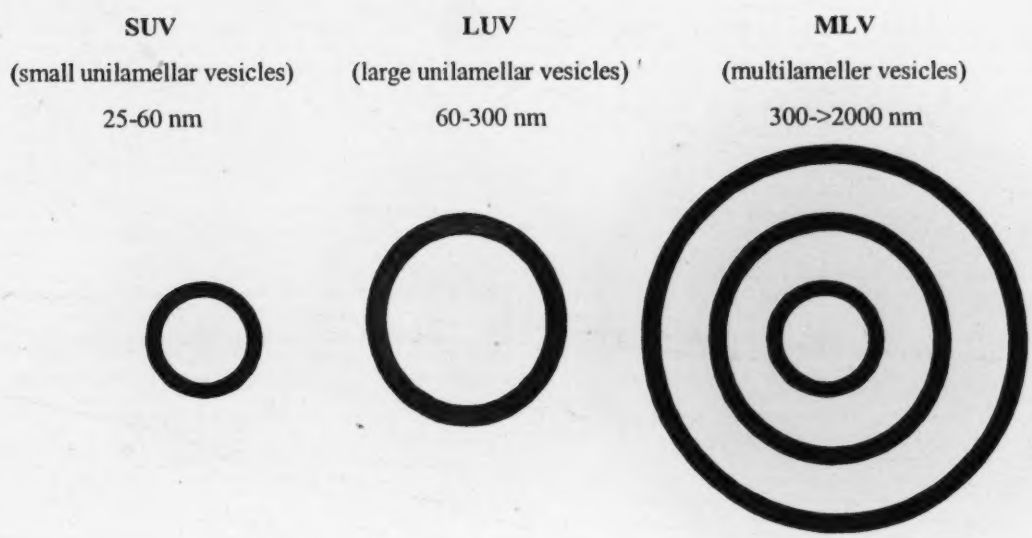

Figure 1.2 Liposome classification.
Liposomes are classified according to their size and the number of bilayers, into small unilamellar (SUVs), large unilamellar (LUVs) or multilamellar vesicles (MLVs). Adapted from (48).

hydrophilic or hydrophobic drugs are generally 'passively loaded' in liposomes at the time of hydration or liposome formation (47, 49). Amphipathic drugs with intermediate solubility can also be suitable for association with liposomal carriers. Amphipathic drugs that are weak bases or weak acids can be efficiently loaded into preformed liposomes using 'remote loading' methods like the ammonium sulfate method for doxorubicin (DXR) (50) or the pH gradient method for vincristine (VCR) (51). The acidobasic constant (pKa) of DXR is 8.5. The pKa_1 of vincristine is 5.2 and pKa_2 is 7.4. In these methods, a chemical or pH gradient (inside acidic) is established across the liposome bilayers. Drug molecules exist in equilibrium between a neutral and an ionized form outside the liposomes. Only drug molecules in the uncharged state can cross the lipid bilayer; they are then are protonated within the liposome interior and retained inside the liposome in the charged state (50, 52-56). In the case of DXR, a gel-like precipitate is formed in the presence of sulphate ions (50, 57) (Figure 1.3). Using remote loading techniques, encapsulation efficiencies of > 95% can be achieved for both DXR and VCR and they both can be loaded at high drug:lipid ratios.

1.5 Techniques for coupling ligands to liposomes

A variety of techniques for coupling targeting ligands to liposomes have been described (58-60) (reviewed in (61, 62)). In general, coupling methods for the formation of LTLs should be simple, fast, efficient, and reproducible, yielding stable, non-toxic bonds. The biological properties of the ligands, e.g., target recognition and binding efficiency, should not be substantially altered. The LTLs should have

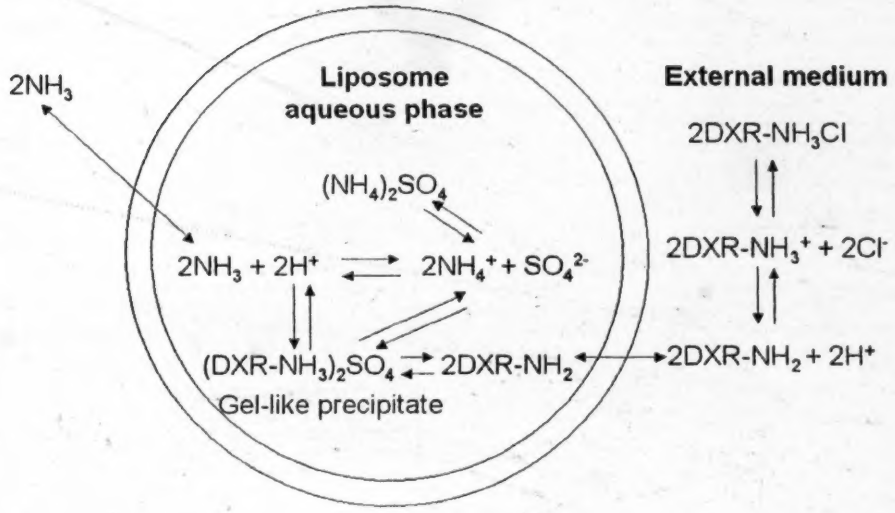

Figure 1.3 Remote loading of DXR into liposomes using an ammonium suphate gradient across the liposomal bilayer.
Uncharged DXR crosses the lipid bilayer, where it is protonated and reacts with SO_4^{2-} anions to form a gel-like precipitate, $(DXR\text{-}NH_3)_2SO_4$. This causes the further dissociation of $(NH_4)_2SO_4$ into NH_4^+ and SO_4^{2-} and, causes the further dissociation of NH_4^+ into H^+ and NH_3 (ammonia). Ammonia efflux from the liposomes is the driving force for the influx of DXR; it produces a transmembrane H^+ gradient ($[H^+]$ internal > $[H^+]$external). This procedure permits encapsulation efficiencies of 95-100%. Adapted from (50).

stabilities and circulation half-lives long enough to allow them to reach and interact with the target cells. Further, the coupling reaction should not impact negatively on drug loading efficiency and drug release rates.

1.5.1 Coupling strategies

Whole Abs were amongst the first ligands to be coupled to classical liposomes, but they proved to be largely ineffective therapeutically due to their rapid elimination from the circulation by cells of the MPS (63-65). Development of Stealth® technology renewed interest in the advancement of immunoliposomes as carriers of therapeutics. Initially, Abs were coupled to phospholipid headgroups, e.g., phosphatidylethanolamine, at the surface of Stealth® liposomes, but the steric barrier imparted by the PEG polymer resulted in low coupling efficiencies and interfered with binding of the LTLs to their targets, particularly when higher concentrations of PEG with high molecular weights were present (66, 67). To avoid this, Abs were coupled to the PEG terminus. This strategy avoids masking of the Abs by the PEG layer, and provides perfect access of the Ab molecules to their target cells (59, 68-70). Several end-functionalized derivatives of PEG have been synthesized for coupling Abs to the PEG terminus. Some commonly used PEG derivatives include pyridyldithiopropionoylamino (PDP)-PEG (71) hydrazide (Hz)-PEG (72) and maleimide (Mal)-PEG (60). A description of these coupling reactions in given in Figure 1.4.

In this thesis, whole mAbs or Fab' fragments were coupled to the PEG terminus of Stealth® liposomes using the Mal-PEG method. In this method, whole

A. PDP-PEG-PE Method

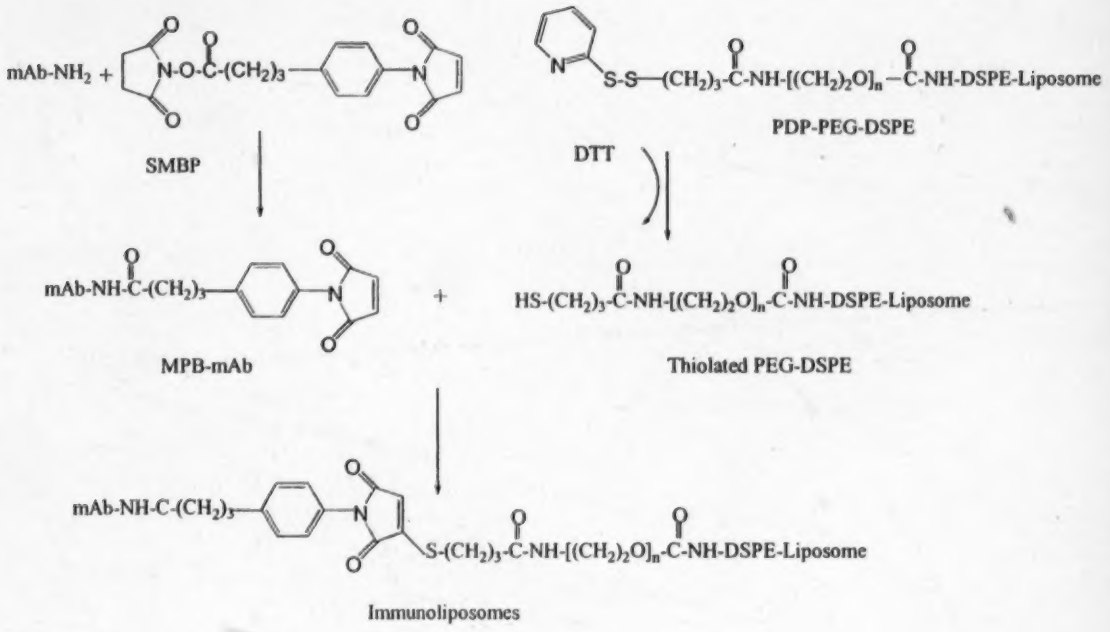

B. HZ-PEG-PE Method

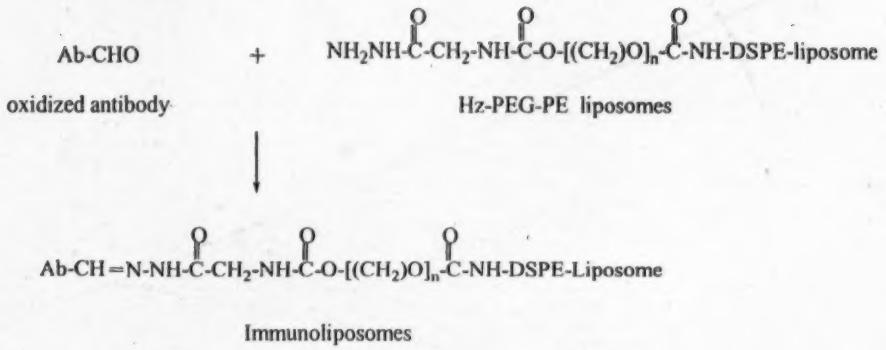

C. Mal-PEG-PE Method

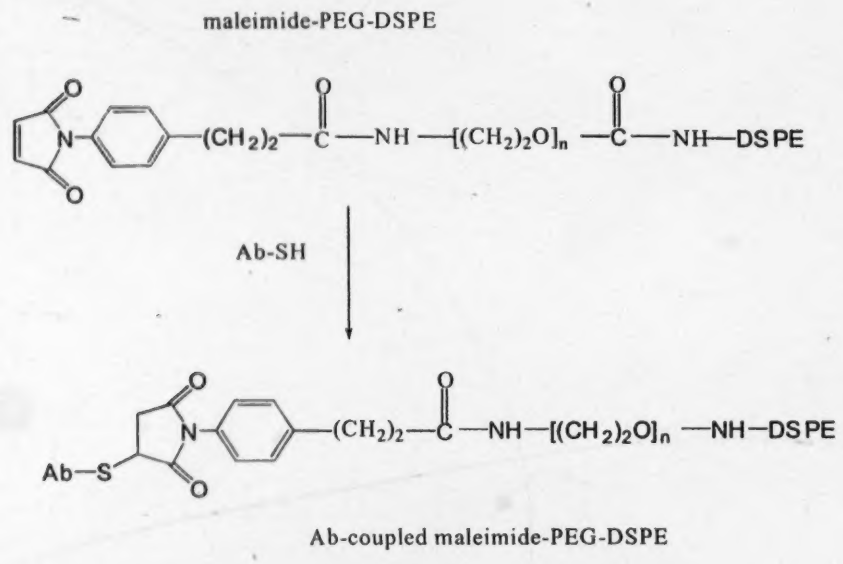

Figure 1.4 Methods for coupling antibodies to liposomes.
The PDP-PEG and Mal-PEG methods rely on the formation of thioether bonds between the liposome and Ab molecules. In Hz-PEG method, hydrazone linkage is formed between the liposome and Ab molecules. The abbreviations are as follows: SMBP, succinimidyl-4-(*p*-maleimidophenyl)butyrate; PDP, *N*-pyridyldithioproprionate; DSPE, distearoyl phosphatidylethanolamine; DTT, dithiolthreitol; MBP, *N*-maleimidophenylbutyrate; Hz, Hydrazide; Mal, Maleimide; PEG, polyethylene glycol. Adapted from (59, 73)

Ab molecules are thiolated using 2-iminothiolane (Traut's reagent), which converts the amine groups of the lysine residues into free sulfhydryl (-SH) group. The thiolated Ab molecules are then reacted with maleimide groups on the PEG-termini to form stable thioether bonds. A disadvantage with this method is that the free thiol groups may react amongst themselves to produce disulphide bonds leading to cross-linking of Ab molecules or immunoliposomes, further promoting their aggregation and faster clearance from the circulation. However, the presence of PEG serves to inhibit aggregation to a large extent. In addition, the random introduction of thiol groups in the Ab molecule may interfere with the biological properties of the molecule leading to interference with the binding of the Ab to its receptor, receptor activation and/or endocytosis. When thioether bonds are formed between liposomes and whole Abs having multiple thiolation sites, random orientation of the Ab molecules on the liposome surface results and the Fc region of a portion of the Abs may be available to bind to Fc receptors, increasing clearance of the immunoliposomes (74) (Figure 1.5). Using the Mal-PEG method, Ab fragments (Fab') can also be coupled to liposomes through thiol groups generated by cleavage of the disulphide bridge of the hinge region of $F(ab')_2$ (60) (Figure 1.5). Alternatively, single chain antibody fragments (scFv) with terminal cysteine groups could be coupled to liposomes via the Mal-PEG method (28). Coupling Ab fragments to liposomes avoids problems associated with potential thiolation of the antigen recognition site (75, 76). In addition, Fab' and scFv fragments lack the Fc

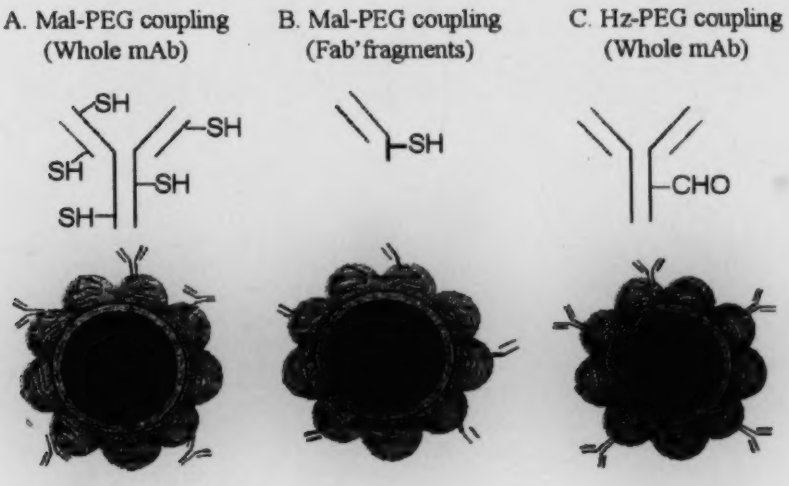

Figure 1.5 Coupling methods influence the orientation of Ab molecules on the liposome surface.
Coupling of whole mAbs through thiol groups formed from lysines, in the Mal-PEG method, result in random orientation of the Ab molecules on the liposomes (A). Coupling of Fab' fragments through thiol groups in the hinge region, released on cleavage of $F(ab')_2$, result in a defined orientation of the molecules, leaving the antigen binding sites accessible for target binding (B). In the Hz-PEG method, whole Ab molecules are coupled through carbohydrate groups present in the Fc-region of the Ab, again leaving the antigen binding sites accessible and preventing the binding of liposomes to the Fc receptors (C).

domain, so they should be cleared less rapidly from circulation. In the Hz-PEG method, carbohydrates in the Fc-region of whole Abs are oxidized to form reactive aldehydes, which form hydrazone linkages with the hydrazide groups on the PEG-terminus (59, 77). Both of the above coupling strategies avoid recognition of the immunoliposomes by the Fc-receptors of the macrophages and favors orientation of the Ab molecules so that their antigen-binding domains are exposed to the target epitopes (Figure 1.5).

The PDP-PEG method also relies on the formation of thioether bonds between proteins and liposomes (59, 61). In this method, a maleimide group is incorporated onto the Ab molecules via reaction with succinimidyl-4-(p-maleimidophenyl)butyrate (SMPB) and the Abs are then incubated with thiolated PDP-PEG. The methods described above, although effective, require a separate step of Ab modification prior to attachment to liposomes. Torchilin *et al.* have recently described a new method, which allows a single step binding of ligands containing amino groups (e.g., mAbs) to the PEG-terminus of the liposomes using a amphiphilic PEG derivative, p-nitrophenylcarbonyl-PEG-PE (pNP-PEG-PE) (78). pNP-PEG-PE incorporates into liposomes via its phospholipid residues, and binds amino groups via its water-exposed pNP group, forming a stable, non-toxic urethane (carbamate) bond. The method permits the binding of several dozen protein molecules per liposome, with retention of their specific activities. Bendas *et al.* have also introduced a new methodology for attaching Abs, without prior derivatization, on the PEG-terminus of liposomes. Anti E-selectin mAbs are coupled, in mild basic conditions, to a new

PEG-PE derivative that is endgroup-functionalized with cyanuric chloride (79). Cyanuric chloride links Abs via nucleophilic substitution at basic pH.

1.5.2 Post-insertion approach

In a different approach, Stealth® liposomes can be converted into LTLs by a versatile 'post-insertion technique' (80). Ligands are coupled to end-functionalized groups in PEG micelles and the ligand-PEG conjugates are then transferred in a simple incubation step from the micelles into the outer monolayer of pre-formed, drug-loaded liposomes. This method allows a combinatorial approach to the design of targeted liposomes that minimizes manufacturing complexities, allowing a variety of ligands to be inserted into a variety of pre-formed liposomes containing a variety of drugs. This allows the LTLs to be tailored to the patient's disease profile without the need for separate manufacturing procedures for each ligand and drug combination. Also, since the conditions for the insertion of the ligand are now decoupled from the conditions for the preparation of and loading of drug into liposomes, conditions can be optimized for both drug loading and ligand insertion. Targeted liposomes prepared using the post-insertion approach have been shown to have *in vitro* drug leakage rates, cell association, cytotoxicity profiles and therapeutic responses that are comparable to liposomes made by conventional coupling procedures like the Mal-PEG coupling method (74, 81, 82). In this thesis, in some experiments, Abs were coupled to the PEG terminus of liposomes using the post-insertion approach.

1.6 Advantages of ligand-targeted Stealth® liposomes

LTLs combine the advantages of a colloidal drug delivery system (liposomes) with the specificity of targeting ligands. Advantages of LTLs include the following. Relatively few ligand molecules per liposome (10-20) are required to selectively deliver high payloads of drugs to target cells via the mechanism of receptor-mediated internalization. Unlike other delivery systems such as drug-immunoconjugates or immunotoxins, which deliver few molecules of drug or toxin (<10), per Ab molecule, LTLs can be exploited to deliver thousands of molecules of drug using few tens of molecules of Abs or ligands on the liposome surface (83-86). In addition, the presentation of multiple targeting molecules on the surface of individual liposomes can restore multivalent binding of monovalent Ab fragments, and hence increase their binding avidity for the target antigens. This can eliminate the need for extensive re-engineering of, e.g., scFv fragments, to increase their valency.

Another advantage of immunoliposomes lies in the potential for additivity or synergy between the signaling mAbs present at liposome surface and liposomal drug, entrapped in the liposome interior. In animal xenograft studies of human cancers, therapeutic Abs showed additive, or even synergistic activities when used in combination with chemotherapeutic drugs (87-90). The response rate (complete and partial) in low-grade lymphoma to anti-CD20 mAb (Rituxan®) alone was 48% (91); however, when Rituxan® was combined with a combination of cyclophosphamide, hydroxydaunomycin, VCR (Oncovin®) and prednisone (CHOP regimen), response rates of over 90% were documented (92). Anti-HER2 mAb (Herceptin®) was

demonstrated to have synergistic effects when used in combination with cisplatin and carboplatin, and additive effects with cyclophosphamide, paclitaxel and DXR. On the downside, it has also been shown that Ab-drug combinations can exacerbate toxicities for, e.g., cardiac toxicity with a combination of free DXR and anti-HER2 (89). Another advantage of immunoliposomal anticancer drugs is the amelioration of toxicities associated with the administration of free drugs, given either alone or in combination with therapeutic Abs.

Liposomes can be targeted using mAbs having unique signaling properties, such as inhibition of DNA repair (93), induction of cell cycle arrest (94), blockade of P-glycoprotein (Pgp) (95) or induction of apoptosis (96). This can lead to anticancer effects that may synergize with the cytotoxic effects of the liposomal anticancer drugs (87-89).

There are other advantages to the use of targeted liposomes. Liposomes are generally made from naturally-occurring phospholipids and hence unlike other colloidal drug delivery systems, liposomes have a high degree of biocompatiblity. They can also protect drugs from premature degradation by enzymes present in blood and can be used as a non-toxic excipient for the solublization of hydrophobic drugs. Furthermore, liposomes can be formulated in ways that improve drug pharmacokinetics and drug biodistribution to target tissues by either passive or active targeting as described above.

Despite several advantages, LTLs are complex delivery systems. Sections 1.7 to 1.10 outlines the principles to be considered for designing effective LTLs.

1.7 Choice of target receptor

1.7.1 Receptor expression

The target receptor or antigen for LTLs should either be selectively expressed or over-expressed on malignant cells compared to normal cells. Since few tumor antigens exist with exclusive specificty, researchers have mainly targeted antigens or receptors that are over-expressed on tumor cells relative to normal cells.

Evidence is emerging that receptor density is an important determinant of therapeutic response. In a recent study, it was demonstrated that a receptor density of at least10^5 ErbB2 receptors per cell was required before improved therapeutic response of anti-ErbB2-targeted liposomal DXR was observed relative to non-targeted liposomal DXR in a metastatic model of breast cancer (28). In a B-cell lymphoma (Namalwa) model (used in this thesis), improved therapeutics could be demonstrated when target cells had receptor densities (CD19) in the range of 10^4-10^5 (24).

Target cells should demonstrate minimal heterogeneity in their antigen or receptor expression. Tumor cells are notorious for having heterogenous expression of tumor antigens. This heterogeneity is a result of genetic instability of cells in the necrotic region of tumor tissue, and of the expression of the antigen in different glycosylation patterns within tumor tissue (97). In addition, certain tumor-specific antigens have been observed to disappear from the surface of tumor cells in the presence of Abs and reappear when Abs are no longer present (98). In heterogenous tumor cell populations, cells that lack the target receptor or antigen may escape the

cytotoxic effects of the LTLs and subsequent re-growth of these cells will lead to disease relapse or emergence of resistant cell populations. However, some antigen-negative cells may be killed via the so-called 'bystander effect', i.e., by drug released from the LTLs in the vicinity of the as targeting agents, which are capable of recognizing a large percentage of the cells in antigen-negative cells. A possible approach to overcoming the heterogeneity of tumor cells would be to have a 'cocktail' of ligands as targeting agents, which are capable of recognizing a large percentage of cells in heterogenous populations. This approach would also increase the number of cell surface epitopes available for interaction with the LTLs, hypothetically leading to increased drug delivery to the target cells. A study has demonstrated that the use of a cocktail of CD19, CD22 and CD38 immunotoxins is curative in B-cell lymphoma in severe combined immunodeficient (SCID) mice (99).

The antigen or receptor should not be shed during treatment. Considerable sloughing of target antigen into blood occurs with some types of tumors, e.g., the sloughing of MUC-1 antigen from breast cancer cells (100). Shed antigens, circulating in the blood, can compete with tumor cell-bound antigens for binding of LTLs (101). This can also lead to aggregation of LTLs in the bloodstream, leading to potential problems like vascular occlusion. Injection of free Ab or ligand prior to injecting the targeted liposomes could help in clearing shed antigens from the blood.

1.7.2 Internalization

The ability of target cells to internalize LTLs is an important selection criterion in choosing a targeting ligand. If the ligand triggers receptor-mediated

internalization of the entire liposome-drug package into the cell interior, then arguably more drug will be delivered to the target cells (Figure 1.6). This mechanism should work well for drugs such as DXR, VCR or methotrexate that escape degradation by lysosomal enzymes and low pH (102). However, for drugs such as cytosine arabinoside (ara-C) that are acid labile and/or don't survive lysosomal degradation, liposomal targeting to internalizing epitopes will be less efficacious. If non-internalizing ligands are used, liposome contents will be released over time at or near the cell surface, and a portion of the released drug will enter the cell by passive diffusion or other normal transport mechanisms (Figure 1.6). Although increased concentrations of drug may be achieved at the cell surface by this mechanism, it can be argued that, in the dynamic *in vivo* environment (e.g., plasma or lymph), the rate of diffusion and redistribution of the released drug away from the cell may exceed the rate at which the drug enters the cell, particularly for drugs such as DXR, which have a large V_d. Targeting to non-internalizing epitopes might be efficacious in solid tumors through the bystander effect, in which cells lacking the target epitope can be killed by drug released at the surface of neighbouring cells having bound liposomes (103). The impact on the bystander effect of LTLs targeted to internalizing receptors is unknown, but one could predict that it would decrease if the cells ingested significant proportion of the LTLs before drug could be released. LTLs directed against internalizing receptors have demonstrated increased therapeutic activity in some tumor models (24, 27, 28, 86). In other tumor models, LTLs did not improve

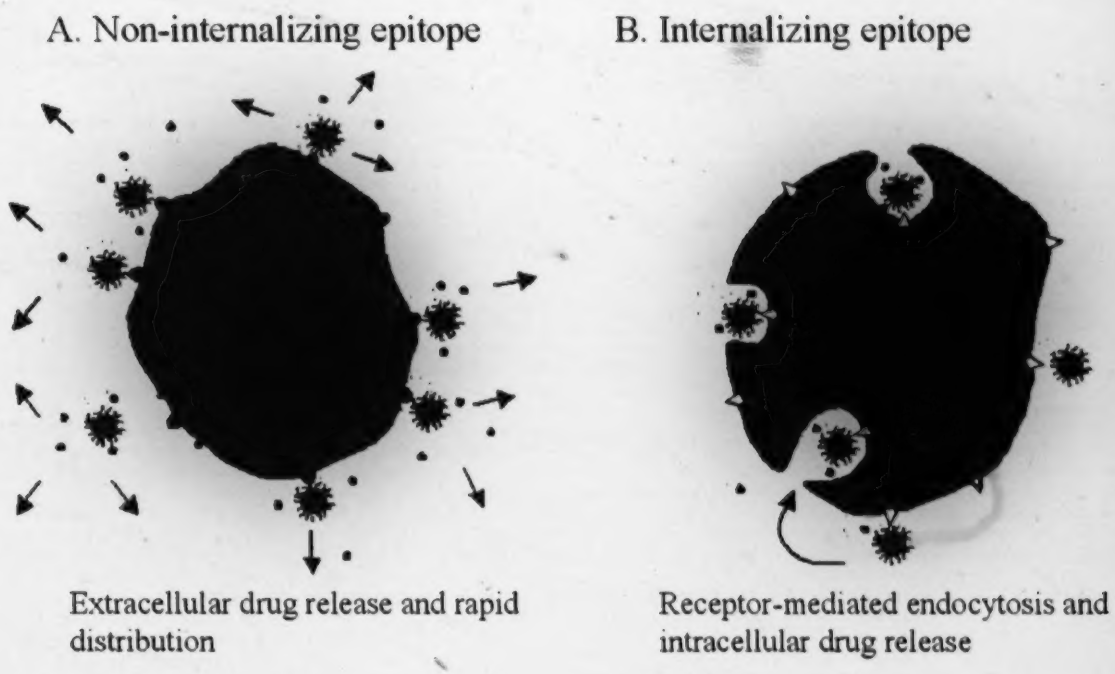
A. Non-internalizing epitope
B. Internalizing epitope
Extracellular drug release and rapid distribution
Receptor-mediated endocytosis and intracellular drug release

Figure 1.6 Mechanisms of action of Stealth® immunoliposomes.
Immunoliposomes can bind to non-internalizing epitopes on cell surface and release the drug extracellularly. Alternatively, they can bind to internalizing epitopes; the drug-liposomes package can be taken inside the cell by receptor-mediated endocytosis and drug can be released intracellularly. (From T.M. Allen)

therapeutic responses over non-targeted liposomes, which was hypothesized to be due to the lack of internalization of the LTLs into the cells (104, 105). Internalization of LTLs has been verified by direct electron microscopic analysis and confocal microscopy (106-108).

Internalization of Abs or other ligands into the target cells is also required for other LTTs, such as immunotoxins and Ab-drug conjugates. Internalization of LTTs depends on various factors such as type of receptor or epitope, antigen/receptor density, Ab valency, and rate of internalization and re-expression of the target epitope (109). Hence it is desirable to develop rapid and efficient methods to screen Abs or other ligands for internalization. Direct selection of Abs or their fragments demonstrating efficient internalization is now possible by panning on target cells using Ab phage display libraries (110). LTLs selected by this methodology, coupled to scFv fragments that bind to ErbB2 (HER2/neu), demonstrated efficient internalization by ErbB2-expressing tumor cells. ScFv-targeted liposomes containing DXR had significant antitumor activity in mouse xenografts having high tumor cell receptor density compared to non-targeted liposomes containing DXR or free DXR (111).

1.8 Choice of targeting ligand

1.8.1 Whole antibody versus antibody fragments versus non-antibody ligands

An advantage of using whole mAbs or divalent (or multivalent) engineered Ab fragments as liposomal targeting agents, is their higher binding avidity due to the presence of two (or more) binding domains on the same molecule (Figure 1.7). Whole mAbs, due to the presence of an Fc domain, can trigger complement-mediated cytotoxicity (CDC) and antibody-dependent cell-mediated cytotoxicity (ADCC) leading to apoptosis and cell kill. This may help in achieving additive or synergistic responses between signaling Abs and the liposomal drug. Also, whole Ab molecules may have some stability advantages over Ab fragments. However, on the down side, Fc-mediated mechanisms are also responsible for initiating immunogenic responses and for rapid clearance of immunoliposomes from the circulation. To this end, the use of Fab' fragments to target LTLs has been shown to reduce immunogenicity of the immunoliposomes as well as increase their circulation times (112). The use of Ab fragments may also be helpful in reducing the uptake of immunoliposomes by tumor-associated macrophages, thus providing better penetration of the immunoliposomes into solid tumors. Smaller Ab fragments usually have the advantage of faster localization to disease sites and better penetration of tumor tissue (113). Although Ab avidity is lost with the use of smaller fragments (Fab' or scFv), due to the loss of multivalent binding, coupling of Ab fragments to the liposomes is expected to restore multivalency and avidity to the system. Due to their ease of production (e.g., from Escherichia coli fermentation) and decreased immunogenicity, scFv fragments might

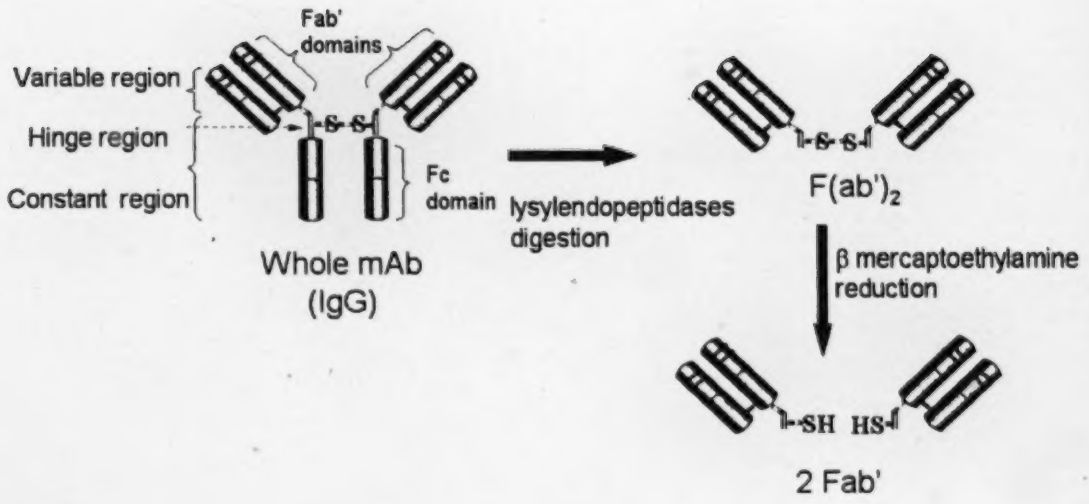

Figure 1.7 Antibody fragmentation.
Whole mAb (IgG) can be enzymatically cleaved at the hinge region, to release a $F(ab')_2$ molecule. The disulphide bridges of $F(ab')_2$ can be reduced to form two Fab' molecules, releasing -SH groups. Fab' molecules can be coupled to liposomes via thioether bonds formed between maleimide groups on liposomes and -SH groups of Fab'.

be more advantageous than Fab' fragments as targeting agents. Naturally occurring ligands to cell-surface receptors (such as folate, transferrin, growth factors) have lower molecular weights than Abs, are less immunogenic, more cost-effective and easy to handle and store. Receptors for these ligands are often over-expressed on tumor cells, which provide the basis for selective drug delivery (reviewed in (86, 114-116)). However, receptor expression is generally not specific for tumor cells and normal cells might suffer toxicities (86). In many cases, the receptors for these ligands have demonstrated receptor-mediated internalization of LTLs (reviewed in (86)).

1.8.2 Immunogenicity and new developments in Ab engineering

Development of hybridoma technology, for production of mAbs of murine origin, fostered an interest in LTTs (117). It has long been recognized that introduction of mouse mAbs into humans evokes HAMA (human anti-mouse antibody) responses, which are mediated in part by Fc receptor-mediated mechanisms (85, 118, 119). In the case of LTLs targeted via murine mAbs, this can result in hypersensitivity reactions and removal of the LTLs from the circulation due to their recognition and uptake by Fc receptors in the MPS (63, 120-122). The decrease in circulation $t_{1/2}$ compromises targeting to disease cells and, hence, therapeutic responses. This is especially limiting when multiple treatments are desired. Harding *et al.* showed that, although repeated i.v. administration of free chimerized murine mAb into rats did not trigger an immune response, a single injection of chimeric Ab-targeted Stealth® liposomes did. Subsequent injections of the LTLs resulted in their

rapid clearance, which was accompanied by a significant increase in Ab-specific antisera in the animal plasma. Interestingly, the antiserum was primarily detected against the Fc portion of the Ab and hence the authors proposed the use of small Ab fragments (Fab'fragments) as targeting moieties for liposomes (122).

In attempts to reduce the immunogenicity of murine mAbs, genetic engineering has been used to generate chimeric (where the constant region is human) (123) or humanized mAbs (where only the complementary determininant region (CDR) in the variable region is murine) (124). Since the constant region of the Ab molecule contain most of the antigenic sites, humanized or chimeric Abs are less immunogenic. Of the approximately 200 mAbs currently undergoing clinical trials and of the several with clinical approval for the treatment of cancer, transplant rejection, rheumatoid arthritis and Crohn's disease, most are humanized or chimeric. More recent developments in Ab technology include techniques for the production of fully human Abs or Ab fragments using phage display libraries and transgenic mice (125, 126) but whether anti-idiotype (85, 127) responses (directed to the mAb binding site) will be seen after repeated doses is unknown (128).

Another approach to reducing the immunogenicity of the murine Abs is to use Ab fragments like Fab' or scFv, which lack the constant region mainly responsible for generating immunogenic responses. Researchers are now focusing on the use of these Ab fragments or genetically engineered Abs as targeting moieties for liposomes (27, 28, 32, 129).

The immunogenicity associated with Ab-targeted liposomes could also be avoided by using natural ligands such as vitamins and hormones as targeting moieties against receptors over-expressed on cancer cells. Not enough data are available at this point to comment on the potential immunogenicity of liposomes targeted by these types of ligands.

1.8.3 Pharmacokinetics of ligand-targeted liposomes

Liposomal encapsulation of anticancer drugs can result in substantial changes in the pharmacokinetics and biodistribution of the drug. The drug assumes the pharmacokinetics of the carrier, until it is released from the liposome. Care should be taken in the development of LTL formulations to ensure that the targeting moiety does not seriously compromise the pharmacokinetics of the liposome. As discussed in Sections 1.5 and 1.8.1, the choice of coupling method and the choice of ligand will both influence the rate of clearance of LTLs, particularly when Abs containing Fc domains are involved. For example, Fab'-coupled liposomes had a 6-fold increase in circulation half-lives compared to whole mAb-coupled liposomes, even though the density of Fab'molecules was approximately 10-fold higher than that of whole mAbs on the surface of liposomes (112). Liposomes coupled to Fab' fragments at the PEG-terminus had a log-linear pharmacokinetic profile very similar to non-targeted PEG-liposomes. In contrast, whole mAb-coupled liposomes had biphasic clearance from the circulation, which is characteristic of rapid clearance by the MPS, and a late phase of slow clearance (32, 129).

Previous results from our laboratory have shown that the circulation half-life of anti-CD19-targeted liposomes is shorter in tumor-bearing mice compared to naïve mice (24, 74). In the Namalwa cell murine xenograft model, the cancer cells sequester in the bone marrow and spleen, sites that are readily accessible to immunoliposomes administered by the i.v. route. This likely accounts for the more rapid removal of the immunoliposomes from circulation. Koning *et al.* have also observed an increased clearance of immunoliposomes from the circulation in tumor-bearing mice, compared to healthy animals (130).

1.8.4 Ligand density and binding affinity

The issue of what is the optimal ligand density on the surface of liposomes remains to be resolved. High Ab densities on the surface of immunoliposomes may be desirable for Ab fragments, as it will lead to better binding avidity of the immunoliposomes for the target antigen. In addition, high Ab density will decrease the intermolecular distances between Ab molecules on the surface of liposomes and this may help in initiating signal transduction mechanisms. However, high density of whole mAbs will compromise the pharmacokinetics of the immunoliposomes and give rise to potential immunogenicity concerns, as discussed above.

The issue of binding affinity also remains to be resolved. Although it has been suggested that ligands having high binding affinities are desirable, low affinity ligands might prove to be better ligands as they may allow liposomes to penetrate further into the tumor interior, decreasing the 'binding site barrier' (131).

1.9 Choice of drug

1.9.1 Drug release rates and the concept of bioavailability

While internalization of liposomes by receptor-mediated endocytosis increases the amount of liposomal drug delivered into the target cell, it is not necessarily rapidly bioavailable, even though this would be highly desirable. Methods that facilitate intracellular release of liposomal drugs are being developed. For example, pH-sensitive lipids like dioleoylphosphatidylethanolamine (DOPE) assume the hexagonal phase at physiological pH and temperature, but they can be stabilized in the bilayer phase by other lipids including thiolytically cleavable polyethyleneglycol-lipid derivatives or pH-sensitive peptides or fusion proteins (132-134). Liposomes made of pH sensitive lipids can be formulated so they revert to hexagonal phase on exposure to low pH, enzymes or glutatione in the endosomal compartment, rapidly releasing their contents (triggered release) (135). pH-Titratable polymers have also been used to destabilize membranes following change of the polymer conformation at low pH (136-138).

1.9.2 Mechanism of action of drug

Cancer cells are not normally synchronized with respect to the cell cycle. Depending on the mechanism of action of the drug, either faster or slower release rates of the drug might be desirable. For example, one could argue theoretically that exposure of cancer cells to cell-cycle dependent drugs (e.g., VCR) needs to be sustained over long periods of time to allow cells to cycle through the cell phase where they are susceptible to drug effects. Conversely, rapid exposure of the target

cells to high levels of cell cycle independent drugs (e.g., DXR) would, one could argue, result in greater cytotoxicity than slow, sustained release of these drugs.

1.10 Extravascular vs. vascular targets

Targets within the vasculature or readily accessible from the vasculature should bind LTLs more readily than targets buried deep within tissues. A number of physical barriers are present that prevent or delay delivery of therapeutic agents to tissues, e.g. blood brain barrier, basement membranes or tight junctions. Solid tumors have a heterogenous blood supply, and high interstitial pressures exist within tumor tissue, especially in necrotic zones, which limit the diffusion of drugs, and especially colloidal particles (e.g liposomes), to poorly perfused areas (139). The 'binding site barrier' hypothesis suggests that Abs (or LTLs) bind to the first target cells they encounter, which retards their diffusion through the tumors and limits their therapeutic effects (131). Further, some studies have reported that immunoliposomes containing exposed Fc regions of the Ab are taken up by tumor-associated macrophages, which limits their direct interactions with the target tumor cells (84, 140, 141). Some studies employing mAbs for therapy or imaging have reported an uneven distribution of Ab molecules in the tumor cells (98). Despite these limitations, successful targeting to some animal models of solid tumors has been demonstrated (27, 28).

In our laboratory, the models for which the best *in vivo* results for immunoliposomal DXR were obtained are those in which the cancer cells are readily accessible from the vasculature, i.e., hematological malignancies such as B-cell

lymphoma and multiple myeloma (24, 142), or in pseudometastatic models of solid tumors in which the cells were administered i.v., and the mice were treated when the tumors were just beginning to be established (83, 143). When established solid tumors were treated in the models employed in our laboratory, although both targeted and non-targeted liposomal DXR gave improved results over free (non-encapsulated) drug, the targeted liposomes were not significantly better than the non-targeted liposomes (143, 144).

Negative therapeutic results in treating solid tumors were also experienced by others (105, 145). Although anti-HER2 Fab' LTLs show improved efficacy compared to non-targeted liposomes against HER2-overexpressing breast cancer cells having high (but not intermediate or low) antigen density, the levels of LTLs and non-targeted liposomes that localized to the tumors were similar (28, 84). The explanation for the improved results may lie in the high level of antigen expression of the target cells and the rapid internalization of the targeted liposomal drugs (28). This conclusion is also borne out by the results of tumor biodistribution experiments done in our laboratory and by others, which have demonstrated that levels of liposomes in developed tumors are not increased by Ab targeting (144, 146, 147).

1.11 Therapeutic applications of ligand-targeted liposomes

1.11.1 Antibodies or antibody fragments as targeting moieties

Some promising uses of Ab-targeted liposomes include the following: anti-HER2/Neu-targeted liposomes against mammary carcinoma cells (28, 84, 146, 148); anti-CD19-targeted liposomes against malignant B cells, (24, 108, 142); anti-GD_2-

targeted liposomes to target neuroblastoma or melanoma (32, 149); and anti-β_1 integrin-targeted liposomes in metastatic lung tumors (27).(Table1.1)

In an early study in our laboratory, a murine model of squamous lung carcinoma was treated with DXR-loaded liposomes targeted via a mAb against a carbohydrate on the surface of the cells. Treatment of mice with these DXR-loaded LTLs resulted in a significant decrease in the number and size of tumors and significant increases in survival times relative to free DXR or non-targeted liposomes containing DXR, with some long-term survivors (83). Treatment of more advanced tumors was unsuccessful, probably due either to receptor down-regulation and/or lack of penetration of the LTLs into larger tumors (83, 150).

The therapeutic effectiveness of anti-CD19-targeted immunoliposomes in a murine model of human B-cell lymphoma (Namalwa) (24), was also demonstrated. *In vivo* survival studies performed in SCID mice xenografts of the Namalwa cell line demonstrated significantly increased life spans for mice treated with anti-CD19-targeted liposomes loaded with DXR, compared to mice treated with DXR-loaded non-targeted Stealth® liposomes or free DXR (24). Treatment of mice was initiated 24 h after i.v. injection of the cells, at which time the target cells had populated the bone marrow, suggesting that some extravasation of the LTLs can occur.

Anti-CD19 is also expressed, although to a much lower extent, on the surface of peripheral blood mononuclear cells from patients with multiple myeloma. Anti-CD19-targeted liposomes were shown to bind selectively to B-cells in mixed B-cell and T-cell populations, and were shown to have higher cytotoxicities against multiple

myeloma patient B-cells compared to non-targeted liposomes, as determined by both decreases in cell proliferation and increased apoptosis (142). A possible therapeutic niche for these LTLs might be the elimination of residual circulating malignant B-cells (the hypothesized mechanism by which multiple myeloma relapse occurs) after bone marrow ablation (151-155).

Park *et al.* have described results in breast cancer for DXR-loaded liposomes coupled to either recombinant human anti-HER2-Fab' or anti-HER2 scFv C6.5 (28). HER2 is a receptor tyrosine kinase, a product of the HER2 (c-erbB2) proto-oncogene, which has been shown to play an important role in the development and progression of breast and other cancers. Subcutaneous implants of several different HER2-overexpressing highly tumorigenic cell lines with different antigen densities were treated with i.v. injections of DXR-loaded anti-HER2 LTLs. DXR-loaded immunoliposomes were superior to DXR-loaded non-targeted liposomes, free DXR or free Ab or Ab fragments. Careful controls demonstrated that the effect was due to the specific targeting of the immunoliposomes, and not due to effects of the targeting agent or free drug alone. In the same murine model, gold-loaded non-targeted liposomes were localized in the extracellular areas of tumor stroma and tissue macrophages, while anti-HER2-targeted liposomes were found within tumor cells (107). The authors therefore concluded that the therapeutic advantage associated with DXR-loaded anti-HER2-targeted liposomes was due to specific intracellular drug delivery to the target cells. The authors discuss the potential for anti-HER2-targeted liposomes in delivering effective antitumor therapy in breast cancer while avoiding

the dose-limiting cardiotoxicity of DXR. DXR-loaded anti-HER2-targeted liposomes are currently undergoing scale-up for clinical studies.

Pastorino *et al*. treated nude mice, inoculated i.v. with human neuroblastoma cells HTLA-230, with DXR-loaded liposomes targeted with anti-GD_2 Fab' fragments and obtained complete inhibition of tumor growth (32). Neither free Fab' fragments, free DXR, empty liposomes conjugated to Fab' fragments, or non-targeted DXR-loaded liposomes had any effect on prolonging the survival times of the tumor-bearing mice. Long-term survival rates approaching 100% were obtained for different doses and dosing schedules of the drug-loaded immunoliposomes. Histological evaluation of the main organs demonstrated that the immunoliposomes selectively inhibited neuroblastoma growth in all the examined organs. This is another example of the successful treatment of a human tumor xenograft in which the tumor is small and relatively undeveloped, allowing the immunoliposomes ready access to the tumor cells.

Another study evaluated the therapeutic effectiveness of DXR-loaded liposomes, targeted via Fab' fragments of anti-β_1 integrins, in a metastatic human lung tumor xenograft mouse model (27). Treatment of mice with these DXR-loaded liposomes resulted in a significant suppression of tumor growth compared to control formulations, as well as prevention of the metastasis of tumor cells to liver and adrenal gland, although no cures were observed. The authors suggest a possible therapeutic niche for these immunoliposomes in the treatment of metastases after

Table 1.1 Selected list of ligand-targeted liposomes that have received evaluation *in vitro* or *in vivo* for delivery of anticancer drugs.

Targeting agent	Cell surface target	Model	Reference
Antibody, antiCD19	CD19	human-B-cell lymphoma (Namalwa)	(24)
Antibody, antiCD19	CD19	human multiple myeloma, ARH77	(142)
Antibody, recombinant human anti-HER2-Fab' or scFv C6.5	HER2	HER2-overexpressing human breast cancer	(28)
Antibody, human anti-CEA 21B2 and human anti-CEA 21B2 Fab'	Human carcinoembryonic antigen, CEA	CEA-positive human gastric cancer, MKN-45	(157)
Antibody, MRK16	P-glycoprotein	human myelogenous leukemia, K562	(158)
Antibody, anti-β_1 – integrin Fab'	β_1 integrins	human non-small cell lung carcinoma	(27)
Antibody, CC52	CC531	rat colon carcinoma	(159)
Antibody, anti-GD_2 and anti-GD_2 Fab'	GD_2	human melanoma or neuroblastoma	(32), (151)

Antibody, anti-idiotype mAb, S5A8	38C13	murine B-cell lymphoma	(156)
Antibody, human anti-E-Selectin	E-Selectins	activated human endothelial cells	(160)
Antibody, anti-ganglioside G_{M3} (DH2) or anti-Le^x (SH1)	carbohydrate, ganglioside (G_{M3}); Lewis X (Le^x)	B16BL6 mouse melanama and HRT-18 human colorectal adenocarcinoma	(161)
Peptide, antagonist G	Vasopressin	human small cell lung cancer, H69	(144)
Peptide, vasoactive intestinal peptide	VIP receptors	rat breast cancer	(162)
Peptide, P_0-protein	intercellular adhesion molecule-1 (ICAM-1)	human M21 and A-375 melanoma	(163)
Synthetic peptide, cyclic peptide inhibitor CTTHWG-FTLC (CTT)	matrix metalloproteinases / gelatinases (MMP-2 and MMP-9)	U937 leukemia and HT1080 sarcoma	(164)
Angiogenic homing peptide, APRPG	integrin, GPIIb-IIIa	Meth-A sarcoma	(147)

Vitamin, folate	folate receptor	M109-R mouse carcinoma tumor	(25)
Vitamin, folate	folate receptor	KB cells, human nasopharyngeal cell-line	(22, 165)
Vitamin, folate	folate receptor β	murine acute myelogenous leukemia	(29)
Vitamin, Folate	folate receptor	chinese hamster ovary and KG-1 human acute myelogenous leukemia cells	(166)
Transferrin	transferrin receptor	murine colon 26 and B16 melanoma	(167)
Transferrin	transferrin receptor	MKN45P human gastric tumor	(30)
Transferrin	transferrin receptor	C6 glioma	(168)
Carbohydrate, hyaluronic acid	CD44	B16F10 murine melanoma	(169)

surgical removal of the primary tumor. Although members of β_1 integrin family have upregulated expression in a number of cancers, they have a wide distribution in normal cells and hence additional studies are required to assess the utility of using anti-β_1 integrins as targeting moieties for immunoliposomes.

Tseng *et al.* used a different approach by targeting DXR-containing liposomes via an anti-idiotype Ab to 38C13 murine B-cell lymphoma cells. These immunoliposomes were shown to bind specifically to, and internalize into 38C13 cells. Further, DXR-loaded immunoliposomes were more effective at prolonging the survival of tumor-bearing mice than non-targeted liposomal DXR or free DXR(156).

Nam *et al.* showed that DXR-loaded liposomes conjugated to mAbs against tumor-associated carbohydrate antigens (ganglioside G_{M3}) were able to reduce *in vivo* tumor growth and metastasis of B16BL6 mouse melanoma cells to a significantly greater extent than free DXR or DXR entrapped in either classical or Stealth® liposomes. In biodistribution experiments, immunoliposomes exhibited higher accumulation in tumor tissues than control liposomal formulations (161).

1.11.2 Peptides and other receptor ligands as targeting moieties

Peptide-targeting of liposomes to disease sites has become possible because of our increased understanding of the discrete peptide sequences of proteins involved in cell-cell and effector-cell interactions. In addition, differential expression of receptors for vitamins, growth factors and other ligands occurs frequently between normal and diseased cells. Hence, ligands that bind to these receptors can be used to target liposomes to diseased cells that over-express the receptors (22, 23, 25, 30, 133,

165, 168, 170-173). The main problems with this approach are the expression of many of these receptors on normal tissues, and the occurrence of circulating ligands in the blood that may compete with binding of the LTLs. Table 1.1 gives the list of ligands that have received evaluation as liposomal targeting moieties for the delivery of anticancer drugs.

1.12 The Model System

Lymphomas are tumors derived from the lymphatic system. They have traditionally been classified as either non-Hodgkin's lymhoma (NHL) or Hodgkin's lymhoma (HL) based primarily on histological differences. NHLs are classified into indolent (low-grade) and aggressive (intermediate, high grade) disease. At the molecular level, the genetic lesions responsible for causing NHLs include the activation of oncogenes by chromosomal translocations, as well as inactivation of tumor suppressor genes by chromosomal deletions and mutations (174). Some of the most common translocations include t(8;14) (q24:32); t(14:18) (q32:21); t(11:14) (q13:32) which can activate protooncogenes like c-MYC, BCL-2 or PAX-5 . Further deletions and mutations of p53 and other unidentified tumor suppressor genes have been demonstrated. In addition, viral infection has been linked with particular subtypes, e.g., Epstein-Barr virus (EBV) with Burkitt's lymhoma (174, 175).

Approximately 85% of all NHLs arise from the cells of the B-lineage. B-lymphocytes are the effector cells of humoral or Ab-mediated immunity. B-cells are generated from bone marrow stem cells that first differentiate into progenitor B-cell (pro B-cells) and then sequentially into pre-B-cells and mature B-cells (98). Mature

but naïve B-cells migrate to secondary lymphoid tissues, where upon encounter with antigen they can become plasma cells, responsible for producing Abs (98). The various stages of B-lymphocyte life cycle may be differentiated by expression of cell surface markers (cluster designation, CD antigens) and by the status of immunoglobulin gene rearrangements. Malignant clones can be derived from any of these developmental stages. New lymphoma classifications are now being proposed, which are expressed in terms of the developmental stage from which the malignant clone appears to derive. These include classifications like Revised European-American Lymphoma (REAL) (176) and World Health Organization (WHO) nomenclature guides (177).

1.12.1 Cell surface antigens: CD19, CD20 and CD22

A $CD19^+/CD22^+/CD20^+$ human B-cell lymphoma (Namalwa cell line) that grows readily in SCID mice was used as the model in this thesis. CD19, a 95 kDa B lineage-specific membrane glycoprotein is expressed on all B-cells from early stages until their terminal differentiation into plasma cells, when it is lost (178, 179). The receptors are absent on hematopoietic stem cells in the bone marrow (180), which allows targeting to the malignant B-cells, leaving the progenitor population intact. In addition, CD19 receptors have been documented to undergo receptor-mediated endocytosis upon Ab binding, which makes this antigen a particularly appealing target (24, 181). CD19 is expressed on greater than 90% of B-cell lymphomas, and malignant B-cells form clonal populations with a very high percentage of the cells expressing this target antigen.

CD19 is a critical signal transduction molecule that regulates B-lymphocyte development, activation and differentiation. On the surface of B-cells, CD19 forms a protein complex with CD21 (complement receptor type 2), CD81 (TAPA-1; a target for antiproliferation Ab), Leu-13 and other unidentified proteins (96, 182). Its function intersects with multiple signaling pathways crucial for modulating intrinsic and antigen-induced signals. Engagement of CD19 by mAbs leads to tyrosine phosphorylation of cytoplasmic and cell surface proteins including CD19, activation of phospholipase C (PLC), inositol phospholipid turnover, intracellular Ca^{2+} mobilization, stimulation of serine specific protein kinases including protein kinase C, and activation of nuclear factor κB (178, 183). Anti-CD19 has been shown to induce cell cycle arrest (94) and inhibit the function of the Pgp pump (95). Recently a study demonstrated that homodimers of anti-CD19 can signal G_0/G_1 arrest (184).

CD20, a 33-37 kDa membrane phosphoprotein, is expressed on more than 90% of B-cell lymphomas (1, 185-187). It is expressed on B-cell precursors and mature B-cells, but is lost following differentiation to plasma cells. Stem cells (B-cell progenitors) in bone marrow lack the CD20 antigen, allowing healthy B-cells to regenerate after treatment with anti-CD20 mAbs, and return to normal levels within several months. CD20 is not modulated or shed upon ligation (186, 188, 189). It does not internalize (188) or internalizes very slowly (190) upon Ab binding. The precise function of CD20 is unknown, but it appears to play a role in the early steps of B-cell activation, proliferation and differentiation (191, 192). It also plays a role in

the activation of protein tyrosine kinases (193) and may function as a Ca^{2+} channel (189, 194).

A chimeric mouse-human anti-CD20 Ab, rituximab (Rituxan™, Genentech, Inc.), was approved by the Food and Drug Administration (FDA) in 1997 for the treatment of relapsed or refractory, CD20-positive, B-cell, low-grade or follicular NHL (195). Rituximab consists of the heavy and light chain variable regions from the murine IgG_1 anti-CD20 mAb, and the constant region from human $IgG_{1\kappa}$ anti-CD20 mAb. It mediates CDC in the presence of human complement (186, 187), and ADCC with human effector cells (186, 196, 197). In addition, it has been shown to induce apoptosis (196, 198) and to sensitize chemoresistant human lymphoma cell lines (88, 199).

CD22 is a 135 kDa B-cell restricted siaologlycoprotein expressed in the cytoplasm of early pre-B-cells and on the surface of mature B-cells (200-202). It is lost prior to differentiation to plasma cells (203). Though the precise function of CD22 is unclear, it is suggested to regulate B-cell responses by recruiting key signaling molecules to the antigen receptor complex (204, 205). Though CD22 is not normally shed from the cell surface, it is rapidly internalized after binding with its natural ligands or Abs (206, 207), and this makes it an excellent target for LTTs such as immunotoxins, Ab-drug conjugates and immunoliposomes. Clinical trials with a humanized anti-CD22 IgG_1 Ab (Epratuzumab, Amgen Inc. and Immunomedics Inc.) in patients with NHL are ongoing (208). In the clinic, anti-CD22 is also being

evaluated as radioimmunoconjugate or immunotoxins (anti-CD22 Abs conjugated to ricin A toxin or pseudomonas endotoxin) (209-213).

1.12.2 Drugs: Doxorubicin and Vincristine

Current chemotherapeutic protocols for B-cell lymphomas consist of a combination of anticancer drugs including cyclophosphamide, DXR, VCR, bleomycin, dexamethasone and prednisone. The most commonly used protocol is the CHOP regimen consisting of cyclophosphamide (C), adriamycin/DXR (H), VCR (O) and prednisone (P). In this thesis, immunoliposomal formulations of two anticancer drugs, DXR and VCR, which work via different mechanisms of action, have different drug-related properties, and have different leakage rates from liposomes, were evaluated for the treatment of B-cell malignancies.

VCR, a vinca alkaloid, is a dimeric alkaloid isolated from the periwinkle plant *Catharanthus rosea*. It is composed of a dihydroindole nucleus (vindoline), which is linked by a carbon-carbon bond to an indole nucleus (catharanthine). VCR has a formyl group attached to the nitrogen of the vindoline nucleus (Figure 1.8A). Vincristine is effective against a wide variety of neoplasms including NHL, HL, acute lymphoblastic leukemia, rhabomyosarcoma, breast cancer, small cell lung cancer, neuroblastoma and Wilm's tumor . VCR is a cell cycle specific agent, which exerts its antitumour activity by binding to the α and β subunits of tubulin, producing interference in microtubule assembly in S phase. The depolymerized tubulin proteins prevent mitotic spindle assembly and cell division is halted in the metaphase stage of mitosis (214-216). Other effects noted at very high concentrations are decreased

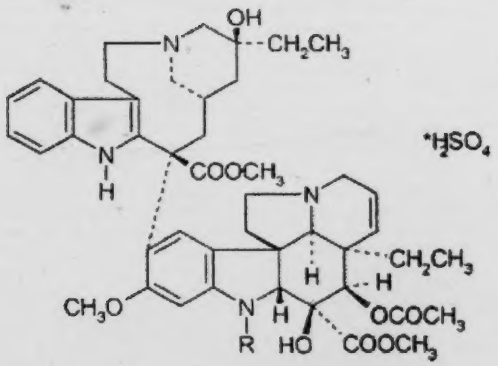

R is CHO

A. Vincristine

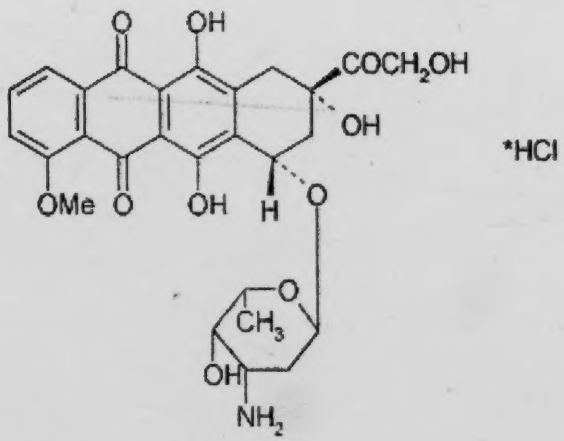

B. Doxorubicin

Figure 1.8 Structural formulae of (A) Vincristine and (B) Doxorubicin

protein and RNA synthesis, altered lipid synthesis, and blocked uptake of glutamic acid. Peripheral neurotoxicity is the dose-limiting toxicity of VCR (216-219) and its severity is related to both the total dose and the duration of treatment (220). Other infrequently occurring side effects include constipation, abdominal cramps, nausea, vomiting, mucositis, diarrhea, paralytic ileus, intestinal necrosis and bladder atony (220). Severe myelosuppression is rare but may occur with VCR overdosage (221). Alopecia and rashes are frequently reported (220). The plasma pharmacokinetics of free VCR fits into a three-compartment model, which includes a large volume of distribution (V_d), high clearance (CL) and long terminal $t_{1/2}$ (222). After i.v. administration, the free drug is rapidly redistributed to body tissues with a $t_{1/2}\ \alpha$ of less than 5 min. The $t_{1/2}\beta$ ranges from 50-155 minutes and $t_{1/2}\chi$ from 23-85 hours (216, 222-225).

In vitro data indicate that the duration of VCR exposure is an important determinant for cytotoxicity (226) and this provides the basic rationale for encapsulating VCR into liposomes. In clinical trials, patients refractory to bolus VCR therapy exhibited increased response rates when VCR was administered as a 5-day infusion (257, 258).

DXR, a cell cycle independent drug, belongs to the anthracycline antibiotics class of chemotherapeutics and is amongst the most widely used anticancer drugs in the clinic. It is known to be particularly active against hematopoietic malignancies including HL and NHL and a number of solid tumors (227). DXR acts by multiple mechanisms. DXR consists of a tetracycline ring, the aglycone. One ring of this is a

quinone and is water insoluble. The molecule also contains a hydrophilic amino sugar moiety (Figure 1.8B). It is belived that, inside the liposomes, DXR is precipitated due to the stacking of the tetracycline rings. DXR is known to inhibit topoisomerase II, resulting in DNA strand breaks. In addition, it can inhibit DNA and RNA polymerase, which in turn inhibits DNA synthesis. It can cause oxidative DNA damage by the production of free radicals, as well increase ceramide levels, leading to apoptosis (227, 228).

Myelosuppression, predominantly neutropenia and leucopenia, is the dose-limiting toxicity of DXR; in addition to this, mucositis, nausea, vomiting and alopecia are frequent, whereas hepatopathy, characterised by elevated bilirubin concentrations, occurs less frequently (227, 229). Cardiotoxicity is the major adverse effect of DXR with cumulative doses that exceed approximately 500 mg/m^2; it is often irreversible and may lead to clinical congestive heart failure (227, 229). DXR has a triexponential clearance from the circulation ($t_{1/2}$ α=10min; $t_{1/2}$ β=1-3 h; $t_{1/2}$ χ=30-50 h). The pharmacokinetics is dominated by tissue binding (V_d=365 L) (227).

Stealth® formulations of DXR have already reached the clinic (Doxil® / Caelyx®) and a conventional (non-PEGylated) liposomal formulation of VCR (Onco-TCS®) is undergoing clinical trails.

1.13 Hypothesis and Objectives

Anticancer chemotherapy is compromised by dose-limiting side effects due to the distribution of anticancer drugs indiscriminately to malignant and normal cells of the body. Ab-mediated targeting of liposomal anticancer drugs to antigens expressed

on the surface of malignant cells is postulated to be an attractive strategy for alleviating some of the side effects and increasing the therapeutic effectiveness of anticancer drugs. The overall hypothesis of this thesis was that the selective targeting of liposomal DXR or liposomal VCR to B-cell surface epitopes will improve the therapeutic effectiveness of these drugs and hence will be an attractive strategy for treating B-cell malignancies. A murine xenograft model of a B-cell malignancy (Namalwa) was used, as our previous experience leads us to believe that immunoliposomes will probably perform best against targets in the vasculature, or readily accessible from the vasculature (see section 1.10). The objective of this thesis was to perform basic research to optimize immunoliposomal formulations of the anticancer drugs, DXR or VCR, for the treatment of B-cell malignancies. Through these studies, we aimed to identify factors that will help design effective immunoliposomal drugs for treating cancer.

The specific objectives were to:

1) Compare whole mAbs with Fab' fragments in order to determine which of the two has more desirable properties as a targeting agent.
2) Compare immunoliposomal formulations of anticancer drugs working via different mechanisms of action, and having different drug-related properties and different leakage rates from the liposomes, i.e., DXR and VCR.
3) Compare immunoliposomal therapeutics targeted against internalizing epitopes (CD19, CD22) with those targeted against non-internalizing epitopes (CD20).

4) Evaluate combination regimens of immunoliposomal DXR or VCR directed against multiple epitopes (CD19, CD22 and CD20).

In chapter 2, liposomes containing either DXR or VCR, and coupled to either whole mAb or Fab' fragments of anti-CD19 were developed and evaluated *in vitro* and *in vivo* in a xenograft model of human B-cell lymphoma (Namalwa). Here, we aimed to compare targeted, sustained release formulations of VCR vs. DXR, in the same model. Also, compared were whole mAb and its Fab' fragments as targeting moieties. The hypothesis was that liposomes targeted via Fab' fragments will demonstrate longer circulation times as compared to immunoliposomes targeted via whole Abs due to the absence of Fc receptor-mediated mechanisms of liposome clearance into immune cells. The longer circulation times would allow more time for the immunoliposomes to bind to the target cells, which would help in increasing the therapeutic effectiveness of immunolisposomal drugs. The chapter presents data on cell association, cytotoxicities, drug release rates, pharmacokinetics, and therapeutics comparing several different formulations of both DXR and VCR. Also described here is a method to prepare Fab' fragments from IgG_{2a} mAbs such as anti-CD19, employed in these studies.

It has long been hypothesized that immunoliposomes targeted against internalizing epitopes will be more effective than those targeted against non-internalizing epitopes, but direct experimental proof was missing. In chapter 3, this hypothesis was verified experimentally by using two separate populations of liposomal DXR, each targeted with a mAb against a different epitope, either

internalizing or non-internalizing, that are both expressed on the surface of the Namalwa cells. Using a xenograft model, immunoliposomal DXR targeted against CD19, an internalizing epitope, was compared with immunoliposomal DXR targeted against CD20, a non-internalizing epitope. The chapter also presents data on cell binding, confocal microscopy and cytotoxicity experiments comparing the different liposome formulations.

In chapters 4 and 4A, combination regimens of immunoliposomal DXR or immunoliposomal VCR targeted to multiple epitopes (CD19, CD22 or CD20) were evaluated. The hypothesis was that targeting of immunoliposomal anticancer drugs against multiple epitopes would be a more effective strategy for treating B-cell malignancies than targeting against a single epitope. *In vitro* cell association and *in vivo* survival experiments were done to evaluate if targeting of liposomal anticancer drugs to multiple epitopes (CD19, CD22 or CD20) will increase the therapeutic effectiveness of immunoliposomal anticancer drugs compared to targeting to a single epitope.

Chapter 5 summarizes the findings of this thesis. Conclusions are drawn and speculations and ideas for future directions of this work, and that of the immunoliposomal field in general, are presented.

CHAPTER 2

Improved therapeutic responses in xenograft models of human B-lymphoma for long-circulating vincristine-loaded liposomes targeted via anti-CD19 IgG_{2a} or Fab' fragments compared to those loaded with doxorubicin.

(manuscript in preparation for submission to Clinical Cancer Research)

2.1 ABSTRACT

Antibody (Ab)-mediated targeting of liposomal anticancer drugs to antigens expressed on malignant B-cells has been shown to be an effective strategy for treating B-cell malignancies. We have compared long-circulating (Stealth®) immunoliposome (SIL) formulations containing anticancer drugs having different mechanisms of action, drug-related properties and drug release rates from liposomes. We evaluated the specific binding and cytotoxicity of anti-CD19-targeted SIL containing vincristine (VCR) versus doxorubicin (DXR) *in vitro* and the pharmacokinetics and therapeutic responses of these formulations *in vivo* in xenograft models of human B-cell lymphoma (Namalwa cell line). Also, SIL formulations of VCR or DXR targeted via the whole monoclonal antibody (mAb), anti-CD19 (SIL[αCD19]) were compared to those targeted via its Fab' fragments (SIL[Fab'CD19]).

Both SIL[αCD19] and SIL[Fab'CD19] demonstrated higher cell association with, and cytotoxicity against, Namalwa cells than non-targeted Stealth® liposomes (SL). In naïve BALB/c mice, coupling of Fab' fragments to the liposomes increased the circulation times of both DXR- and VCR-containing liposomes relative to whole mAb. VCR had faster leakage rates from the liposomes than DXR, both *in vitro* and *in vivo*. The rate of removal of liposomal lipid from circulation was similar for DXR-containing and VCR-containing liposomes. In therapeutic experiments, administration of single i.v. doses of either anti-CD19-targeted liposomal VCR or DXR significantly increased the survival times of mice compared to drug-loaded non-

targeted liposomes or free drugs. Treatment with VCR-loaded SIL resulted in significant increases in life spans compared to DXR-loaded SIL. Mice treated with DXR-loaded SIL[Fab'CD19] had significantly longer survival times than those treated with DXR-loaded SIL[αCD19], but no significant difference was found in the survival times of mice treated with VCR-loaded SIL[αCD19] versus VCR-loaded SIL[Fab'CD19]. These results are the first demonstration of the improved therapeutic responses of targeted, sustained release formulations of the cell-cycle dependent drug, VCR in the treatment of B-cell malignancies. In addition, we describe here for the first time superior therapeutics of liposomal DXR targeted with Fab' fragments over those targeted with whole mAbs.

2.2 INTRODUCTION

Anticancer chemotherapy is compromised by dose-limiting side effects as a consequence of the distribution of anticancer drugs to normal cells and tissues as well as to malignant ones. Trapping cytotoxic drugs in liposomes (phospholipid bilayer vesicles) can reduce their side effects as well as improve their therapeutic responses by enhancing their localization to tissues with increased vascular permeability, e.g. solid tumors undergoing angiogenesis (8, 230). This approach, referred to as passive targeting, has resulted in several liposomal anticancer drugs that have received clinical approval and many more that are in clinical trials.

There is currently increased interest in the use of ligand-mediated or 'active' targeting as a strategy for increasing the therapeutic effectiveness of antineoplastic drugs. To form targeted liposomes, mAbs, peptides or growth factors that bind

selectively to tumor-associated antigens or receptors are coupled to the liposome surface (2, 22-25, 27-29, 84, 112, 149, 231, 232). Abs that are capable of inducing efficient receptor-mediated internalization of immunoliposomes can result in significant increases in the amount of drug delivered to the target cells and hence therapeutic responses, relative to free drugs, non-internalizing Abs or non-targeted liposomes (108, 233, 234). In addition, many mAbs have unique signaling properties, such as inhibition of DNA repair (93), blockade of P-glycoprotein (95) or induction of apoptosis (96), that lead to anticancer effects that may synergize with the cytotoxic effects of liposomal anticancer drugs (87-89).

Despite the observation that immunoliposomes improve the therapeutic effectiveness of anticancer drugs, some further development is required prior to clinical testing. Many of the coupling techniques currently used for the preparation of immunoliposomes rely on thiolation of amino residues on whole IgG Ab molecules (59). Such modifications can alter the biological activity of the Ab molecule, e.g., by randomly thiolating the active site, leading to interference with the binding of the Ab to its receptor, receptor activation and/or endocytosis.

The immunogenicity of therapeutic agents that are based on murine mAbs has been a major barrier to successful therapy in humans since they evoke human anti-mouse Abs (HAMA), mediated in part by the Fc-region of the molecule (85, 118, 119, 235). This can result in hypersensitivity reactions and, in the case of immunoliposomes, enhanced removal of the immunoliposomes by the cells of the mononuclear phagocyte system (MPS) via Fc receptors on macrophages (63, 120,

122). Since the extent of uptake of liposomes by target tissues is directly related to their residence time in the circulation, any decrease in the circulation half-lives of liposomes due to non-specific uptake mechanisms will compromise their selective uptake by the target tissues (236). Further, some studies have reported that targeted liposomes containing exposed Fc regions of the Ab are taken up by tumor-associated macrophages, which limits their direct interactions with the target tumor cells (84, 140, 141).

Ab fragments that contain the relevant antigen binding site, e.g., Fab' or scFv fragments, are attractive alternatives to whole Abs as liposomal targeting agents. Fab' fragments can be coupled to liposomes through the thiol groups of the hinge region, avoiding perturbation of the antigen recognition site and introduction of random amino-acid modifications to the Ab (75, 76). Removal of the Fc domain helps liposomes evade uptake by the Fc-receptors on macrophages and should reduce immunogenicity of the immunoliposomes. It will also increase their circulation time and, therefore, the degree of tumor localization of the immunoliposomes (32, 112). Although binding avidity is lost with the use of univalent Fab' and scFv fragments, coupling of these fragments to liposomes will restore multivalency and binding avidity.

The vinca alkaloid, vincristine (VCR), is used in the treatment of lymphomas. It is a cell-cycle dependent drug that arrests cell mitosis during metaphase by preventing tubulin polymerization as well as by inducing depolymerization. However, dose-limiting toxicities such as peripheral neuropathy associated with VCR

therapy can compromise both the therapeutic outcome and patient quality of life. *In vitro* studies have demonstrated a positive relationship between the therapeutic effectiveness of VCR and the length of exposure of tumor cells to the drug (51). A classical (non-PEGylated) liposomal formulation of VCR is currently in clinical trials (237, 238). The use of an Ab-targeted, long-circulating liposomal formulation of VCR should increase the amount of drug delivered to the target cells and increase the duration of exposure of the target cells to the drug, both of which should result in an improved therapeutic response. The exposure of sensitive tissues to the drug will be decreased, leading to reduced side effects.

The ability of liposome-encapsulated DXR to decrease the side effects of the drug and to increase its therapeutic effectiveness is well established in the clinic (239-241). The utility of liposomal DXR targeted via whole murine anti-CD19 Abs has been previously described in our laboratory in SCID mouse models of human B-lymphoma and multiple myeloma (24, 142). A comparison of Fab'-targeted liposomal DXR with whole mAb-targeted liposomal DXR would allow us to test the hypothesis that Fab'-targeted liposomes will have therapeutic advantages, in part due to their pharmacokinetic advantages.

In this study, we evaluated the binding, cytotoxicity, pharmacokinetics and therapeutic outcome for anti-CD19-targeted liposomal formulations of two different cytotoxic drugs, vincristine (VCR) and doxorubicin (DXR) that act via different mechanisms of action, have different drug-related properties and different drug release rates from liposomes. We compared the therapeutic responses, in a SCID

mouse model of human B-cell lymphoma, of liposomal drugs targeted with whole mAb or Fab' molecules with results obtained for free drugs, non-targeted liposomes and drug-free liposomes. A significant improvement in therapeutic response was associated with drug-loaded Ab-targeted liposomes compared with other treatment groups and with VCR-containing liposomes compared with those containing DXR.

2.3 MATERIALS AND METHODS

2.3.1 Materials

Egg sphingomyelin (SM) and cholesterol (Chol) were purchased from Avanti Polar Lipids (Alabaster, AL). Methoxypolyethylene glycol (MW 2000), covalently linked via a carbamate bond to distearoylphosphatidylethanolamine (mPEG) (242), hydrogenated soy phosphatidylcholine (HSPC) and doxorubicin (DXR) were generous gifts from ALZA Pharmaceuticals, Inc. (Mountain View, CA). Maleimide-derivatized polyethylene glycol (MW 2000)-distearoylphosphatidylethanolamine (Mal-PEG) was custom synthesized by Shearwater Polymers, Inc. (Huntsville, AL), according to a previously described protocol (60). Nuclepore® polycarbonate membranes (pore sizes: 0.2, 0.1, and 0.08 μm) were purchased from Northern Lipids (Vancouver, BC). Vincristine sulphate (1 mg/ml) for injection was purchased from the pharmacy of the University of Alberta Hospital (Edmonton, AB). RPMI 1640 (without phenol red), penicillin-streptomycin and fetal bovine serum (FBS) were purchased from Life Technologies (Burlington, ON). 2-iminothiolane (Traut's reagent), 2-mercaptoethylamine-HCl (2-MEA) and 3-[4,5-dimethylthiazole-2-yl]-2,5-diphenyltetrazolium bromide (MTT) were obtained from Sigma Chemical Co. (St.

Louis, MO). Iodobeads, Protein A/G column, ImmunoPure® IgG Elution buffer, Slide-A-Lyzer dialysis cassettes (MW cut-off of 10,000) and buoys were purchased from Pierce (Rockford, IL). Lysyl endopeptidase enzyme was obtained from Wako Chemicals Inc. (Richmond, VA). SDS-PAGE (sodium dodecyl sulphate-polyacylamide gel electrophoresis) gels (4-20% acrylamide, Tris-HCl buffer system) and BioRad Protein Assay Reagent were purchased from BioRad Laboratories (Mississauga, ON). Sephadex G-25 and G-50, Sepharose CL-4B, aqueous counting scintillant (ASC), [^{3}H]-VCR (1.85 MBq) and [^{14}C]-DXR (185 KBq) were purchased from Amersham Pharmacia Biotech (Baie d'Urfe, QC). [^{14}C]-VCR was a kind gift from Inex Pharmaceuticals, Vancouver, BC. Cholesterol- [1,2-^{3}H-(N)]-hexadecyl ether ([^{3}H]-CHE), 1.48-2.22 TBq/mmol, Solvable™ and Ultima Gold™ were purchased from Perkin-Elmer Biosciences (Boston, MA). Tyraminyinulin (TI) was synthesized and ^{125}I-TI was prepared as described before (243). Centrisart concentrators (MW cut-off of 100,000) were obtained from Sartorius, Goettingen, Germany and Microcon YM-10 concentrators from Millipore Corp., Bedford, MA. All other chemicals were of analytical grade purity or the highest available purity.

2.3.2 Mice

Six-to-eight week-old female BALB/c mice were obtained from the Health Sciences Laboratory Animal Services (University of Alberta, Edmonton, AB) and kept in standard housing. Female 6-8-week old CB17 severe compromised immunodeficient (SCID) mice were purchased from Taconic Farms (Germantown. NY) and housed in the virus antigen-free unit of the Health Sciences Laboratory

Animal Services, University of Alberta. All experiments were approved by the Health Sciences Animal Policy and Welfare Committee of the University of Alberta.

2.3.3 Tumour cell line

The human Burkitt's lymphoma cell line, Namalwa (ATCC CRL 1432) was purchased from American Type Culture Collection, Rockville, MD and cultured in suspension in a humidified 37 °C incubator with a 5% CO_2 atmosphere in RPMI 1640 media supplemented with 10% (v/v) fetal bovine serum (FBS), penicillin G (50 units/ml), and streptomycin sulfate (50 μg/ml). For experiments, only cells in the exponential phase of cell growth were used.

2.3.4 Preparation of liposomes

Non-targeted liposomes, to be loaded with VCR, were composed of SM:Chol:mPEG at a 55:40:5 molar ratio (SM-SL) and were similar to previously described VCR formulations, except that PEG was included (51). VCR was encapsulated by a transmembrane pH gradient-dependent procedure as previously described (54). In some cases, radiolabeled [^{3}H]-VCR sulphate (5 μCi [^{3}H]-VCR sulphate per mg of unlabelled VCR) was added as a radioactive tracer. Targeted liposomes (see below) were composed of SM:Chol:mPEG:Mal-PEG, at a 55:40:4:1 molar ratio (SM-SIL). The dried lipid film was hydrated in 300 mM citrate buffer (pH 4.0) with occasional vortexing and heating at 65°C to give a concentration of 25-30 mM phospholipid (PL). The liposomes were then sequentially extruded at 65°C (Lipex Biomembranes Extruder, Vancouver, BC, Canada) through a series of polycarbonate membranes with pore sizes of 0.2, 0.1 and 0.08 μm to achieve a final

size of 120-130 nm. The liposome particle size was analyzed using a Brookhaven BI90 submicron particle sizer (Brookhaven Instruments Corporation, Holtsville, NY). VCR entrapment was determined either by spectrophotometry (λ=297 nm) in ethanol:water (8:2 by volume) or from the specific activity counts of the [^{3}H]-VCR tracer (Beckman LS-6800 Scintillation Counter). PL concentration was determined using the Barlett colorimetric assay (244) or from the specific activity of the [^{3}H]-CHE tracer. Loading efficiency was determined from the drug:lipid ratio before and after encapsulation of the drug. Trapping efficiencies of 95% and greater could routinely be achieved by this procedure. In some cases, the liposomes were concentrated using Centrisart concentrators.

Non-targeted liposomes, to be loaded with DXR, were composed of HSPC:Chol:mPEG at a 2:1:0.10 molar ratio (HSPC-SL) and targeted liposomes (see below) were composed of HSPC:Chol:PEG:Mal-PEG at a 2:1:0.08:0.02 molar ratio (HSPC-SIL). They were prepared by hydration of thin films, as described previously and were extruded to a diameter of 110 to 120 nm (108). DXR was loaded into liposomes using the ammonium sulfate loading method of Bolotin *et al.* (50).

Liposomes for the *in vitro* binding experiments were radiolabeled with [^{3}H]-CHE, a non-metabolizable, non-exchangeable radioactive tracer for binding studies, and were prepared by hydrating the lipid films in HEPES-buffered saline (HBS, 25 mM 4-(2-hydroxyethyl)-1-piperazine ethanesulphonic acid, 140 mM NaCl, pH 7.4) followed by extrusion as described above. For pharmacokinetic experiments,

liposomes were prepared in the presence of [^{3}H]-CHE and then loaded with drug spiked with either [^{14}C]-VCR or [^{14}C]-DXR.

2.3.5 Preparation of αCD19 antibody and Fab' fragments

The murine monoclonal αCD19 Ab (IgG_{2a}) was produced from the FMC63 murine hybridoma (from Dr. H. Zola, Children's Health Research Institute, Adelaide, Australia (245) and purified as described previously (74). Radioiodinated (^{125}I) mAbs or Fab' fragments were used to measure coupling efficiencies and to determine the amount of mAb or Fab' attached to the liposomes. Iodination was as described previously (24). An isotype-matched (IgG_{2a}) control Ab, αPK136 was produced from the HB191 murine hybridoma (ATCC).

To prepare Fab' fragments, mAb αCD19 was incubated with lysyl endopeptidase at a molar ratio of 1:200 (enzyme:substrate) in HBS (pH 8.0) for 3 h at 37°C (246), after which the digest was chromatographed on an immobilized Protein A/G column equilibrated with Tris buffer, pH 8.0 (0.1M Tris-HCl, 0.15M NaCl) to adsorb any undigested IgG_{2a} and the Fc segment of the Ab. The disulfide bridges of $F(ab')_2$ thus obtained were reduced using 5 mM 2-MEA for 60 min at 37°C. The sample was then eluted over a Sephadex G-25 column equilibrated with degassed HBS (pH 7.4), to remove free 2-MEA. Fab' fragments were maintained in an O_2-free environment. Protein concentrations were determined by the BioRad Protein Assay and the preparation of $F(ab')_2$ and Fab' fragments was confirmed by SDS-PAGE analysis. Fab' fragments of the isotype-matched control Ab (αPK136) were prepared by the same protocol.

2.3.6 Coupling of immunoliposomes

αCD19 or Fab' fragments of αCD19 (Fab' CD19) were coupled to the terminus of the Mal-PEG coupling lipid included in SM-SIL or HSPC-SIL using the coupling procedure previously described (60). Every effort was made to ensure that αCD19 or Fab'CD19 coupled liposomes had comparable numbers of CD19 binding sites on the immunoliposomes in each individual experiment, bearing in mind that IgG_{2a} has two binding sites and Fab' has only one. For coupling of the whole Ab, to give HSPC-SIL[αCD19] or SM-SIL[αCD19], the protocol was as previously described. Briefly, mAb (10 mg/ml) was incubated with 2-iminothiolane in O_2-free HBS, pH 8.0, at a ratio of 20:1 mol/mol for 1 h at room temperature in order to thiolate the amino groups. At the end of the incubation, the sample was chromatographed on a Sephadex G-50 column, equilibrated with O_2-free HBS (pH 7.4) and immediately incubated with liposomes in an O_2-free environment overnight with continuous stirring. For Fab'-coupled liposomes (HSPC-SIL[Fab'CD19] or SM-SIL[Fab'CD19]), the Fab' fragments were generated from $F(ab')_2$ immediately before coupling; they were then incubated with HSPC-SIL or SM-SIL in an oxygen-free environment overnight with continuous stirring. The SIL were separated from the uncoupled mAb or Fab' fragments over a Sephadex CL-4B column equilibrated with HBS (pH 7.4). Coupling efficiency was determined from the ratio of nmol protein/μmol PL, before and after coupling. Coupling of Fab' fragments was assessed by adding a trace amount of [^{125}I]-labeled $F(ab')_2$ at the time of cleavage with 2-MEA. To assess coupling of whole Ab, a trace amount of [^{125}I]-labeled

αCD19 was added to the unlabeled Ab before thiolation. A coupling efficiency of 80-90% for αCD19 and of 50-70% for Fab' fragments could routinely be achieved by this procedure. αPK136, an isotype-matched, non-specific (NS) control Ab, or its Fab' fragments, were coupled to the liposomes in a similar fashion (SM-SIL[αNS], SM-SIL[Fab'NS]).

In two therapeutic studies (Figures 2.8 and 2.9), αCD19 or Fab'CD19 were conjugated to micelles composed of mPEG:Mal-PEG (4:1) and then incubated with preformed SM:Chol (55:45) liposomes, from Inex Pharmaceuticals (Burnaby, BC, Canada) at 65°C for 1 h according to the post-insertion method of Iden *et al.* (74). In all other studies in this thesis, immunoliposomes were made by conventional coupling procedures, as described above.

2.3.7 Binding and uptake of immunoliposomes

In vitro cell association of immunoliposomes was determined at both 37°C and 4°C (non-permissive for internalization) to discriminate between the processes of cell binding and receptor-mediated internalization, as described previously (24). Briefly, Namalwa cells were washed with warm phosphate-buffered saline, pH 7.4 (PBS) to remove the media and plated in 48-well plates (1×10^6 cells/well in a volume of 0.2 ml). Liposomes (SM-SL, HSPC-SL, SM-SIL[αCD19], HSPC-SIL[αCD19], SM-SIL[Fab'CD19] or HSPC-SIL[Fab'CD19]) were radiolabeled with [^{3}H]-CHE and incubated with 1×10^6 Namalwa cells in a humidified incubator containing 5% CO_2 at PL concentrations ranging from 0.1 mM to 1.6 mM PL (in triplicate) for 1 h at 37°C or 4°C. Cells were then washed twice with cold PBS to

remove the unbound liposomes and the amount of [^{3}H]CHE associated with cells was determined. Uptake (pmoles PL uptake per 1 million Namalwa cells) was calculated from the specific activity of the liposomes. Non-specific binding was determined for the corresponding radiolabeled liposomes coupled to the isotype-matched control Ab, αPK136. Specific binding was determined by subtracting non-specific binding from the total binding. The maximum number of binding sites per cell (B_{max}) and the dissociation constant (K_d) values were determined by non-linear regression using GraphPad Prism software (San Deigo, CA).

2.3.8 *In vitro* cytotoxicity

The *in vitro* cytotoxicities of free VCR, free DXR and various liposomal formulations of VCR or DXR were determined using the MTT tetrazolium dye reduction assay as described previously (24). Briefly, 5 x 10^4 Namalwa cells were plated in 96-well round-bottom plates and incubated with increasing concentrations of free or liposomal drug formulations for 1 h or 24 h at 37 °C. At these time points, the cells were gently washed twice with warm PBS to remove any non-associated free or liposomal drug and further incubated for a total period of 48 h in media. At the end of the incubation period, medium in the wells was replaced by tetrazolium dye and further incubated for 4 h. The resulting formazan crystals were then dissolved using dimethyl sulphoxide (DMSO) and the plates were read on a Titertek Multiscan Plus MK II plate reader (Flow Laboratories, Mississauga, ON) at dual wavelengths of 570 and 650 nm. Results are expressed as the concentration required for 50% inhibition of cell growth, IC_{50} (nM for free or liposomal VCR and μM for free or liposomal

DXR). IC_{50} was obtained graphically using SlideWrite software (Advanced Graphics Software, Encinitas CA).

2.3.9 *In vitro* leakage

The leakage of VCR from the various liposomal formulations was determined in 50% adult bovine serum (ABS). Liposomes loaded with radiolabeled VCR, were diluted in ABS (1:1 by volume) loaded in a dialysis cassette (MW cut-off of 10,000) and dialyzed against 50% ABS at 37°C. At different time points, aliquots were counted for [^{3}H]-VCR. The final lipid concentration of all the formulations was 0.5 mM. Results are expressed as $t_{1/2}$ (time in which 50% of drug leaks out from liposomes). Leakage of DXR has previously been determined in our laboratory to have a $t_{1/2}$ of the order of 90 h, when encapsulated in liposomes of the composition used in our experiments (G. Charrois, manuscript in preparation).

2.3.10 Pharmacokinetics and biodistribution

The pharmacokinetics and biodistribution of various liposomal formulations entrapping [^{125}I]-TI was examined in naïve BALB/c or SCID mice bearing 5 x 10^6 Namalwa cells as described previously (24). [^{125}I]-TI was used as an aqueous space marker for intact liposomes. [^{125}I]-TI resists metabolism and breakdown and is rapidly cleared from body following its release from the liposomes (247). Briefly, mice (3/group) were injected with liposomes radiolabelled with [^{125}I]-TI. At selected time points, mice were euthanised by cervical dislocation. A blood sample was obtained by cardiac puncture (0.1 ml) and major organs (liver, spleen, lung, heart, kidneys, thyroid) were dissected out. The blood and organs were counted for cpm of

^{125}I. Blood correction factors were applied to correct for liposomes present in the blood volume of organs (248) and pharmacokinetic parameters were calculated using a polyexponential curve stripping and the least square parameter estimation program PK Analyst 1.0 (MicroMath, Salt Lake City, UT). Results are expressed as percentage of counts remaining in blood and organs relative to the total counts in the body at each time point.

Another series of pharmacokinetic and biodistribution experiments were performed with liposomes which were prepared using [^{3}H]-CHE as a lipid label, and were loaded with [^{14}C]-VCR or [^{14}C]-DXR. These experiments traced liposomal lipid as well as the drug. Naïve BALB/c mice (3/time point) were injected with liposomal formulations of the drugs at the same dose as that chosen for the therapeutic studies (0.66 mg VCR/kg or 3 mg DXR/kg). At selected time points, mice were euthanised by cervical dislocation. Whole blood was collected via cardiac puncture with a heparinized syringe, and liver and spleen were dissected out. Tissues were further processed using a method similar to those described before (249-251). Plasma was isolated from whole blood by centrifugation at 3000 x g for 5 minutes. Liver and spleen homogenates (10% w/v or 5% w/v respectively) were prepared in water using a Polytron homogenizer (Brinkman Instruments, Mississauga, ON, Canada). Next, 500 µl of Solvable™ was added to 200 µl of either tissue homogenates or plasma. The solutions were then digested for 2 h at 60°C. After the vials cooled to room temperature, 50 µl of 200 mM ethylenediaminetetraacetate (EDTA) was added before overnight bleaching with 200 µl of hydrogen peroxide

(30% v/v). Next day 100 µl of 1 N HCl was added before 5 ml of Ultima Gold™, and the samples were counted in a Beckman LS 6500 liquid scintillation counter for [^{3}H] and [^{14}C] counts. Blood correction factors were applied to correct for liposomes present in the blood volume of organs (248). Results are expressed as percentage of injected drug or phospholipid concentration present in blood or organs at each time point.

2.3.11 *In vivo* survival experiments

SCID mice (5-7/group) were injected i.v. into the tail vein with 5 x 10^{6} Namalwa cells in 0.2 ml PBS. Treatments with free or liposomal drugs were given 24 h later as single bolus i.v. doses of either 0.66 mg VCR/kg or 3 mg DXR/kg. VCR dose approximated with the clinical human dose (2 mg/m^{2}) and DXR dose is the maximum tolerated dose (MTD) in SCID mice. In only one set of therapeutic experiments animals were dosed at the MTD of VCR i.e. 2 mg/kg. Mice were monitored daily and euthanised when they developed hind leg paralysis.

2.3.12 Statistical analysis

Comparisons of the cellular binding and uptake, cytotoxicities and pharmacokinetics were done using one-way analysis of variance with InStat software (GraphPad software, Version 3.0, San Diego, CA). The Tukey post-test was used to compare means. Differences were considered significant at a *P* value of less than 0.05. K_d and B_{max} values were calculated using GraphPad Prism software, San Diego, CA). Survival studies were analyzed using Kaplan-Meier plots, using GraphPad Prism software.

2.4 RESULTS

2.4.1 Preparation of anti-CD19 Fab' fragments

The purity of the Fab' fragment was assessed by SDS-PAGE under non-reducing conditions (Figure 2.1). The molecular weights of the $F(ab')_2$ and Fab' fragments of αCD19 were approximately 110 and 55 kD respectively. Purity of the protein was over 90% and the final recovery of Fab' fragments was 50-60%.

2.4.2 *In vitro* cellular association of immunoliposomes

In vitro cell association studies were performed to determine the targeting effectiveness of immunoliposomes to $CD19^+$ Namalwa cells. The term cell association reflects a combination of three processes, a) specific binding of SIL to the CD19 epitope at the cell surface, b) internalization of the SIL into the cell interior and recycling of the epitope back to the cell surface with possible repetition of the process, and c) non-specific binding or attachment of the SIL to the cell surface. Cellular association of SM-SIL[αCD19] or SM-SIL[Fab'CD19] to $CD19^+$ Namalwa cells was higher than that of Ab-free controls (SM-SL) at all PL concentrations (Figure 2.2A). At a PL concentration of 0.4 mM, the total cell association for SM-SIL[αCD19] or SM-SIL[Fab'CD19] was around 3-fold higher than SM-SL ($P<0.05$). In addition, cellular association of SM-SIL[αCD19] and SM-SIL[Fab'CD19] to cells at 37°C was significantly higher than at 4°C (non- permissive for endocytosis),

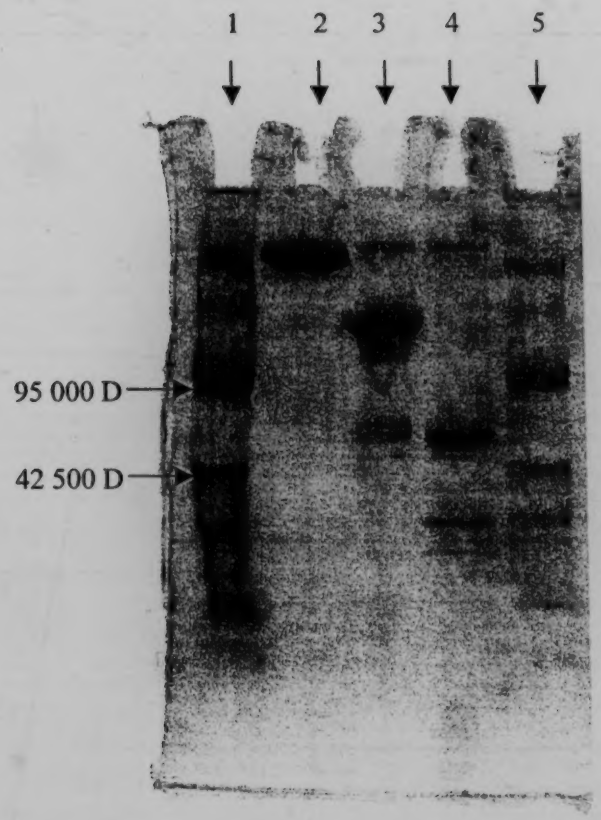

Figure 2.1 SDS-PAGE gel of αCD19 and its fragments under non-reducing conditions

Lane 2: whole mAb, αCD19
Lane 3: $F(ab')_2$ fragment of anti-CD19 generated by digestion with lysyl endopeptidase
Lanes 4: Fab' fragments (Fab'CD19) generated by reduction of disulphide bridges of $F(ab')_2$ fragment with β mercaptoethylamine
Lanes 1 and 5: Molecular weight markers

suggesting a requirement for metabolic processes in the uptake of these immunoliposomes (Figure 2.2A). SM-SIL[Fab'CD19] had a higher level of association to the Namalwa cells than SM-SIL[αCD19], although the total number of binding domains on the Fab'-coupled liposomes was actually lower than on the Ab-coupled liposomes (Figure 2.2A). The B_{max} was found to be 910 ± 100 pmoles/10^6 cells for SM-SIL[αCD19] and 1760 ± 130 pmoles/10^6 cells for SM-SIL[Fab'CD19] ($P< 0.005$). Also there was a significant difference in the K_d values of SM-SIL[αCD19] (250 ± 90 μM) and that of SM-SIL[Fab'CD19] (460 ± 80 μM) ($P<0.05$). Non-specific cellular association was determined by using radiolabeled liposomes coupled to an isotype-matched control Ab (anti-PK136) or its Fab' fragments. Non-specific association of anti-PK136-coupled liposomes with Namalwa cells increased linearly with increasing PL concentration and was very similar to that observed for the non-targeted liposomes, SM-SL (Figure 2.2B). Specific cell association was determined by subtracting non-specific association from the total cell association (Figure 2.2C).

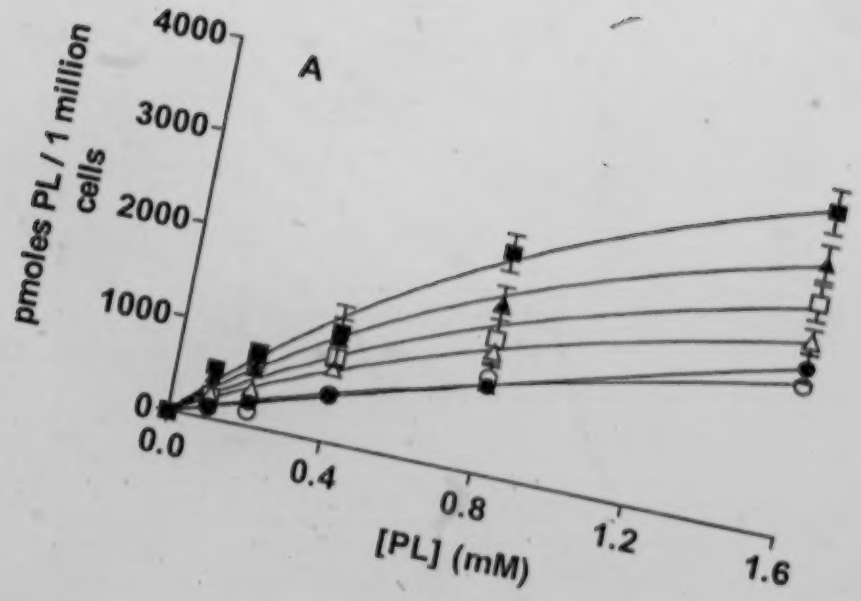
A
pmoles PL / 1 million cells
4000
3000
2000
1000
0
0.0
0.4
0.8
1.2
1.6
[PL] (mM)

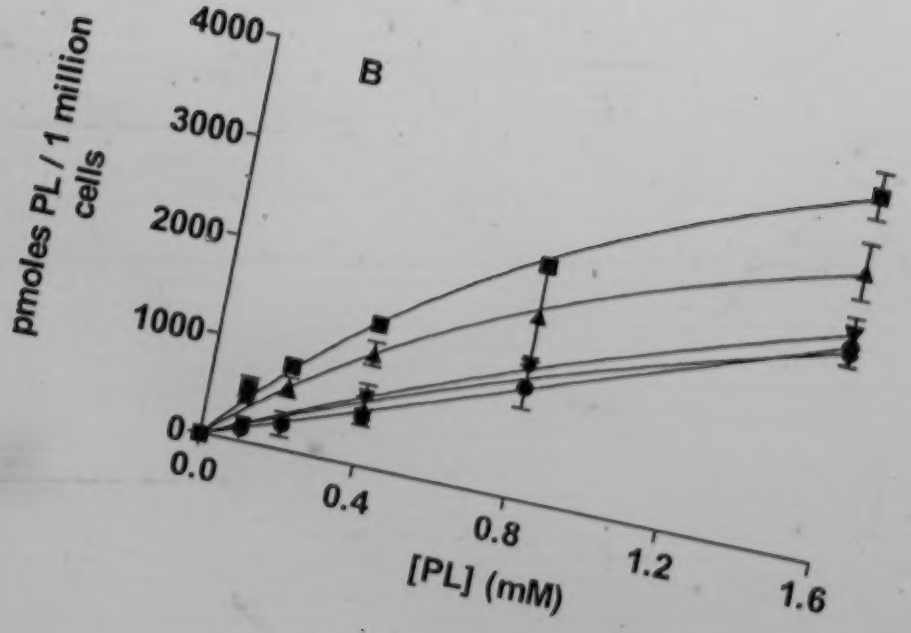
B
pmoles PL / 1 million cells
4000
3000
2000
1000
0
0.0
0.4
0.8
1.2
1.6
[PL] (mM)

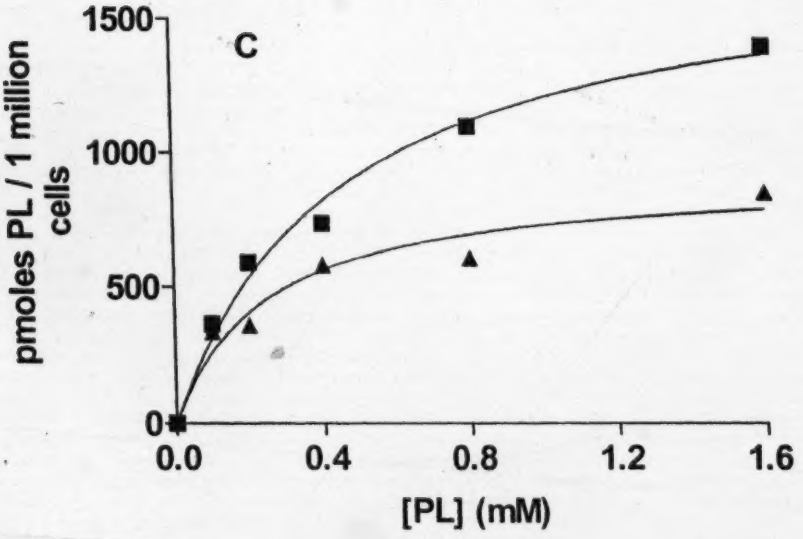

Figure 2.2 ***In vitro*** **cellular association of liposomes to Namalwa cells.** Liposomes were labeled with [^{3}H]-CHE and incubated with 1 million Namalwa cells after which the cells were washed with cold PBS to remove the unbound liposomes. The concentration of mAb on SIL[αCD19] was 0.53-0.66 nmol binding domains of αCD19/μmol PL, while the concentration of Fab' fragments on SIL[Fab'CD19] was 0.36-0.45 nmol binding domains of Fab'/μmol PL. Data are expressed as pmoles PL / 1 million cells. Each point is an average of 3 replicates ± S.D., from one representative experiment. Panels A and B represents data from two separate experiments. Panel C is the specific binding of immunoliposomes calculated from the experiment reported in Panel B. **(A)** Total cellular association of liposomes with cells as a function of concentration at 37°C (closed symbols) or 4°C (open symbols). SM-SL(●,○); SM-SIL[αCD19] (▲,△); SM-SIL[Fab'CD19] (■,□). **(B)** Total cellular association of liposomes with cells at 37°C compared to control liposomes targeted with isotype-matched control mAb anti-PK136 (αNS). SM-SL (●); SM-SIL[αCD19] (▲); SM-SIL[Fab'CD19] (■); SM-SIL[αNS] (◆); SM-SIL[Fab'NS] (▼). **(C)** Specific binding of SM-SIL[αCD19] (▲) or SM-SIL[Fab'CD19] (■) to Namalwa cells.

2.4.3 *In vitro* cytotoxicity

The *in vitro* cytotoxicities of free drugs and various drug-loaded liposome formulations were determined for 1 or 24 h incubations. This helps to differentiate between effects due to cellular uptake of drugs still encapsulated in the immunoliposomes following receptor binding and internalization of the drug package versus uptake of drug as free drug following its release (leakage) from the liposomes outside the cell. The αCD19-targeted liposomal VCR formulations, i.e., VCR-SM-SIL[αCD19] or VCR-SM-SIL[Fab'CD19], displayed 23 to 28-fold higher cytotoxicity than the non-targeted formulations (VCR-SM-SL) ($P<0.005$) for 1 h incubations (Table 2.1A). At the longer time point (24 h), no significant difference between targeted and non-targeted formulations was observed ($P>0.05$). The cytotoxicity of VCR-SM-SIL[αCD19] was not significantly different from that of VCR-SM-SIL[Fab'CD19] at either 1 h or 24 h ($P>0.05$). In addition, the cytotoxicity of targeted formulations approached that of free drug ($P>0.05$). The IC_{50} values for liposomal formulations coupled to the isotype-matched Ab, i.e., VCR-SM-SIL[αNS] or VCR-SM-SIL[Fab'NS], were significantly higher than those obtained for VCR-SM-SIL[αCD19] ($P<0.05$) or VCR-SM-SIL[Fab'] ($P<0.05$) and were similar to that of VCR-SM-SL ($P>0.05$) for 1 h incubations.

Since cytotoxicity studies with DXR-loaded immunoliposomes have been reported previously (24), the current experiments comparing whole mAb with Fab'

Table 2.1A Cytotoxicity of free or liposomal VCR formulations against Namalwa cells.

Namalwa cells (5 x 10^4/well) were plated in 96-well plates and incubated with a range of concentrations of free VCR or liposomal VCR for 1 h or 24 h. The liposomes were composed of SM:Chol:mPEG (55:40:5) or SM:Chol:mPEG:Mal-PEG (55:40:4:1), with 0.6 to 0.8 nmoles binding domains of αCD19/μmol PL or 0.45-0.64 nmol Fab'CD19/μmol PL. At the end of the incubation time, cells were washed with PBS and plated with fresh medium. The plates were further incubated for a total of 48 h, after which a MTT (tetrazolium) assay was performed. The data are expressed as mean IC_{50} in nM ± S.D for 3-5 separate experiments.

	IC_{50} (nM)	
Formulation	**1 h**	**24 h**
Free VCR	39 ± 19	4.4 ± 1.1
VCR-SM-SL	1070 ± 400	5.8 ± 2.2
VCR-SM-SIL[αCD19]	46 ± 10	3.9 ± 1.4
VCR-SM-SIL [Fab'CD19]	37 ± 12	5.1 ± 4.2
VCR-SM-SIL[αNS]	610 ± 370	6.4 ± 2.5
VCR-SM-SIL [Fab'NS]	400 ± 260	2.6 ± 2.0

Table 2.1B Cytotoxicity of free or liposomal DXR formulations against Namalwa cells.

In vitro cytotoxicity against Namalwa cells (see above) of free DXR or liposomal DXR composed of HSPC:Chol:mPEG (2:1:0.1) or HSPC:Chol:mPEG:Mal-PEG (2:1:0.08:0.02) with 0.4 nmol binding domains of αCD19/μmol PL of 0.39 nmol Fab'CD19/μmol PL. The data are expressed as mean IC_{50} in nM ± S.D for 3 separate experiments.

Formulation	IC_{50} (μM), 1 h
Free DXR	1.5 ± 0.9
DXR-HSPC-SL	>350
DXR-HSPC-SIL[αCD19]	32 ± 9
DXR-HSPC-SIL[Fab']	34 ± 4

fragments were done only for a 1 h incubation time and demonstrated that the IC_{50} values for DXR-HSPC-SIL[Fab'CD19] and DXR-HSPC-SIL[αCD19] were similar (Table 2.1B). IC_{50} values for both types of targeted liposomes were lower than that obtained for non-targeted liposomes (DXR-HSPC-SL) but higher than the values obtained for free DXR.

2.4.4 *In vitro* leakage experiments

The leakage of VCR from targeted or non-targeted liposomes was determined in 50% ABS at 37°C to check if the coupling of Ab to VCR-SM-SL altered the leakage rate for VCR from the liposomes. SM-containing formulations of VCR are known to have faster VCR leakage rates than those seen for leakage of DXR from DXR-HSPC-SL or DXR-HSPC-SIL (51, 108). The PL concentration of all the formulations was 0.5 mM. The rate of leakage of VCR from VCR-SM-SIL[αCD19] ($t_{1/2}$ = 6.8 ± 0.2 h) was found to be similar to that for VCR-SM-SL ($t_{1/2}$ = 7.2 ± 1.8 h). In previous experiments we have found that the $t_{1/2}$ for leakage of DXR from DXR-HSPC-SL was approximately 90 h (G.Charrois manuscript in preparation).

2.4.5 Pharmacokinetics and tissue distribution

First, the pharmacokinetics and biodistribution of SM-SL, SM-SIL[αCD19] and SM-SIL[Fab'CD19] were examined in naïve BALB/c mice (Figure 2.3, Table 2.2) using [^{125}I]-TI as a liposomal aqueous-space radioactive marker. SM-SIL[αCD19] was rapidly cleared from the circulation compared to SM-SIL[Fab'CD19], which demonstrated a pharmacokinetic profile very similar to the non-targeted SM-SL. Clearance of SM-SIL[αCD19] from the blood was biphasic

and characterized by a rapid initial phase of clearance of immunoliposomes and a second, slower, phase of elimination (Figure 2.3, Table 2.2). In contrast SM-SIL[Fab'CD19] demonstrated a log-linear uniphasic elimination profile very similar to that of SM-SL (Figure 2.3, Table 2.2). The mean residence time of SM-SIL[Fab'CD19] (23.1 ± 1.8 h) was significantly higher than that for SM-SIL[αCD19] (11.0 ± 0.9 h) (P<0.005, Table 2.2). Pharmacokinetics of HSPC-SL, HSPC-SIL[αCD19] and HSPC-SIL[Fab'CD19] were essentially the same as that found for their SM-containing counterparts (E. Moase, unpublished results).

We compared the biodistribution of SM-SIL[αCD19] to liver and spleen in naïve BALB/c mice with that of SM-SIL[Fab'CD19] (Figure 2.4 A, B). The uptake of SM-SIL[αCD19] into liver was initially significantly higher than that of SM-SIL[Fab'CD19] (P<0.001, Figure 2.4 A), likely due to Fc receptor-mediated mechanisms. In addition, the spleen had a significantly higher uptake of SM-SIL[αCD19] compared to SM-SIL[Fab'CD19] (Figure 2.4B) at all time points (P<0.001).

The pharmacokinetics of the liposomes was also determined in tumor-bearing SCID mice at 24 h post-inoculation i.v. of 5 x 10^6 Namalwa cells, using the aqueous space marker ^{125}I-TI, and the results were similar to those found in naïve mice (Figure 2.5). The blood level for SM-SIL[Fab'CD19] was not significantly different from that of SM-SL at 2 h (87% and 85% of injected cpm, respectively) and 24 h (33% and 37%, respectively) post-injection of liposomes (Figure 2.5).

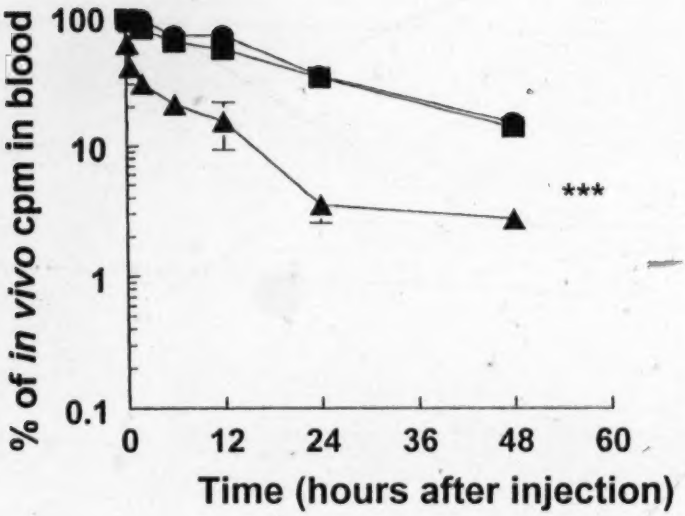

Figure 2.3 Blood clearance of targeted versus non-targeted liposomes in naive BALB/c mice.

Liposomes loaded with an aqueous space marker, [^{125}I]-TI were injected with a single bolus dose of liposomes (0.5 μmol PL/mouse) i.v. At selected time points, mice were euthanised and a blood sample and various organs were analyzed for ^{125}I. SM-SL (●); SM-SIL[αCD19] (▲) and SM-SIL[Fab'CD19] (■); The area under the curve (AUC) of SM-SIL[αCD19] was significantly lower than that of SM-SL or SM-SIL[Fab'CD19] (***P<0.001) (n=3)

Table 2.2 Comparison of the pharmacokinetic parameters of targeted and non-targeted liposomes.
Non-targeted liposomes (SM-SL) were composed of SM:Chol:mPEG (55:40:5) and targeted liposomes (SM-SIL) were composed of SM:Chol:mPEG:Mal-PEG (55:40:4:1). Liposomes loaded with an aqueous space marker, [^{125}I]-TI, were injected via the tail vein as a single bolus dose into female BALB/c mice (0.5 μmol PL/mouse). At selected time points, mice were euthanised and a blood sample and various organs were analyzed for ^{125}I. Pharmacokinetic parameters for SM-SL and SM-SIL[Fab'CD19] were calculated using a one-compartment uniexponential model assuming bolus administration and first-order output, and the least squares parameter estimation program PK analyst (MicroMath Scientific Software, Salt Lake City, UT). The SM-SIL[αCD19] graph was fitted to a two-compartment model and for this the K_E value was calculated from β half-life. (n=3)

Formulation	MRT [a] (h)	$t_{1/2}\alpha$ [b] (h)	$t_{1/2}\beta$ [c] (h)	K_E [d] (h^{-1})
SM-SL	27.5 ± 0.4	19.1 ± 0.3		0.036 ± 0.005
SM-SIL[αCD19]	11.0 ± 0.9	0.2 ± 0.1	9.0 ± 1.3	0.078 ± 0.010
SM-SIL[Fab' CD19]	23.1 ± 1.8	16.0 ± 1.2		0.043 ± 0.003

[a] Mean residence time
[b] half-life for initial clearance phase
[c] half-life for terminal clearance phase
[d] elimination rate constant from the central compartment

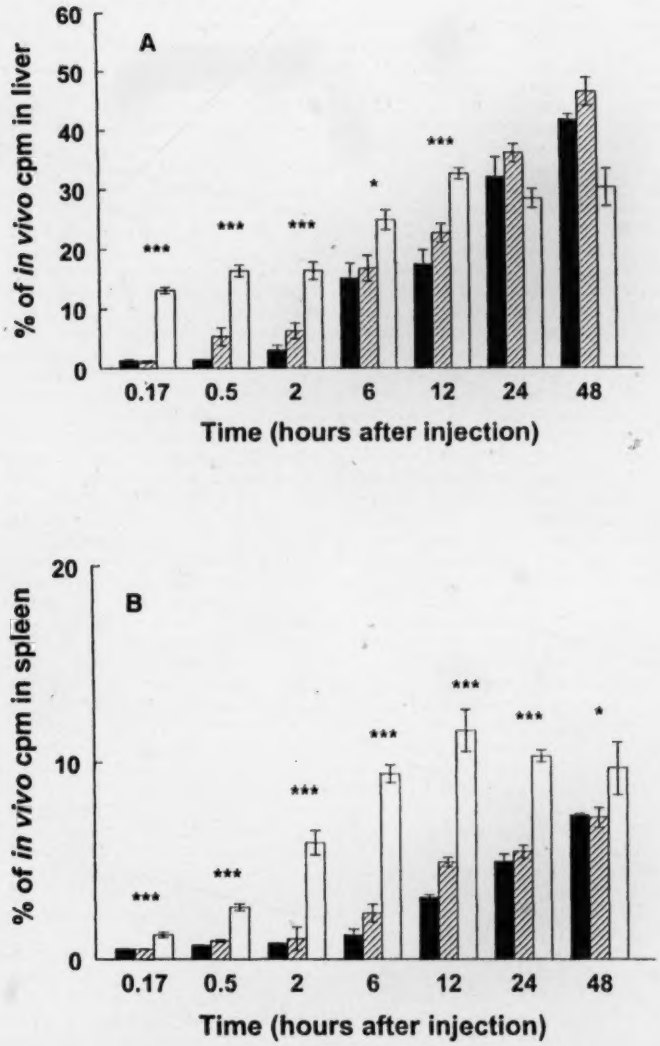

Figure 2.4 Biodistribution of liposomes to liver and spleen in naïve BALB/c mice.

Liposomes (SM-SL, SM-SIL[αCD19], SM-SIL[Fab'CD19] loaded with an aqueous space marker, [^{125}I]-TI were injected with a single bolus dose of liposomes (0.5 μmol PL/mouse) i.v. At selected time points after liposome injection, mice were euthanised and a blood sample and various organs were analyzed for ^{125}I. Data represents the percentage of total counts in the liver (**A**) and spleen (**B**) at each time point. SM-SL (solid bars); SM-SIL[αCD19] (open bars); SM-SIL[Fab'CD19] (hatched bars). Data are mean ± S.D, n=3; **P*<0.05, ****P*<0.001.

SM-SIL[αCD19], on the other hand, was rapidly cleared from the circulation. At 2 h and 24 h only 44% and 13%, respectively, of SM-SIL[αCD19] were still in blood ($P<0.05$ compared to SM-SIL[Fab'CD19]).

The pharmacokinetics and biodistribution of non-targeted or targeted liposomes loaded with either VCR or DXR were then examined, in naïve BALB/c mice (Figure 2.6). For both VCR-loaded or DXR-loaded SIL formulations, SIL[αCD19] were rapidly cleared from the circulation compared to SIL[Fab'CD19], which demonstrated a pharmacokinetic profile very similar to the non-targeted SL (Figure 2.6 C, D). For both DXR- or VCR-containing formulatiomns, the uptake of SIL[αCD19] into MPS (liver and spleen) was significantly higher than that of SIL[Fab'CD19] ($P<0.001$), at all time points likely due to Fc receptor-mediated mechanisms (Figure 2.7).

VCR had faster leakage rates from the liposomes than DXR as seen from drug:lipid ratios (Figure 2.6 E, F). The levels of % injected drug in plasma was lower for VCR-containing liposomes than for DXR-containing liposomes due to the faster leakage of VCR from the liposomes (Figure 2.6 A, B). The removal of the liposomal lipid (liposomes) from circulation was similar for DXR-containing and VCR-containing liposomes (Figure 2.6 C, D). In other words, for the VCR-containing formulations at the longer time points, some drug-depleted liposomes were present in plasma.

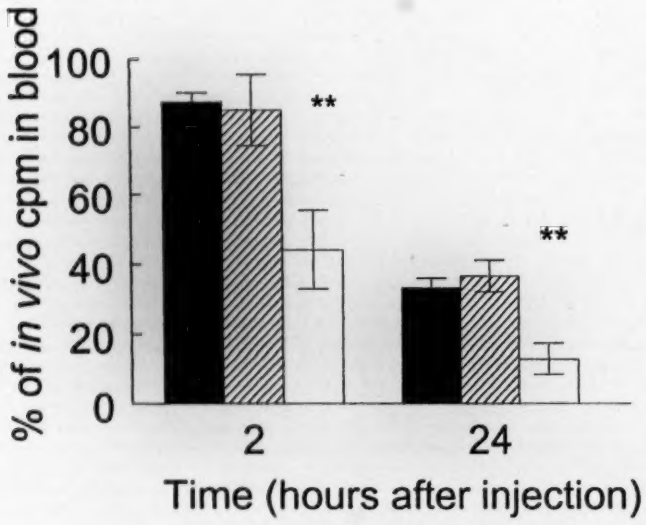

Figure 2.5 Blood clearance of targeted versus non-targeted liposomes in SCID mice bearing Namalwa cells.
Liposomes (0.5 μmol PL/mouse) loaded with an aqueous space marker, [^{125}I]-TI were injected i.v to SCID mice bearing 5 X 10^6 Namalwa cells 24h post-inoculation of cells. At selected time points, mice were euthanised and a blood sample and various organs were analyzed for ^{125}I. Data represents the percentage of total counts in blood at each time point. SM-SL (solid bars); SM-SIL[αCD19] (open bars); SM-SIL[Fab'CD19] (hatched bars). Data are mean ± S.D, n=3; $^{**}P<0.01$.

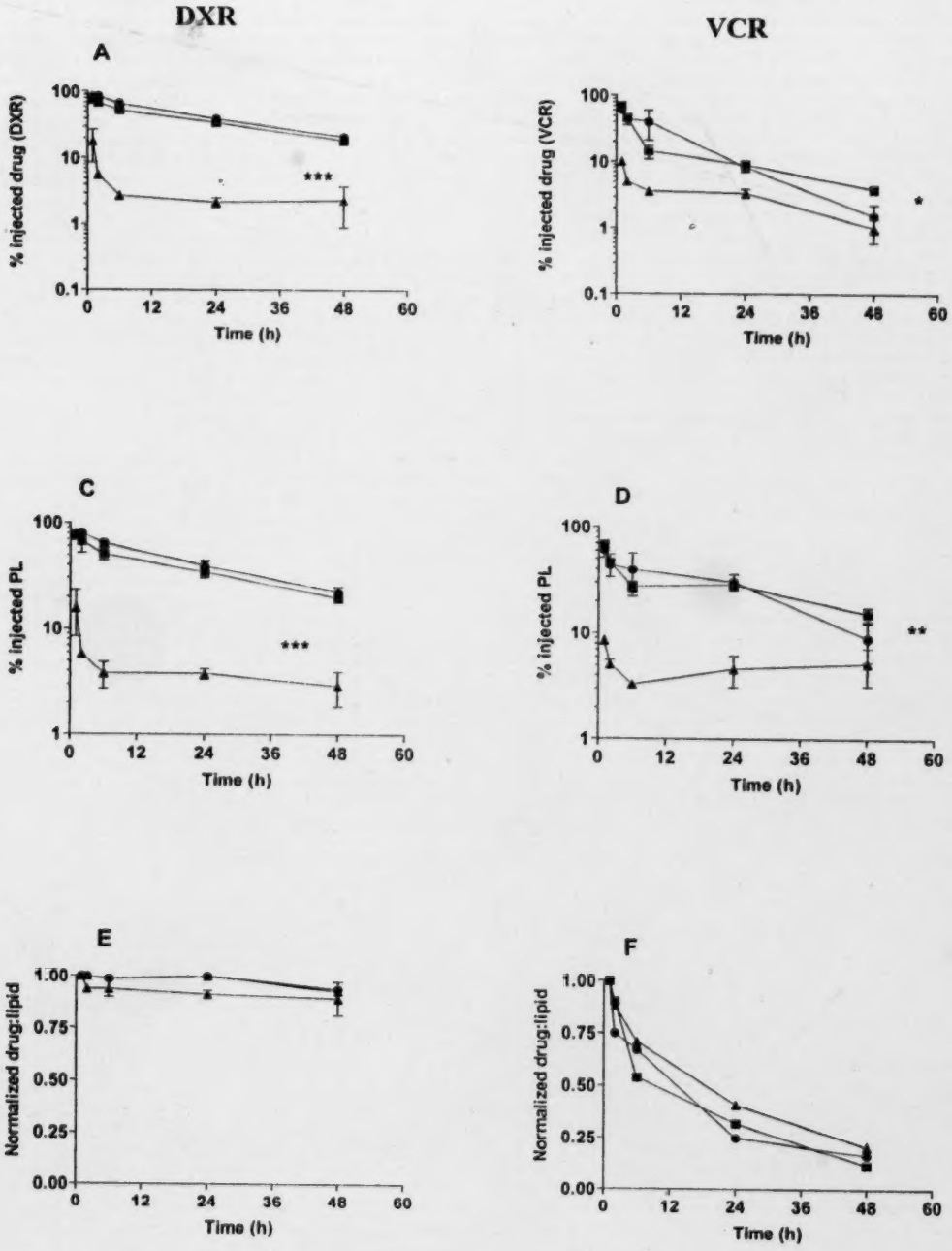
DXR
VCR
A
% injected drug (DXR)
100
10
1
0.1
0
12
24
36
48
60
Time (h)
***
% injected drug (VCR)
*
C
% injected PL
***
D
% injected PL
**
E
Normalized drug:lipid
1.00
0.75
0.50
0.25
0.00
F
Normalized drug:lipid

Figure 2.6 Blood clearance of drug-loaded targeted versus non-targeted in naive BALB/c mice.

Non-targeted liposomes loaded with VCR were composed of SM:Chol:mPEG (55:40:5, mol/mol). Targeted liposomes loaded with VCR were composed of SM:Chol:mPEG:Mal-PEG (55:40:4:1, mol/mol) and had 0.93 nmol binding domains of αCD19/μmol PL or 1.1 nmol Fab'CD19/μmol PL. Non-targeted liposomes loaded with DXR were composed of HSPC:Chol:mPEG (2:1:0.1). Targeted liposomes loaded with DXR were composed of HSPC:Chol:mPEG:Mal-PEG (2:1:0.08:0.02) and had 1.3 nmol binding domains of αCD19/μmol PL or 1.6 nmol Fab'CD19/μmol PL. Liposomes were radiolabeled with [^{3}H]-CHE and loaded with either [^{14}C]-VCR or [^{14}C]-DXR. Naïve BALB/c mice (3/time point) were injected i.v. with a single bolus dose of 0.66 mg/kg liposomal VCR or 3 mg/kg liposomal DXR. At selected time points, mice were euthanised and blood, liver and spleen samples were analyzed for radioactivity. Data represents mean ± S.D of the percentage of injected drug (Panels A and B for DXR and VCR respectively) or phospholipid (Panels C and D for DXR or VCR respectively) in blood (n=3). Panels E and F gives the normalized drug:lipid ratios for DXR or VCR containing liposomes respectively. SL (●); SIL[αCD19] (▲); SIL[Fab'CD19] (■). For both DXR- and VCR-loaded liposomes, the area under the curve (AUC) of SIL[αCD19] was significantly lower than that of SL or SIL[Fab'CD19] *P<0.05, **P<0.01,***P<0.001 (n=3).

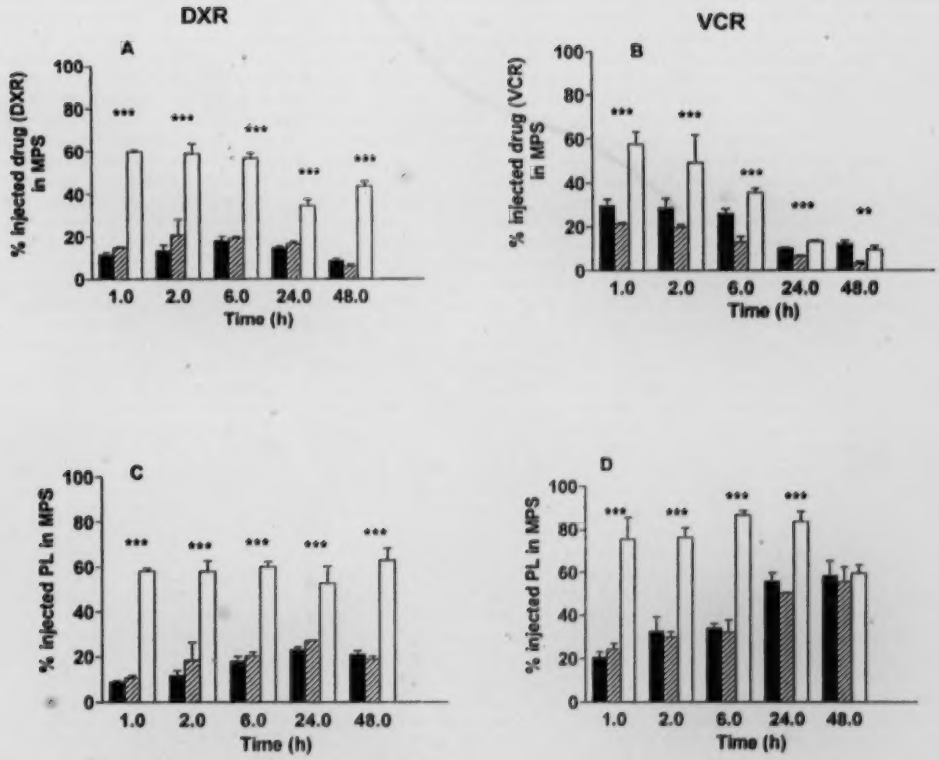

Figure 2.7 Biodistribution of drug-loaded liposomes to liver and spleen in naïve BALB/c mice.

Non-targeted liposomes loaded with VCR were composed of SM:Chol:mPEG (55:40:5, mol/mol). Targeted liposomes loaded with VCR were composed of SM:Chol:mPEG:Mal-PEG (55:40:4:1, mol/mol) and had 0.93 nmol binding domains of αCD19/μmol PL or 1.1 nmol Fab'CD19/μmol PL. Non-targeted liposomes loaded with DXR were composed of HSPC:Chol:mPEG (2:1:0.1). Targeted liposomes loaded with DXR were composed of HSPC:Chol:mPEG:Mal-PEG (2:1:0.08:0.02) and had 1.3 nmol binding domains of αCD19/μmol PL or 1.6 nmol Fab'CD19/μmol PL. Liposomes were radiolabeled with [^{3}H]-CHE and loaded with either [^{14}C]-VCR or [^{14}C]-DXR. Naïve BALB/c mice (3/time point) were injected i.v. with a single bolus dose of 0.66 mg/kg liposomal VCR or 3 mg/kg liposomal DXR. At selected time points, mice were euthanised and blood, liver and spleen samples were analyzed for radioactivity. Data represents mean ± S.D. of the percentage of injected drug (Panels A and B for DXR and VCR respectively) or phospholipid (Panels C and D for DXR or VCR respectively) in the MPS (liver + spleen) (n=3). SL (solid bars); SIL[αCD19] (open bars); SIL[Fab'CD19] (hatched bars). $^{**}P<0.01$,$^{***}P<0.001$ (n=3).

2.4.6 *In vivo* survival experiments in xenograft models of human B-lymphoma

Therapeutic experiments were performed in SCID mice bearing Namalwa cells. The first therapeutic study performed, compared free VCR and various formulations of VCR-loaded liposomes (VCR-SM-SL, VCR-SM-SIL[αCD19] and VCR-SM-SIL[Fab'CD19]). Treatments were given as a single dose of 2 mg/kg VCR (MTD reported in literature for VCR). With this dose, mice in all the treatment groups showed signs of adverse reactions, namely lack of energy and scruffy appearance for the initial 4-5 days. These effects were not observed after this time. The control / no-treatment group (PBS) mice had a mean survival time of 25.2 ± 3.0 days. Only one mouse in the free VCR group was sacrificed on day 55. Mice in all the other groups and the remaining 4/5 mice in the free VCR group were long-term survivors.

Two separate therapeutic experiments were then performed to compare VCR-loaded liposomes at a lower dosage of VCR (0.66 mg/kg). This dose approximates with the clinical human dose of 2 mg/m^2. Figures 2.8 and 2.9 gives the Kaplan-Meier plots for tumor-bearing mice treated with free VCR, or liposomal VCR formulations. All treatments significantly increased the survival of mice compared to controls (P<0.005) (Figures 2.8 and 2.9). VCR-SM-SL did not have a therapeutic advantage over free VCR in this model (P>0.5). On the other hand, both VCR-SM-SIL[αCD19] and VCR-SM-SIL[Fab'CD19] increased the survival of mice to a significantly greater extent than VCR-SM-SL (P<0.005) or free VCR (P<0.05) and

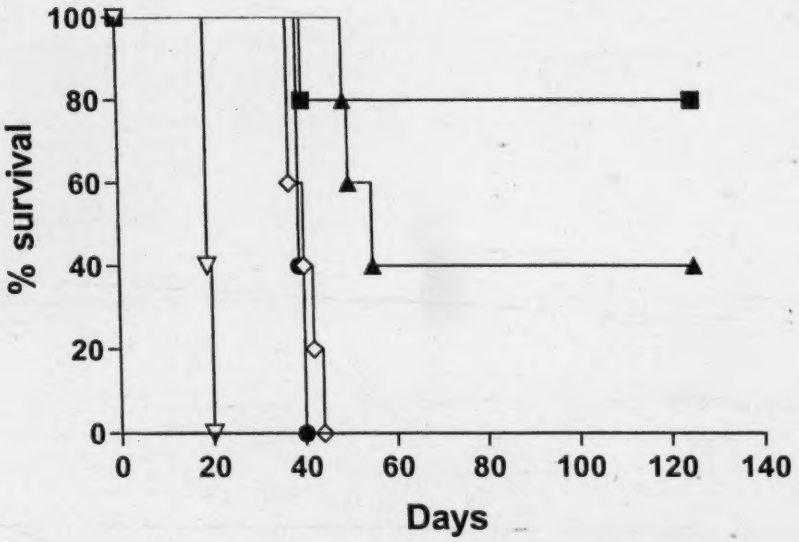

Figure 2.8 Therapeutic efficacy of free VCR or liposomal formulations of VCR in SCID mice injected with Namalwa cells.
SCID mice (5/group) were injected i.v. with 5 x 10^6 Namalwa cells in 0.2 ml at 24 h prior to i.v. treatment with a single bolus dose. Liposomes were composed of SM:Chol:mPEG (55:40:5) or SM:Chol:mPEG:Mal-PEG (55:40:4:1, mol/mol). Targeted liposomes had 0.71 nmol binding domains of αCD19/μmol PL or 0.44 nmol Fab'CD19/μmol PL. Free VCR or liposomal VCR was administered at a dose of 0.66 mg/kg. Saline control (▽); free VCR (◇); VCR-SM-SL (●); VCR-SM-SIL[αCD19]; (▲); VCR-SM-SIL[Fab'CD19] (■).

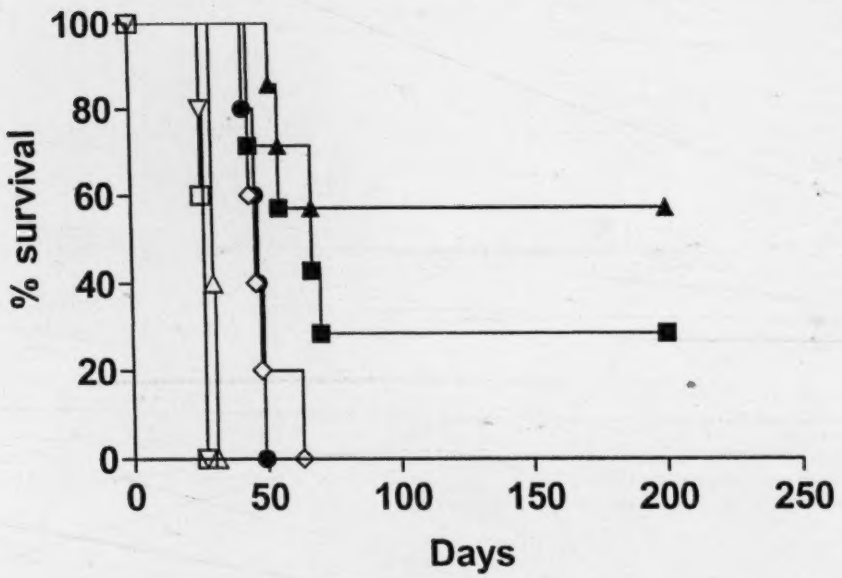

Figure 2.9 Therapeutic efficacy of free VCR or liposomal formulations of VCR in SCID mice injected with Namalwa cells.
SCID mice (5-7/group) were injected i.v. with 5 x 10^6 Namalwa cells in 0.2 ml at 24 h prior to i.v. treatment with a single bolus dose. Liposomes were composed of SM:Chol:mPEG (55:40:5) or SM:Chol:mPEG:Mal-PEG (55:40:4:1, mol/mol). Targeted liposomes had 1.0 nmol binding domains of αCD19/μmol PL or 1.1 nmol Fab'CD19/μmol PL. Free VCR or liposomal VCR was administered at a dose of 0.66 mg/kg. Saline control (▽); free VCR (◇); VCR-SM-SL (●); VCR-SM-SIL[αCD19] (▲); VCR-SM-SIL[Fab'CD19] (■); SM-SIL[αCD19] (△); SM-SIL[Fab'CD19] (□).

both treatments resulted in long-term survivors. Survival rates for VCR-SM-SIL[Fab'] were not significantly different from those of VCR-SM-SIL[αCD19] (P>0.05) (Figures 2.8 and 2.9). Mice did not show any signs of VCR toxicity in any of the treatment groups.

Mice injected with drug-free liposomes conjugated to Fab' fragments of antiCD19 (SM-SIL[Fab'CD19]) had survival times that were the same as controls, while mice injected with drug-free liposomes conjugated to whole Ab (SM-SIL[αCD19]) had modestly increased survival times (30 days versus 27 days, Figure 2.9). This suggests that αCD19 coupled to liposomes, at the concentrations tested, had mild cytotoxic effects through Fc-mediated complement-dependent cytotoxicity (CDC) and/or antibody-dependent cell-mediated cytotoxicity (ADCC).

Finally, a therapeutic study was performed to compare free or liposomal formulations of either VCR or DXR (Figure 2.10). All treatments except free DXR significantly increased the survival of mice compared to control (P<0.05). DXR-HSPC-SL resulted in higher survival times than free DXR (P<0.05), but VCR-SM-SL resulted in similar survival times to free VCR (P>0.05). Both VCR-SM-SIL[αCD19] and VCR-SM-SIL[Fab'CD19] increased the survival of mice significantly compared to VCR-SM-SL (P<0.005) or free VCR (P<0.05), and both treatments resulted in long-term survivors. Mice receiving either DXR-HSPC-SIL[Fab'CD19] or DXR-HSPC-SIL [αCD19] (at the MTD, 3 mg/kg) exhibited significantly increased survival times compared with either free DXR (P<0.005) or DXR-HSPC-SL (P<0.005). Of interest is the observation that, while the survival rates for VCR-SM-SIL[Fab'CD19]

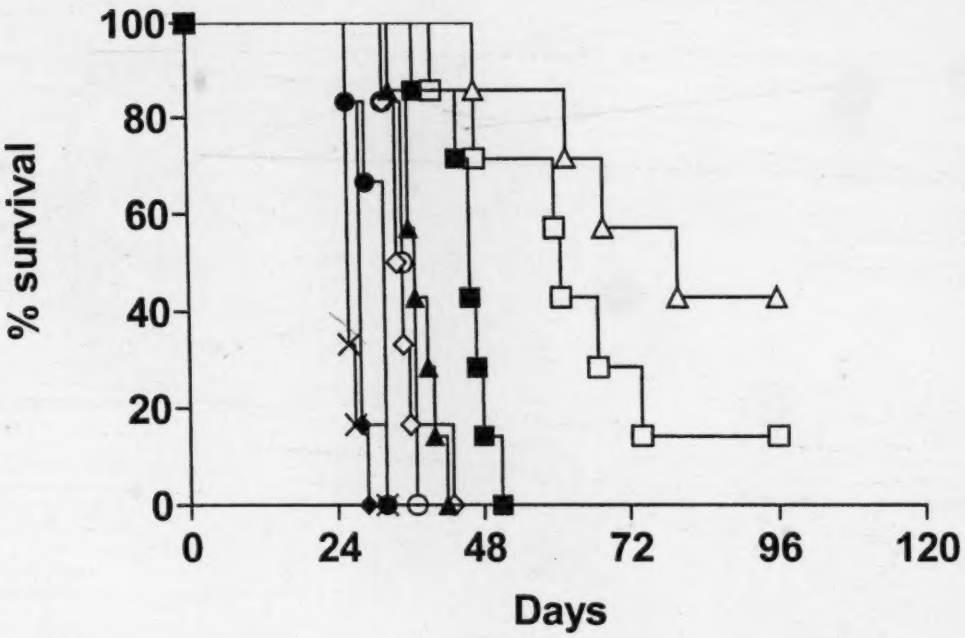

Figure 2.10 Therapeutic efficacy of free drugs or liposomal formulations of drugs in SCID mice injected with Namalwa cells.
SCID mice (6-7/group) were injected i.v. with 5 x 10^6 Namalwa cells in 0.2 ml PBS, 24 h prior to i.v. treatment with a single bolus dose of free or liposomal drugs. Non-targeted liposomes loaded with VCR were composed of SM:Chol:mPEG (55:40:5). Targeted liposomes loaded with VCR were composed of SM:Chol:mPEG:Mal-PEG (55:40:4:1, mol/mol) and had 0.82 nmol binding domains of αCD19/μmol PL or 0.89 nmol Fab'/μmol PL. Non-targeted liposomes loaded with DXR were composed of HSPC:Chol:mPEG (2:1:0.1). Targeted liposomes loaded with DXR were composed of HSPC:Chol:mPEG:Mal-PEG (2:1:0.08:0.02) and had 0.74 nmol binding domains of αCD19/μmol PL or 0.76 nmol Fab'/μmol PL. Free VCR or liposomal VCR was administered at a dose of 0.66 mg/kg and free DXR or liposomal DXR was administered at a dose of 3 mg/kg. Saline control (X); free VCR (◇); VCR-SM-SL (○); VCR-SM-SIL[αCD19] (△); VCR-SM-SIL[Fab'] (□); free DXR (◆); DXR-HSPC-SL (●); DXR-HSPC-SIL[αCD19] (▲); DXR-HSPC-SIL[Fab'] (■).

were not significantly different from those of VCR-SM-SIL[αCD19] (P>0.05), mice treated with DXR-HSPC-SIL[Fab'CD19] had significantly increased survival times compared to those receiving DXR-HSPC-SIL[αCD19] (P<0.005). Also, the results achieved with VCR-SM-SIL[αCD19] and VCR-SM-SIL[Fab'CD19] were superior to those obtained with their DXR-containing counterparts, in spite of the lower dose of VCR (0.66 mg/kg) administered relative to its MTD (approximately 2 mg/kg) in SCID mice.

2.5 DISCUSSION

This study compares, for the first time, the binding, cytotoxicity, pharmacokinetics and therapeutic outcome in the same model system for immunoliposomal formulations of two different anticancer drugs, i.e, VCR and DXR. These drugs work by different mechanisms of action, have different drug-related properties such as mechanisms of resistance and other physical and chemical properties, and different release rates from the liposomes. The study also compares the results for immunoliposomes targeted via αCD19 whole mAb compared to Fab' fragments.

We demonstrated specific binding for VCR and DXR formulations of both SIL[αCD19] and SIL[Fab'CD19] to $CD19^+$ human B-lymphoma cells. In these experiments every effort was made to ensure comparable number of antigen binding sites on the two types of formulations. Utilizing the thiol groups in the hinge region of Fab' fragments to couple them to liposomes avoids three problems; a) loss of Ab activity due to random thiolation of the protein, b) decreased binding due to random

orientation of the Abs at the liposome surface because of the random formation of thioether bonds between the whole mAbs and the liposome, and c) the potential for cross-linking of either the Abs or the liposomes. However, one may lose Ab avidity by coupling Fab' fragments, with only one antigen binding site, to liposomes instead of whole mAbs, with two binding sites. Since the binding of the SIL[Fab'CD19] was equivalent to, or higher than, that seen for the SIL[αCD19], this suggests that coupling of Fab' fragments to liposomes restores their avidity by restoring multivalent binding.

The K_d value for SM-SIL[αCD19] was similar to that found for HSPC-SIL[αCD19] (24), suggesting that the liposome composition, although affecting drug leakage rates (252), does not affect antigen binding of the immunoliposomes.

We observed higher levels of cell association of both SM-SIL[αCD19] and SM-SIL[Fab'CD19] to the Namalwa cells at 37°C compared to 4°C, where endocytosis does not occur. We hypothesize that this is due to binding of the SIL to the cells via the pan B-cell differentiation antigen, CD19, followed by receptor-mediated endocytosis and recycling of the epitope back to the cell surface where it will be available to partake in further binding and internalization events (24, 180, 181, 253).

Following internalization of the liposomal drug packages, we have published evidence that the breakdown of the drug-liposome package by lysosomal and endosomal enzymes and release of drug into the cytoplasm is responsible for the cytotoxic effect produced by targeted liposomal DXR (108, 254, 255). This

mechanism probably applies for the targeted liposomal VCR as well, since VCR-SM-SIL[αCD19] and VCR-SM-SIL[Fab'CD19] demonstrated significantly higher cytotoxicity against the Namalwa cells than VCR-SM-SL after a 1 h incubation, when release and uptake of the free drug into the cells is unlikely to play a major role in mediating cytotoxicity (Table 1A). At a longer time point (24 h), our leakage studies demonstrate that a significant portion of the drug would have already been released from VCR-containing liposomes. This may explain why no significant differences were observed between targeted or non-targeted VCR formulations and free drug at this time point. In the case of the DXR-loaded liposomes, the IC_{50} values of targeted liposomes were lower than for non-targeted liposomes after 24 h incubation (24), which can be explained by the significantly slower rate of leakage of DXR from liposomes composed of HSPC:Chol:mPEG (G.Charrois, manuscript in preparation).

Results from the pharmacokinetic and tissue distribution studies suggest that linkage of whole mAbs to the PEG terminus of liposomes using the Mal-PEG coupling method results in a random orientation of the Ab at the liposome surface, which leads to enhanced uptake of SIL[αCD19] by liver, spleen and other macrophages via Fc-receptor-mediated mechanisms. In contrast, linkage of Fab' fragments to the liposomes appeared to retard their uptake by macrophages, increasing their circulation half-lives. Previous studies from our laboratory have used a hydrazide-derivatized coupling lipid, Hz-PEG, to couple mAbs to liposomes (24). This method involves the oxidation of carbohydrate groups present in the Fc region of the Ab, forming a hydrazone bond between the whole mAb and the liposomes. This

coupling method resulted in increased circulation half-lives compared to the Mal-PEG coupling method; the half-lives were similar to those found for the Fab'-coupled liposomes (24). This further supports the idea that random orientation of Ab molecules on the liposome surface, such as occurs with the Mal-PEG coupling method, leads to an increase in the numbers of exposed Fc regions, resulting in enhanced binding and Fc-receptor-mediated uptake of the immunoliposomes into cells of the MPS. Coupling methods that prevent exposure of the Fc region (Hz-PEG or coupling of Fab' rather than whole mAbs), result in immunoliposomes that have clearance rates more similar to non-targeted liposomes (112). Because therapeutic outcomes are correlated with increased circulation times, strategies that result in decreased clearance of liposomes have been predicted to result in increased survival times (236).

We performed therapeutic studies in a xenograft model of human B-cell lymphoma at a VCR dose approximating the clinical dose in humans, and a DXR dose that is the maximum tolerated dose in SCID mice. Our therapeutic results demonstrated that targeted formulations containing either VCR or DXR were both superior to non-targeted liposomes or to the free drugs. Although the rate of clearance of SIL[αCD19] liposomes from the circulation was significantly higher than that of SLs, mice injected with either VCR-SM-SIL[αCD19] or DXR-HSPC-SIL[αCD19] had significantly increased life spans compared to mice injected with VCR-SM-SL or DXR-HSPC-SL, respectively. Since binding and internalization of αCD19 is a rapid process, our results suggest that SIL[αCD19] bound to, and were

internalized by, the target cells more rapidly than they were cleared from the circulation into macrophages. However, the longer circulation times and the improved antigen accessibility of the SIL[Fab'CD19] probably played an important role in further improving the therapeutic outcome of mice injected with DXR-HSPC-SIL[Fab'CD19] over mice injected with DXR-HSPC-SIL[αCD19].

Two drawbacks of VCR-loaded liposomes in the past were their fast rates of drug release and their relatively rapid rate of clearance from circulation (51). Insertion of PEG-DSPE conjugates onto the surface of VCR-loaded liposomes can increase the circulation time of the liposomes but it also increases the leakage rate for the drug (252). As a result, it was shown previously that PEG-containing liposomes loaded with VCR had no therapeutic advantages over those lacking PEG (252). Our experiments showed that linking Abs to the PEG-terminus of VCR-loaded liposomes did not increase the rate of release of VCR over that seen for non-targeted liposomes, but it significantly improved the therapeutic outcome. This is probably because the targeted formulations could rapidly deliver their drug to the target cells, before their contents were released.

No difference was observed between VCR-SM-SIL[αCD19] and VCR-SM-SIL[Fab'CD19], unlike the superior performance of DXR-HSPC-SIL[Fab'CD19] over DXR-HSPC-SIL[αCD19]. We believe that this is because the rate of release of VCR from the liposomes is faster relative to their rate of plasma clearance, and hence increasing their circulation times would not result in significantly more drug being delivered to the target cells. In other words, delivering drug-depleted liposomes to

the cells is not expected to have a therapeutic advantage. On the other hand, for DXR-containing immunoliposomes, which release their drug slowly on the time scale of plasma clearance, long circulation times would be expected to increase the amount of drug delivered to the target cells over time. However our speculations are based on the experimental results with only two immunoliposomal drugs with different drug release rates. In future, rigorous experiments need to be performed comparing immunoliposmal drugs having a spectrum of different drug release rates to further comment on these results.

We observed that free VCR, the non-targeted formulations and the targeted VCR-containing formulations resulted in better therapeutic responses than each of the corresponding DXR-containing formulations ($P<0.005$). It appears that the Namalwa cells are more sensitive to VCR than to DXR. Treatment of the tumor-bearing mice with free VCR resulted in a significant increase in survival relative to untreated controls, but this was not observed for free DXR relative to controls. Free DXR has little or no effect in this lymphoma model.

Another explanation may involve the differential rate of release from liposomes of VCR and DXR and their different mechanisms of action. These drugs are cell cycle dependent and cell cycle independent, respectively. VCR acts by destabilizing microtubules, resulting in arrest of cells in the metaphase. Since cancer cells are not normally synchronized with respect to the cell cycle, exposure of the cancer cells to VCR for a period of time as long as or longer than the cell cycle would allow cells in different phases of cell cycle to enter metaphase and be susceptible to

the action of the drug. If the rate of release of VCR from the targeted liposomes is on a similar time scale as the doubling time of the cells, this may result in the cells being exposed to high concentrations of drug as they go through the M phase of the cell cycle and to good levels of cytotoxicity. Both *in vitro* studies (226, 256) and clinical trials (257, 258) have established the correlation between increased duration of VCR exposure to neoplastic cells and improved responses.

DXR, on the other hand is not a cell-cycle specific drug. It acts by multiple mechanisms including inhibition of topoisomerase II, resulting in DNA strand breaks, inhibition of DNA and RNA polymerase, oxidative DNA damage and increasing ceramide levels leading to apoptosis. Hence, we can predict the cytotoxicity of DXR would be highest if the drug were delivered rapidly and in high concentrations to the target cells. The slow rate of release of DXR from the targeted liposomes, both before and after endocytosis, means that there may be a delay in exposure of the intracellular sites of action to cytotoxic levels of drug, resulting in delayed cell kill and in lower overall cytotoxicity. We have previously published data showing that the rate of intracellular release of DXR from internalized formulations of DXR-HSPC-SIL[αCD19] was very slow, with appearance of DXR in the nucleus of Namalwa cells taking from 24 h to 48 h (108, 255). In support of this concept, we have previously shown that engineering the targeted liposomes for increased rates of intracellular release of entrapped drugs from endosomes leads to increased cytotoxicities of liposomal formulations of DXR (254, 255). However, again these speculations are based on the results obtained from experiments with only two drugs

that work via different mechanisms of action. Future experiments should compare immunoliposomal formulations of other schedule-dependent drugs such as 5-fluorouracil, methotrexate, topotecan with other schedule-independent drugs such as cisplatin and daunorubicin to further refine these results.

Besides acting via different mechanisms of action, VCR and DXR have other differences in drug-related properties like mechanisms of drug resistance, potencies and other physical and chemical properties. Any of these factors could be responsible for the improved therapeutics observed for VCR-containing immunoliposomes over DXR-containing immunoliposomes. Further, in the experiments reported in chapter 4, we observe synergistic cytototoxic effects of DXR- or VCR-containing liposomes with anti-CD19. The synergistic effects between the encapsulated drug and the coupled antibody may be due to different mechanisms for DXR and VCR and this may also account for the differences in the results observed for DXR- and VCR-containing immunoliposomes.

This study has evaluated the application of VCR- and DXR-loaded immunoliposomes in a B-cell malignancy where the target cells either reside in the vasculature or appear to be readily accessible from the vasculature. Our responses in this haematological model are significantly improved over responses achieved in advanced solid tumor models in our laboratory, e.g. Caov.3, a human ovarian cancer cell line, 4T1-MUC1, a MUC1-expressing mouse mammary carcinoma cell line or NCI-H69, a small cell lung cancer (143, 144, 150). When well-developed tumors in these models were treated with drug-loaded liposomes targeted with specific whole

Abs or peptides, no significant reduction of tumor growth was observed compared to non-targeted liposomes. Explanations for this failure to observe comparable results in the developed solid tumor models compared to the haematological models are several. SIL, according to the 'binding site barrier' hypothesis, will bind to the first target cells they encounter, which will retard their diffusion through the tumor and limit their therapeutic effects (131). In addition, whole Abs may induce Fc receptor-mediated endocytosis of the targeted liposomes by macrophages residing around the tumor cells, lowering the amount of drug that reaches the target cells. Further, the more rapid clearance of liposomes coupled to whole mAbs from the circulation may limit their ability to localize to tumors. However, another solid tumor model system, using anti-HER2 Fab' fragments as targeting agents against a highly overexpressing HER2 breast cancer cell line, has shown improved therapeutic efficacies of immunoliposomes over non-targeted liposomes in solid tumors (27, 28). Increased tumor localization of the Fab'-targeted liposomes compared to non-targeted liposomes could not be demonstrated in this model despite the long circulation time of the Fab'-targeted liposomes, so the explanation for the improved results may lie in the very high antigen density of the target cells and the rapid internalization of the targeted liposomal drugs (28).

In conclusion, we have demonstrated that Ab-mediated targeting of VCR- or DXR-loaded liposomes to an internalizing epitope is a promising approach to the treatment of B-cell malignancies. We compared the therapeutic effectiveness of two

different liposome formulations containing two anticancer drugs having different drug-related properties, targeted using either whole Abs or Fab' fragments. Fab' fragments are expected to decrease the incidence of HAMA when used in human therapy. We anticipate the use of even smaller Ab fragments, e.g., scFv,instead of whole mAbs or Fab' fragments, and the development of fully human Abs as liposomal targeting moieties will overcome the final obstacles to clinical trials for these formulations. The excellent results that we obtained in our human B-lymphoma xenograft model for targeted formulations of liposomal VCR suggests that these formulations should be evaluated for therapeutic responses in human lymphoma.

CHAPTER 3

Internalizing antibodies are necessary for improved therapeutic responses of DXR-containing immunoliposomes

Cancer Res., *62:* 7190-7194, 2002

3.1 ABSTRACT

We have compared two populations of immunoliposomal doxorubicin (DXR), each targeted against a different epitope, either internalizing (CD19) or non-internalizing (CD20), which are both expressed on the surface of the human B-lymphoma cell line (Namalwa). Anti-CD19-targeted liposomes were rapidly internalized into Namalwa cells, while those targeted with anti-CD20 were not internalized. Similar *in vitro* binding and cytotoxicity was observed for anti-CD19-targeted and anti-CD20-targeted liposomal formulations of DXR. Therapeutic experiments were performed in SCID mice inoculated i.v. with Namalwa cells. Administration of single i.v. doses of DXR-loaded anti-CD19-targeted liposomes resulted in significantly greater survival times than either DXR-loaded anti-CD20-targeted liposomes or DXR-loaded non-targeted liposomes. The therapeutic advantage of targeting internalizing vs. non-internalizing epitopes has been directly demonstrated.

3.2 INTRODUCTION

Antibody (Ab)-mediated targeting of liposomal anticancer drugs to epitopes expressed at the surface of cancer cells is being investigated as a means of increasing the site-specific delivery of drug to cancer cells (2, 24, 27, 28, 112). Either internalizing or non-internalizing epitopes are possible targets for liposomal anticancer drugs conjugated to monoclonal antibodies (immunoliposomes), but the mechanism of delivery of the drug into the cell is different in each case. When targeted liposomal drugs bind to non-internalizing epitopes, liposome contents are

released over time at or near the cell surface, and the released drug will enter the cell by passive diffusion or by normal transport mechanisms. Although increased concentrations of drug may be achieved at the cell surface by this mechanism, it can be argued that, in the dynamic *in vivo* environment, the rate of diffusion and redistribution of the released drug away from the cell will exceed the rate at which the drug enters the cell, particularly for drugs such as DXR, which have a large volume of distribution. When targeted liposomal drugs bind to internalizing epitopes, they trigger receptor-mediated uptake of immunoliposomal drug packages into the cell interior where the drug contents are released subsequent to liposomal degradation by lysosmal and endosomal enzymes. Hence, one can hypothesize that targeting to internalizing epitopes should result in delivery of higher concentrations of drug to the cell interior than targeting to non-internalizing epitopes, resulting in improved therapeutic outcomes for liposomal drugs such as DXR that are resistant to degradation by the enzyme-rich, low pH environment of endosomes and lysosomes. Some indirect experimental evidence supports this hypothesis. Liposomes targeted to internalizing receptors have demonstrated better therapeutic responses in some tumor models (24, 27, 28). In other tumor models, targeted liposomes did not improve therapeutic responses over non-targeted liposomes, which was hypothesized to be due to the lack of internalization of the drug-liposome package into the cells (104, 105). This study aims, in a B-lymphoma model system, to verify directly the hypothesis that internalizing epitopes make better targets than non-internalizing epitopes for liposomal anticancer drugs. The binding, internalization, cytotoxicity and therapeutic

responses of immunoliposomes targeted against CD19 (internalizing epitope) were compared with those targeted against CD20 (non-internalizing epitope). Significant improvements in therapeutic responses were associated with the liposomes targeted against the internalizing epitope.

3.3 MATERIALS AND METHODS

3.3.1 Materials

Hydrogenated soy phosphatidylcholine (HSPC) and methoxypolyethylene glycol) (MW 2000), covalently linked to distearoylphosphatidylethanolamine (mPEG) , were generous gifts from ALZA Pharmaceuticals, Inc. (Mountain View, CA). Cholesterol (Chol) was purchased from Avanti Polar Lipids (Alabaster, AL). Maleimide-derivatized polyeythylene glycol (MW 2000)-DSPE (Mal-PEG) was custom synthesized by Shearwater Polymers, Inc. (Huntsville, AL). Nuclepore® polycarbonate membranes (pore sizes: 0.2, 0.1, and 0.08 μm) were purchased from Northern Lipids (Vancouver, BC). 2-Iminothiolane (Traut's reagent) and 3-[4,5-dimethylthiazole-2-yl]-2,5-diphenyltetrazolium bromide (MTT) were purchased from Sigma Chemical Co. (St. Louis, MO). Rhodamine dihexadecanoyl-phosphatidylethanolamine (Rh-PE) was obtained from Molecular Probes (Eugene, OR). RPMI 1640 media (without phenol red), penicillin-streptomycin and fetal bovine serum (FBS) were obtained from Life Technologies (Burlington, ON). Iodobeads were purchased from Pierce (Rockford, IL) and BioRad Protein Assay Reagent from BioRad Laboratories (Mississauga, ON). Sephadex G-50, Sepharose CL-4B, aqueous counting scintillant (ASC) were purchased from Amersham

Pharmacia Biotech (Baie d'Urfe, QC). Cholesterol- [1,2-^{3}H-(N)]-hexadecyl ether ([^{3}H]-CHE), 1.48-2.22 TBq/mmol, and ^{125}I-NaI (185 MBq) were purchased from Mandel Scientific (Mississauga, ON). Goat anti-mouse-FITC IgG and goat anti-human-FITC IgG were purchased from Sigma Chemical Co. (St. Louis, MO). All other chemicals were of analytical grade purity.

3.3.2 Animals, antibodies and cell lines

Six-to-eight week-old female CB17 severe compromised immunodeficient (SCID) mice were purchased from Taconic Farms (Germantown. NY) and housed in the virus antigen-free unit of the Health Sciences Laboratory Animal Services, University of Alberta. All experiments were approved by the Health Sciences Animal Policy and Welfare Committee of the University of Alberta.

The murine monoclonal antibody (mAb) whole anti-CD19 IgG_{2a} (αCD19) was produced from the FMC63 murine hybridoma (245) and purified as described previously (74). Rituximab, a chimeric IgG_1 whole mAb, was used as a source of anti-CD20 (αCD20). Iodinated Abs were used to measure coupling efficiencies and to determine the amount of mAb attached to the liposomes (24). The human Burkitt's lymphoma cell line, Namalwa (ATCC CRL 1432) was purchased from American Type Culture Collection, Rockville, MD and cultured in suspension in a humidified 37°C incubator with a 5% CO_2 atmosphere in RPMI 1640 media supplemented with 10% (v/v) fetal bovine serum (FBS), penicillin G (50 units/ml), and streptomycin sulfate (50 μg/ml). For experiments, only cells in the exponential phase of cell growth were used.

Immunophenotyping of Namalwa cells using single color flow cytometry was performed to examine the cell surface expression of CD19 and CD20 epitopes. Namalwa cells (1×10^6) were first stained with 10 μg primary mAb followed by 20 μl of a 1:32 dilution of goat anti-mouse-FITC IgG for αCD19 or goat anti-human-FITC IgG for αCD20. Cell associated fluorescence was analyzed on a Becton-Dickinson FACScan using Lysis II software (Beckton Dickinson, San Jose, CA). FITC-fluorecent markers were excited with an argon laser (488nm) and emitted fluorescence was detected using a 530nm band pass filter.

3.3.3 Preparation of liposomes

Non-targeted liposomes, to be loaded with DXR for cytotoxicity and therapeutic studies or radiolabeled with [^{3}H]-CHE for binding studies, were composed of HSPC:Chol:mPEG at a 2:1:0.1 molar ratio (HSPC-SL) and targeted liposomes were composed of HSPC:Chol:mPEG:Mal-PEG at a 2:1:0.08:0.02 molar ratio (HSPC-SIL). For confocal microscopy studies, 0.1 mol% of Rh-PE was incorporated into the lipid mixture. Liposomes were prepared by hydration of thin films, as described previously and were extruded to mean diameter in the range of 100 ± 10nm (108). DXR was loaded into liposomes using the ammonium sulfate loading method (50).

αCD19 mAb or αCD20 mAb were coupled to the terminus of the Mal-PEG at 2000:1 (lipid:protein). For cell association studies, liposomes were coupled at 1000:1 (lipid:protein) molar ratios, using the coupling procedure previously described (60). Briefly, mAb (10 mg/ml) was incubated with 2-Iminothiolane in O_2-free HEPES-

buffered saline (HBS), pH 8.0, at a ratio of 20:1 mol/mol for 1 h at room temperature in order to thiolate the amino groups. At the end of the incubation, the sample was chromatographed on a Sephadex G-50 column, equilibrated with O_2-free HBS (pH 7.4) and immediately incubated with liposomes in an O_2-free environment overnight with continuous stirring. To assess coupling efficiency of the Abs, a trace amount of [^{125}I]-labeled αCD19 or αCD20 was added to the unlabeled Ab before thiolation. Ab coupling is expressed as μg mAb / μmol phospholipid (PL). A coupling efficiency of 80-90% for either Ab could routinely be achieved by this procedure and particular attention was taken to ensure that similar Ab densities (within ± 10%) occurred at the surface of either type of immunoliposome.

3.3.4 *In vitro* binding and cytotoxicity of immunoliposomes

In vitro cell association of immunoliposomes labeled with [^{3}H]-CHE was determined, as described previously, at both 37°C and 4°C, i.e., permissive and non-permissive temperatures for endocytosis, respectively (24). Briefly, liposomes (HSPC-SL, HSPC-SIL[αCD19] or HSPC-SIL[αCD20]) were radiolabeled with [^{3}H]-CHE and incubated with 1 x 10^6 Namalwa cells (in FACS tubes) at PL concentrations ranging from 0.1 mM to 1.6 mM PL (in triplicate) for 1 h. Cells were then washed twice with cold PBS to remove unbound liposomes and the amount of [^{3}H]-CHE associated with cells was determined. Cell association (pmoles PL / 1 x 10^6 cells) was calculated from the specific activity of the liposomes. Specific binding was determined by subtracting binding due to non-targeted liposomes from the total binding.

The *in vitro* cytotoxicities of free DXR, free Abs and various liposomal formulations of DXR were determined using the MTT tetrazolium dye reduction assay as described previously (24) and in chapter 2. Results are expressed as IC_{50}, which was obtained graphically using SlideWrite software (Advanced Graphics Software, Encinitas CA).

For confocal studies, Namalwa cells (1×10^6) were incubated with Rh-PE-labeled liposomes either non-targeted or targeted via αCD19 or αCD20 mAbs for 1 h at 37°C or 4°C. Cells were then washed twice with cold PBS to remove unbound liposomes and resuspended in ~0.1 ml of PBS. Cells were allowed to adhere to poly-L-lysine-coated slides prior to mounting with Permaflor (Lipshaw Immunon, Pittsburgh, PA). Cells were then visualized on a ZEISS LSM 510 confocal microscope consisting of a 100W HBO mercury burner (for direct observation) and a He Ne laser with excitation at 543 nm. Emission was collected with LP560. The pinhole was adjusted to obtain 1.0 μm optical sections and images (512 x 512 pixels) were collected.

3.3.5 *In vivo* survival experiments

SCID mice (5-7/group) were injected i.v. in the tail vein with 5×10^6 Namalwa cells in 0.2 ml PBS. Treatments were given as a single bolus i.v. dose of 3 mg DXR/kg as free DXR, DXR-HSPC-SL, DXR- HSPC-SIL[αCD19] or DXR-HSPC-SIL[αCD20]. The density of αCD19 or αCD20 on the liposomes was 76 μg/μmol PL (40 mAb/liposome equaling 80 antigen binding sites) or 70 μg/μmol PL (37 mAb/liposome), respectively; i.e. each mouse received 15 μg αCD19 or 13 μg

αCD20 conjugated to the DXR-containing immunoliposomes. As controls, the same amounts of free mAbs were administered, and empty immunoliposomes also contained comparable doses of Ab and PL. Mice were monitored daily and euthanised when they developed hind leg paralysis.

3.3.6 Statistical analysis

Comparisons of cellular binding and uptake, cytotoxicities and therapeutic efficacies were done using one-way analysis of variance with InStat software (GraphPad software, Version 3.0, San Diego, CA). The Tukey post-test was used to compare means. Differences were considered significant at a *P* value of less than 0.05.

3.4 RESULTS AND DISCUSSION

3.4.1 Immunophenotyping of Namalwa cells

Immunophenotyping of Namalwa cells demonstrated that this cell line had a high expression of both of the B-cell differentiation antigens CD19 and CD20; CD20 had a mean fluorescence intensity (MFI) of 259 vs. an MFI of 175 for CD19 against a background MFI of 15-18, indication that CD20 had a slightly higher expression. The % population of gated cells that expressed these epitopes was 99.9 and 99.1 for CD19 and CD20, respectively. CD20 seemed to have a more heterogeneous distribution than CD19 with a coefficient of variation (CV) for CD20 of 78 and for CD19 of 45. The CV of unstained cells was 44.

3.4.2 *In vitro* cell association and confocal experiments

Ab-mediated specific targeting effect of both HSPC-SIL[αCD19] and HSPC-SIL[αCD20] could be demonstrated *in vitro* (Figure 3.1A). Binding of HSPC-SIL[αCD19] to Namalwa cells saturated at a PL concentration of approximately 0.4 mM (Figure 3.1B). Binding of HSPC-SIL[αCD20] had not reached saturation by a dose of 1.6 mM PL, which could be due to the higher expression of the CD20 epitope on the Namalwa cells and/or higher avidity of SIL[αCD20] for Namalwa cells than SIL[αCD19] (Figure 1B). Cellular association of SIL[αCD19] with cells at 37°C was higher than at 4°C (Figure 3.1A). This was probably due to binding of the SIL[αCD19] to the cells via the pan B-cell differentiation antigen, CD19, followed by receptor-mediated endocytosis and recycling of the epitope back to the cell surface where it was available to partake in further binding and internalization events (24, 180, 181, 253). No significant difference in cellular association of SIL[αCD20] to cells at 37°C vs. 4°C was observed.

Confocal fluorescence microscopy studies using Rh-PE-labeled liposomes showed that, after 1 h incubation at 4°C, both SIL[αCD19] and SIL[αCD20] were largely found on the cell surface, suggesting that both types of immunoliposomes could efficiently bind to the Namalwa cells (Figure 3.3). After 1 h incubation at 37°C, SIL[αCD20] remained largely on the cell surface, which is consistent with its poor ability to internalize (Figure 3.3 and Figure 3.4). SIL[αCD19], on the other hand, showed evidence of internalization, with aggregates of red fluorescence

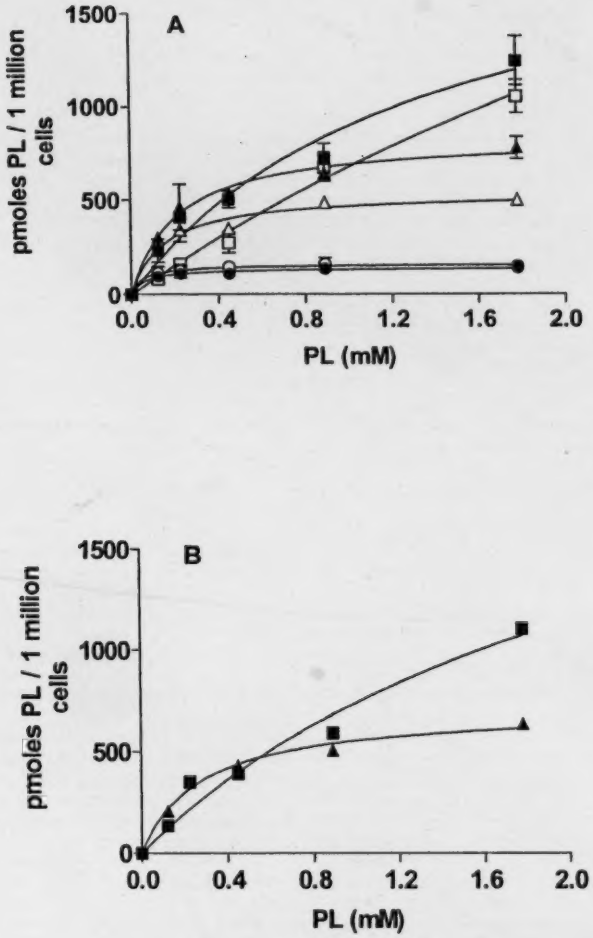

Figure 3.1 ***In vitro*** **cellular association of liposomes to Namalwa cells as a function of concentration at 37°C (closed symbols) or 4°C (open symbols).** Non targeted liposomes HSPC-SL(●,○); Targeted HSPC-SIL[αCD19] (▲,△); Targeted HSPC-SIL[αCD20] (■,□). Liposomes were composed of HSPC:Chol: mPEG (2:1:0.1) or HSPC:Chol: mPEG:Mal-PEG (2:1:0.08:0.02) and were labeled with [^{3}H]CHE. Liposomes were incubated with 1 million Namalwa cells after which the cells were washed with cold PBS to remove the unbound liposomes. The concentration of mAb on both SIL[αCD19] and SIL[αCD20] was 110 μg mAb/μmol PL (58 mAb/liposome). Data are expressed as pmoles PL / 1 million cells. Each point is an average of 3 replicates ± S.D. from one representative experiment. (**A**) Total cellular association of liposomes (**B**) Specific cell association of HSPC-SIL[αCD19] or HSPC-SIL[αCD20].

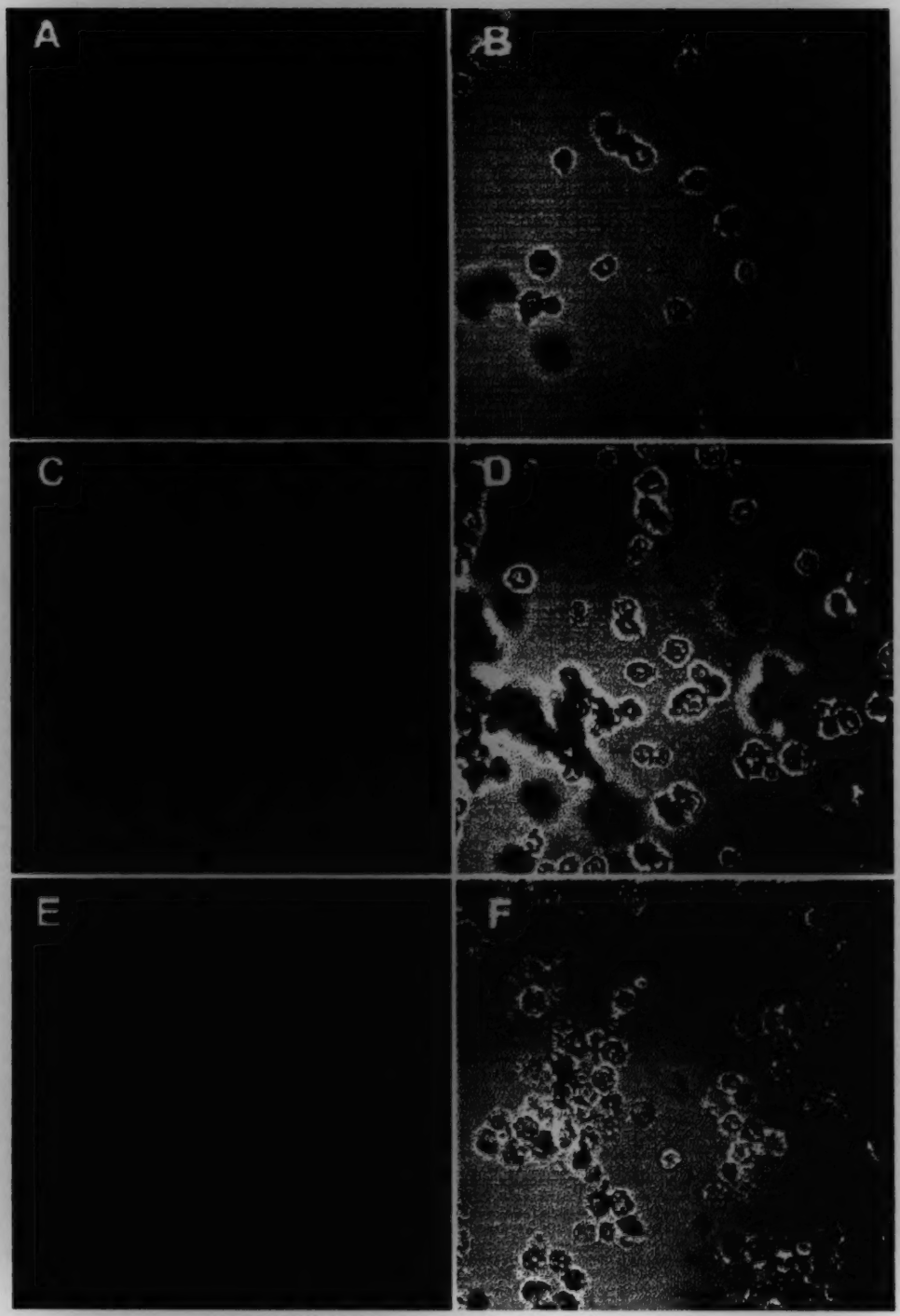
A
B
C
D
E
F

Figure 3.2 Confocal micrographs of Namalwa cells treated with Rh-PE-labeled immunoliposomes at 37°C.
Namalwa cells (1 x 10^6) were incubated with different liposome formulations, composed of HSPC:Chol:mPEG (2:1:0.1) or HSPC:Chol:mPEG:Mal-PEG (2:1:0.08:0.02) labeled with Rh-PE, at 37°C. The concentration of mAb on HSPC-SIL[αCD19] and HSPC-SIL[αCD20] was 74 and 85 μg mAb/μmol PL, respectively. Images show fluorescence images (A, C, E) or superimposed fluorescence and differential interference contrast (DIC) images (B, D, F). HSPC-SL (A, B); HSPC-SIL[αCD19] (C, D); HSPC-SIL[αCD20] (E, F). *Bar*, 20 μm.

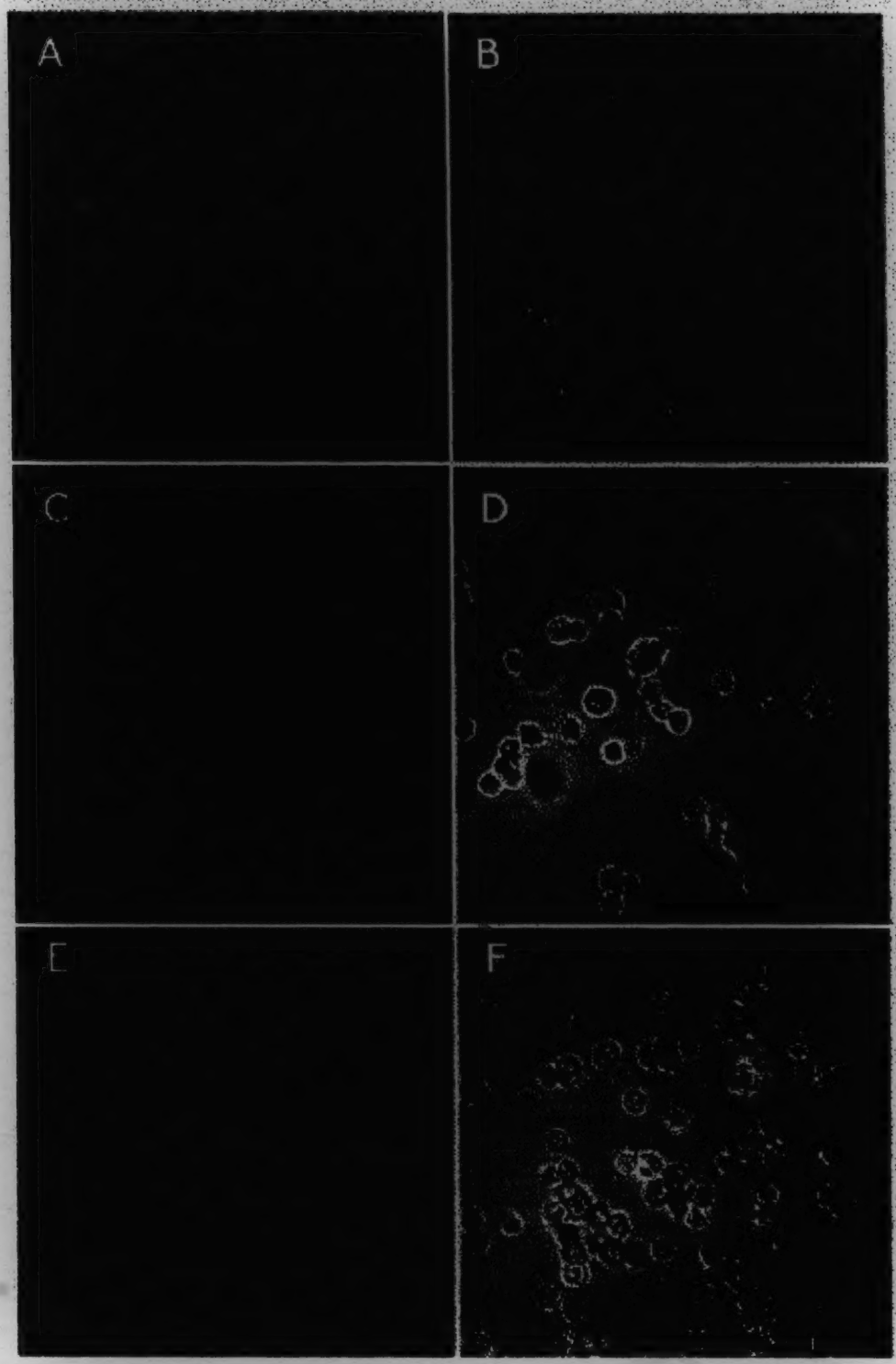
A
B
C
D
E
F

Figure 3.3 Confocal micrographs of Namalwa cells treated with Rh-PE-labeled immunoliposomes at 4°C.
Namalwa cells (1 x 10^6) were incubated with different liposome formulations, composed of HSPC:Chol:mPEG (2:1:0.1) or HSPC:Chol:mPEG:Mal-PEG (2:1:0.08:0.02) labeled with Rh-PE, at 4°C (non-permissive for endocytosis). The concentration of mAb on HSPC-SIL[αCD19] and HSPC-SIL[αCD20] was 74 and 85 μg mAb/μmol PL, respectively. Images show fluorescence images (A, C, E) or superimposed fluorescence and differential interference contrast (DIC) images (B, D, F). HSPC-SL (A, B); HSPC-SIL[αCD19] (C, D); HSPC-SIL[αCD20] (E, F). *Bar*, 20 μm.

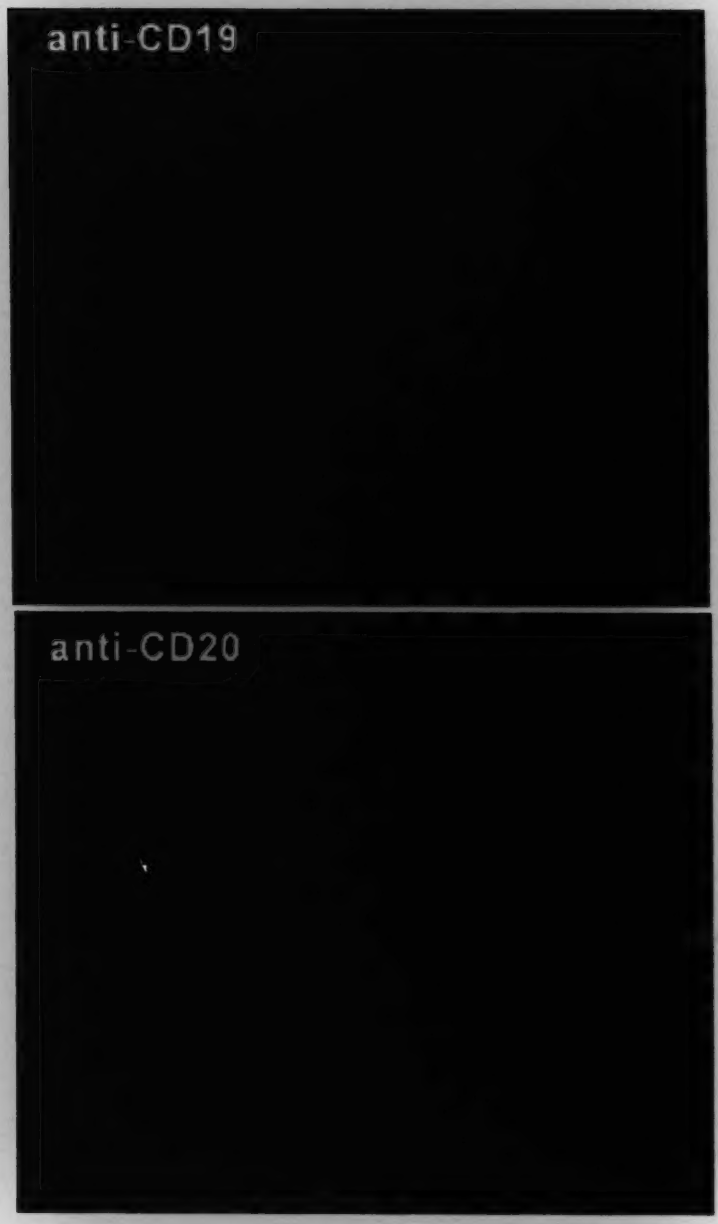

Figure 3.4 Enlarged confocal micrographs of anti-CD19 (top) vs. anti-CD20 (bottom) HSPC-SIL at 37°C.

distributed throughout the cytoplasm (Figure 3.2 and Figure 3.4). Little fluorescence was observed in the cells incubated with non-targeted liposomes consistent with their low levels of non-selective binding to the cells.

3.4.3 *In vitro* cytotoxicity studies

Results from *in vitro* cytotoxicity assays demonstrated that liposomes conjugated to either αCD19 or αCD20 had similar cytotoxicities against Namalwa cells and both had significantly higher cytotoxicities than non-targeted liposomes at an incubation time of 1 h (Table 3.1). Neither drug-free immunoliposomes, nor free Abs displayed any cytotoxicity against Namalwa cells at the concentrations tested, suggesting that these Abs were unable to signal cell growth arrest or death via cell-signaling mechanisms *in vitro* at the concentrations present on the immunoliposomes. The cytotoxicity of DXR-HSPC-SIL[αCD19] was most likely due to the receptor-mediated endocytosis of the drug-loaded liposomes into the cells and release of the drug in the cell interior, as previously reported (108, 255). DXR-HSPC-SIL[αCD20] on the other hand, probably produced its cytotoxicity by release of DXR from the bound liposomes at the cell surface and uptake of the released drug into the cells. In cell culture dishes there is no opportunity for released drug to redistribute away from the cells, unlike the *in vivo* situation.

3.4.4 *In vivo* survival studies

Table 3.2 gives the survival times for tumor-bearing mice inoculated with Namalwa cells and treated with immunoliposomal formulations of DXR and a variety of control treatments. The most interesting observation is that treatment of mice with

Table 3.1 Cytotoxicity of various treatments against Namalwa cells.
$CD19^+/CD20^+$ Namalwa cells (5 x 10^4/well) were plated in 96-well plates and incubated with increasing concentrations of free DXR, liposomal DXR, free Abs or drug-free liposomes for 1 h or 24 h. Cells were then washed with phosphate-buffered saline and incubated further with fresh medium for a total of 48 h after which a MTT (tetrazolium) assay was performed. The liposomes were composed of HSPC:Chol:mPEG (2:1:0.1) or HSPC:Chol:mPEG:Mal-PEG (2:1:0.08:0.02). The data are pooled from 3-4 individual experiments and are expressed as mean IC_{50} in μM ± S.D. Ab concentrations of αCD19 or αCD20 on liposomes in individual experiments were within ± 10% and ranged from 45 to 70 μg mAb/μmol PL (24 to 37 mAb/liposome).

Formulation (compound for which the IC_{50} is given)	IC_{50}, 1h	IC_{50}, 24h
free DXR (μM DXR)	0.4 ± 0.3	0.08 ± 0.06
DXR- HSPC-SL (μM DXR)	60 ± 0.3	0.6 ± 0.2
DXR- HSPC-SIL[αCD19] (μM DXR)	3 ± 0.7	0.4 ± 0.2
DXR- HSPC-SIL[αCD20] (μM DXR)	5 ± 0.2	0.6 ± 0.2
free αCD19 (μM mAb)	>6.7	>6.7
free αCD20 (μM mAb)	>6.7	>6.7
Drug-free HSPC-SL (μM PL)	>900	>900
Drug-free HSPC-SIL[αCD19] (μM PL)	>870	>870
Drug-free HSPC-SIL[αCD20] (μM PL)	>810	>810

DXR-HSPC-SIL[αCD19] resulted in significantly increased life-spans relative to those treated with DXR-HSPC-SIL[αCD20] ($P<0.001$). This observation directly supports the hypothesis that internalizing epitopes make better targets than non-internalizing epitopes for immunoliposomal drugs.

We have published evidence that, following internalization of the liposomal drug packages, the breakdown of the drug-liposome package by lysosomal and endosomal enzymes and release of drug into the cell interior is responsible for the cytotoxic effect produced by targeted liposomal DXR (108, 254, 255). The higher concentrations of drugs delivered into the cell interior by this mechanism is the most probable reason for the increased life-spans observed for immunoliposomes directed against internalizing vs. non-internalizing epitopes. The drug released at the cell surface from DXR-HSPC-SIL[αCD20], on the other hand, will be rapidly redistributed away from the target cells *in vivo* and the lower drug concentrations delivered to the target cells, we hypothesize, is the reason for the lesser therapeutic effect. DXR-HSPC-SIL[αCD19] also increased the survival of mice to a significantly greater extent compared to DXR-HSPC-SL ($P<0.001$) or free DXR ($P<0.001$). No significant difference was observed between mice treated with DXR-HSPC-SIL[αCD20] and free DXR ($P>0.05$). Mice treated with DXR-HSPC-SIL[αCD20] had survival times that were marginally different from DXR-HSPC-SL ($P<0.05$).

Another explanation for the improved therapeutic responses of DXR-HSPC-SIL[αCD19] over DXR-HSPC-SIL[αCD20] may lie in the differential expression of

CD19 versus CD20 on the surface of Namalwa cells. Immunophenotyping of Namalwa cells demonstrated that although over 99% of Namalwa cells expressed both the epitopes (CD19 and CD20), CD20 had a more heterogeneous expression on Namalwa cells than CD19. Immunoliposomes target and kill individual cells based on the presence of the target antigen. Therefore, in a heterogeneous tumor cell population, cells that have no target antigen, or low levels of target antigen may escape the cytotoxic effects of immunoliposomal drugs. The antigen-negative cells, which evade therapy, can regrow and lead to disease relapse or emergence of resistant cell population. DXR-HSPC-SIL[αCD20] may have been ineffective against cells which had low or no expression of the CD20 epitope on Namalwa cells. In contrast, DXR-HSPC-SIL[αCD19] could have been more effective against the majority of the Namalwa cell population due to a more homogeneous expression of the CD19 epitope.

Injection of mice with drug-free liposomes conjugated to either αCD19 or αCD20 did not improve the survival times of mice compared to untreated controls, unlike comparable amounts of free αCD19 or αCD20 ($P<0.01$). The cytotoxic effects of free αCD19 or αCD20 may be mediated through Fc-mediated complement-dependent cytotoxicity (CDC) and/or Ab-dependent cell-mediated cytotoxicity (ADCC). Alternatively, the cytotoxic action may be mediated through signal transduction mechanisms activated by antigen-antibody interactions, which could lead to apotosis or cell kill. Drug-free immunoliposomes, in spite of the multivalent

Table 3.2 Survival times of SCID mice after immunoliposomal treatments. SCID mice (5-7/group) were injected i.v. with 5 x 10^6 Namalwa cells in 0.2 ml phosphate-buffered saline. After 24 h they were injected i.v. in the tail vein with a single bolus dose of 3 mg/kg as free DXR or liposomal DXR. Free Abs were dosed at 15 μg of αCD19 or 13 μg of αCD20 per mouse. Liposomes were composed of HSPC:Chol:mPEG (2:1:0.1) or HSPC:Chol:mPEG:Mal-PEG (2:1:0.08:0.02). Liposomes targeted with αCD19 or αCD20 had 76 μg mAb/μmol PL or 70 μg mAb/μmol PL (40 mAb/liposome or 37 mAb/liposomes), respectively. Empty liposomes had 36 mAb/liposome or 33 mAb/liposomes of αCD19 or αCD20, respectively.

Group	Mean survival time ± S.D. (number of animals)	% increase life span
Control (saline)	27.6 ± 0.5 (5)	
free DXR	31.3 ± 2.7 (5)	13
DXR-HSPC-SL	28.6 ± 0.9 (5)	4
HSPC-SIL[αCD20]	30.5 ± 1.0 (6)	11
HSPC-SIL[αCD19]	31.5 ± 2.4 (6)	14
αCD20	34.3 ± 1.1 (6)	24
αCD19	34.8 ± 0.9 (6)	26
DXR-HSPC-SIL[αCD20]	34.3 ± 4.1 (7)	24
DXR-HSPC-SIL[αCD19]	45.6 ± 4.7 (7)	65

display of mAbs at the liposomes surface, may be less effective than similar concentration of free Abs because the orientation of the bound Abs with respect to the liposome surface might shield the Fc-segment and hinder its activity. Alternatively, different cellular processing pathways for the free mAbs and the immunoliposomes may account for the different effects of each.

In conclusion, it can be suggested that internalization of liposome-drug packages into the cell interior can be an important factor in determining the therapeutic effectiveness of immunoliposomal drugs. Internalization of Abs or other ligands into the target cell is also required for other targeted therapeutics, such as immunotoxins, Ab-drug conjugates and for targeted delivery of genes or viral DNA into cells (2). Direct selection for Abs that have efficient internalization is now possible by panning on target cells using Ab phage display libraries (110).

CHAPTER 4

Treatment of B-cell lymphoma with combinations of immunoliposomal anticancer drugs targeted to both the CD19 and CD20 epitopes.

(manuscript in preparation for submission to Cancer Research)

4.1 ABSTRACT

Internalization of liposome-drug package into cells has been suggested to be a requirement for successful immunoliposomal-drug therapy (234). Here we report that this requirement can vary with the type of drug encapsulated in immunoliposomes. Administration of vincristine (VCR)-loaded immunoliposomes targeted via a non-internalizing antibody, anti-CD20, to severe combined immunodeficient (SCID) mice bearing human B-lymphoma cells (Namalwa) resulted in significantly improved therapeutics compared to doxorubicin (DXR)-loaded liposomes targeted via the same antibody. Indeed, therapeutic results for anti-CD20-targeted liposomal DXR were no better than those found for free DXR and were barely improved over those found for non-targeted liposomal DXR.

In experiments using a combination of anti-CD19-and anti-CD20-targeted VCR-loaded liposomes, over 70% mice were cured. However, mice injected with the combination of anti-CD19- and anti-CD20-targeted liposomes, loaded with DXR instead of VCR, did not have improved survival rates over anti-CD19-targeted liposomal DXR by itself. Hence the success of immunoliposomal therapy in combination regimens requires careful attention to the type of encapsulated drug and the nature of the target epitopes.

4.2 INTRODUCTION

Antibody (Ab)-mediated targeting of liposomal anticancer drugs to antigens expressed selectively or over-expressed on the surface of tumor cells is increasingly being recognized as an effective strategy for increasing the therapeutic effectiveness

of anticancer drugs (24, 27, 28, 32, 149, 234). However, like other Ab-based therapies, important factors that may limit the therapeutic effectiveness of immunoliposomal anticancer drugs, are low density and heterogeneous expression of the target antigen at the cell surface (2, 3, 128, 259, 260).

Evidence is accumulating that high antigen density on target cells may be a requirement for improving the efficacy of targeted, relative to non-targeted, liposomal drugs (28). For immunoliposomal drugs, Abs are presented in a multivalent fashion at the liposome surface and high antigen density may facilitate the simultaneous engagement of multiple antigenic sites, which can initiate signal transduction mechanisms, increasing cell kill. Since increasing the density for a single population of receptors at the cell surface is impractical, a possible approach to increasing the total population of receptors that can be targeted would be to use a cocktail of immunoliposomal drugs, with the immunoliposomes in the mixture being targeted against different populations of receptors.

Ab-based therapies including immunoliposomes target and kill individual cells based on the presence of target antigens, and therefore tumor cells that have little or no target antigen may escape cytotoxic effects. The antigen-negative cells can result in disease relapse and emergence of resistant cell populations (261). Using cocktails of immunoliposomes would also facilitate delivery of drugs to a higher percentage of tumor cells in populations of cells that have heterogenous expression of receptors. Several studies have shown significantly improved therapeutic responses

when using combinations of immunotoxins, compared to single immunotoxin therapy in animal cancer models (99, 262-266).

Immunoliposomal therapy has, to date, relied on targeting to a single antigen on tumor cell surfaces. In this study, we evaluated the therapeutic efficacy, in xenograft models of human B-lymphoma, of combination regimens of immunoliposomes, loaded with either doxorubicin (DXR) or vincristine (VCR), targeted to two different epitopes, CD19 (internalizing) and CD20 (non-internalizing). We show that this strategy resulted in a significant cure rate for VCR-loaded liposomes, but not for DXR-loaded liposomes.

Internalization of liposome-drug packages is generally accepted to be a requirement for successful immunoliposomal drug therapy (234). In chapter 3, it was shown that DXR-loaded immunoliposomes required internalization into Namalwa cells in order to improve the therapeutic response over that obtained with non-targeted liposomes (234). Here we report, in the same animal model, the unexpected finding that mice injected with VCR-loaded immunoliposomes targeted via αCD20, had significantly increased survival rates, which were comparable to those found in mice injected with αCD19-targeted immunoliposomal VCR. These results are the first evaluation of combination regimens of immunoliposomal anticancer drugs in animal models of cancer, and also the first demonstration of improved therapeutic responses of an immunoliposomal formulation of an anticancer drug targeted to a non-internalizing epitope.

4.3 MATERIALS AND METHODS

4.3.1 Materials

Egg sphingomyelin (SM) and cholesterol (Chol) were purchased from Avanti Polar Lipids (Alabaster, AL). Hydrogenated soy phosphatidylcholine (HSPC) and methoxypolyethylene glycol (MW 2000), covalently linked via a carbamate bond to distearoylphosphatidylethanolamine (mPEG) (242), were generous gifts from ALZA Pharmaceuticals, Inc. (Mountain View, CA). Maleimide-derivatized PEG_{2000}-DSPE (Mal-PEG) was custom synthesized by Shearwater Polymers, Inc. (Huntsville, AL), according to a previously described protocol (60). Nuclepore® polycarbonate membranes (pore sizes: 0.2, 0.1, and 0.08 μm) were purchased from Northern Lipids (Vancouver, BC). 2-Iminothiolane (Traut's reagent) and 3-[4,5-dimethylthiazole-2-yl]-2,5-diphenyltetrazolium bromide (MTT) were purchased from Sigma Chemical Co. (St. Louis, MO). RPMI 1640 media (without phenol red), penicillin-streptomycin and fetal bovine serum (FBS) were obtained from Life Technologies (Burlington, ON). Iodobeads were purchased from Pierce (Rockford, IL) and BioRad Protein Assay Reagent from BioRad Laboratories (Mississauga, ON). Sephadex G-50, Sepharose CL-4B, aqueous counting scintillant (ASC) were purchased from Amersham Pharmacia Biotech (Baie d'Urfe, QC). Cholesterol- [1,2-^{3}H-(N)]-hexadecyl ether ([^{3}H]-CHE), 1.48-2.22 TBq/mmol, and ^{125}I-NaI (185 MBq) were purchased from Mandel Scientific (Mississauga, ON). Centrisart concentrators (MW cut-off of 100,000) were obtained from Sartorius, Goettingen, Germany. All other chemicals were of analytical grade purity.

4.3.2 Animals, antibodies and cell lines

Six-to-eight week-old female CB17 severe compromised immunodeficient (SCID) mice were purchased from Taconic Farms (Germantown. NY) and housed in the virus antigen-free unit of the Health Sciences Laboratory Animal Services, University of Alberta. All experiments were approved by the Health Sciences Animal Policy and Welfare Committee of the University of Alberta.

The murine monoclonal antibody (mAb) whole anti-CD19 IgG_{2a} (αCD19) was produced from the FMC63 murine hybridoma (245) and purified as described previously (74). Rituximab, a chimeric whole IgG_1 mAb, was used as a source of anti-CD20 (αCD20). The human Burkitt's lymphoma cell line, Namalwa (ATCC CRL 1432) was purchased from American Type Culture Collection, Rockville, MD and cultured in suspension in a humidified 37°C incubator with a 5% CO_2 atmosphere in RPMI 1640 media supplemented with 10% (v/v) fetal bovine serum (FBS), penicillin G (50 units/ml), and streptomycin sulfate (50 μg/ml). For experiments, only cells in the exponential phase of cell growth were used.

4.3.3 Preparation of liposomes

Non-targeted liposomes, to be loaded with DXR for therapeutic studies or radiolabeled with [^{3}H]-CHE for binding studies, were composed of HSPC:Chol:mPEG at a 2:1:0.1 molar ratio (HSPC-SL) and targeted liposomes were composed of HSPC:Chol:mPEG:Mal-PEG at a 2:1:0.08:0.02 molar ratio (HSPC-SIL). Liposomes were prepared by hydration of thin films, as described in chapter 2

and were extruded to mean diameter in the range of 100 ± 10 nm (108). DXR was loaded into liposomes using the ammonium sulfate loading method .

Non-targeted liposomes, to be loaded with VCR for therapeutic studies or radiolabeled with [^{3}H]-CHE for binding studies, were composed of SM:Chol:mPEG at a 55:40:5 molar ratio (SM-SL) and targeted liposomes were composed of SM:Chol:mPEG:Mal-PEG at a 55:40:4:1 molar ratio (SM-SIL). Liposomes were prepared by hydration of lipid film in citrate buffer (pH 4) and extruded to a mean diameter of 120 ± 10 nm (51) (as described in chapter 2). VCR was loaded using the transmembrane pH gradient-dependent procedure (54).

αCD19 or αCD20 mAbs were coupled to the terminus of the Mal-PEG at 2000:1 (lipid:protein) molar ratios, using a previously described coupling procedure (60). Briefly, mAb (10 mg/ml) was incubated with 2-Iminothiolane in O_2-free HEPES-buffered saline (HBS), pH 8.0, at a ratio of 20:1 (mol/mol) for 1 h at room temperature in order to thiolate the amino groups. At the end of the incubation, the excess reagent was removed by chromatography on a Sephadex G-50 column, equilibrated with O_2-free HBS (pH 7.4) and the thiolated Ab was immediately incubated with liposomes in an O_2-free environment overnight with continuous stirring. To assess coupling efficiency of the Abs, a trace amount of [^{125}I]-labeled αCD19 or αCD20 was added to the unlabeled Ab before thiolation. Ab coupling is expressed as μg mAb / μmol phospholipid (PL). A coupling efficiency of 80-90% for either Ab could routinely be achieved by this procedure and particular attention was

taken to ensure that similar Ab densities (within ± 10%) occurred at the surface of either type of immunoliposome.

4.3.4 Cell association of immunoliposomes

In vitro cell association of immunoliposomes labeled with [^{3}H]-CHE was determined, as described previously, at both 37°C and 4°C, i.e., permissive and non-permissive temperatures for endocytosis, respectively (24). Briefly, liposomes (SM-SL, HSPC-SL, SM-SIL[αCD19], HSPC-SIL[αCD19], SM-SIL[αCD20] or HSPC-SIL[αCD20]) were radiolabeled with [^{3}H]-CHE and incubated with 1 million Namalwa cells (in FACS tubes) at PL concentrations ranging from 0.1 mM to 1.6 mM PL (in triplicate) for 1 h. For evaluating cell association of combinations of immunoliposomes, HSPC-SIL[αCD19] and HSPC-SIL[αCD20] or SM-SIL[αCD19] and SM-SIL[αCD20] were mixed at a ratio of 1:1, before incubating with the Namalwa cells. Cells were then washed twice with cold PBS to remove unbound liposomes and the amount of [^{3}H]-CHE associated with cells was determined. Cell association (pmoles PL / 1 million cells) was calculated from the specific activity of the liposomes. Specific binding was determined by subtracting cell association of non-targeted liposomes from the total cell association.

4.3.5 *In vivo* survival experiments

SCID mice (5-7/group) were injected i.v. in the tail vein with 5 x 10^6 Namalwa cells in 0.2 ml phosphate-buffered saline (PBS). After 24 h, treatments were given as a single bolus i.v. dose of 3 mg DXR/kg as free DXR, or DXR-loaded liposomes (DXR-HSPC-SL, DXR-HSPC-SIL[αCD19] or DXR-HSPC-SIL[αCD20]).

Alternatively, mice were injected with 0.66 mg VCR/kg as free VCR, or VCR-loaded liposomes (VCR-SM-SL, VCR- SM-SIL[αCD19] or VCR-SM-SIL[αCD20]). The Ab density on drug-loaded immunoliposomes was used to calculate appropriate doses of either free mAb or empty immunoliposomes that were used as experimental controls. Where combinations of two drug-loaded immunoliposomal formulations, two free mAbs or two empty immunoliposomal formulations were used, the total dose administered composed of equal parts of each component. Mice were monitored daily for 150 days, and were euthanised when they developed hind leg paralysis. Mice surviving to 150 days were determined to be long-term survivors and were subsequently sacrificed and subjected to gross pathological examination.

4.3.6 Statistical analysis

Comparisons of cellular binding and uptake and survival studies reported in Table 4.1 were done using one-way analysis of variance with InStat software (GraphPad software, Version 3.0, San Diego, CA). The Tukey post-test was used to compare means. Survival studies reported in Table 4.2 were analyzed using Kaplan-Meier plots, using GraphPad Prism software. Differences were considered significant at a P value of less than 0.05.

4.4 RESULTS AND DISCUSSION

4.4.1 *In vitro* cell association

The levels of cellular association of either SIL[αCD19] or SIL[αCD20] with Namalwa cells were significantly higher than seen for non-targeted SLs at either 37°C or 4°C (Figure 4.1). In addition, the levels of cellular association of SIL[αCD19]

with cells were significantly higher at 37°C than at 4°C (non-permissive for endocytosis) (Figure 4.1), suggesting a requirement for metabolic processes in the uptake of these immunoliposomes. No significant differences were observed in the levels of cellular association of SIL[αCD20] with cells at 37°C vs. 4°C. Specific cell association (targeted minus non-targeted) is given in Figure 4.2. As expected, the levels of cellular association of 1:1 combinations of SIL[αCD19] and SIL[αCD20] were higher than those seen for either of the individual immunoliposome formulations at all the PL concentrations and appeared to be additive. This was observed for both SM- and HSPC-liposomes at either 37°C or 4°C (Figure 4.2). Only at one concentration (1.6 mM PL), at 37°C, the cell association of the combination of HSPC-SIL[αCD19] and HSPC-SIL[αCD20] appeared to be sub-additive.

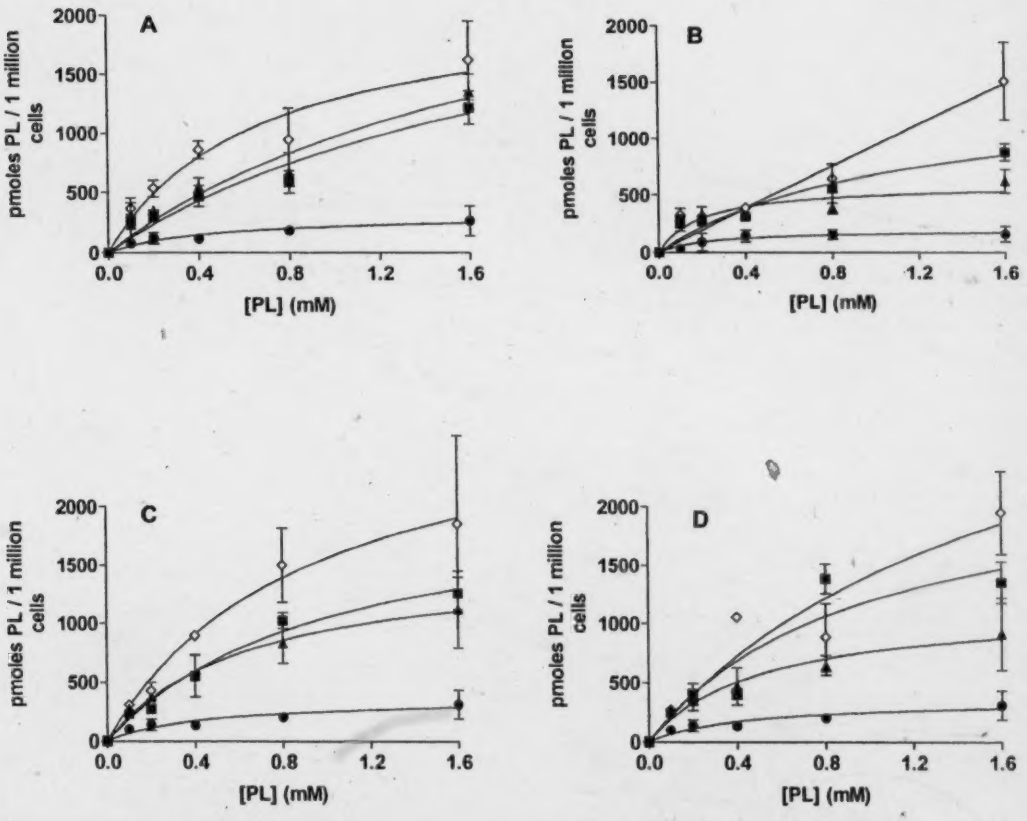

Figure 4.1 ***In vitro*** **cellular association of liposomes with Namalwa cells as a function of concentration at 37°C (Panels A and C) or 4°C (Panels B and D).** Non targeted liposomes SL(●); Targeted SIL[αCD19] (▲); Targeted SIL[αCD20] (■); Targeted combination of SIL[αCD19] + SIL[αCD20] (◇).
Panels A and B: Liposomes were composed of HSPC:Chol:mPEG (2:1:0.1) or HSPC:Chol: mPEG:Mal-PEG (2:1:0.08:0.02). Panels C and D: Liposomes were composed of SM:Chol: mPEG (55:40:5) or SM:Chol: mPEG:Mal-PEG (55:40:4:1). Liposomes were labeled with [^{3}H]CHE and incubated with 1 million Namalwa cells for 1 h after which the cells were washed with cold PBS to remove the unbound liposomes. The concentration of mAbs on HSPC-SILs was 64 μg αCD19/μmol PL or 54 μg αCD20/μmol PL and that on SM-SILs was 59 μg αCD19/μmol PL or 56 μg αCD20/μmol PL. Data are expressed as pmoles PL / 1 million cells. Each point is an average of 3 replicates ± S.D. from one representative experiment.

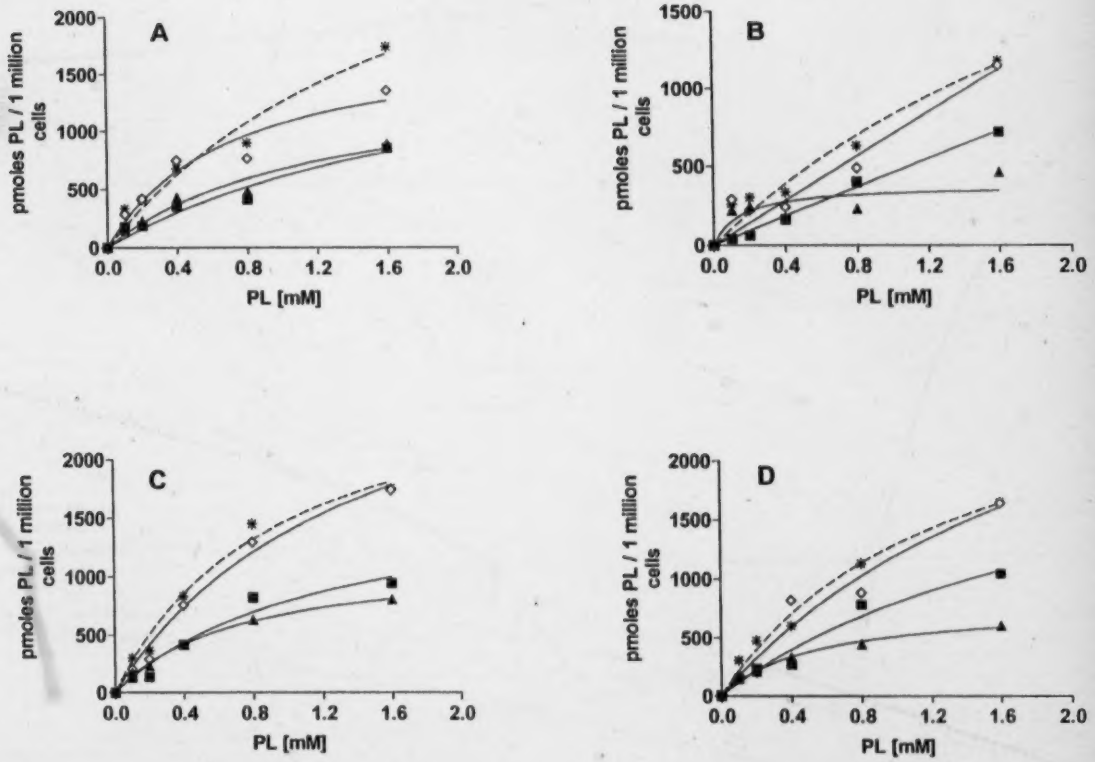

Figure 4.2 Specific cell association of immunoliposomes with Namalwa cells as a function of concentration at 37°C (Panels A and C) or 4°C (Panels B and D). Targeted SIL[αCD19] (▲); Targeted SIL[αCD20] (■); Targeted combination of SIL[αCD19] + SIL[αCD20] (◇). (*) represents the calculated sum of cell association of SIL[αCD19] and SIL[αCD20]. Panels A and B: Liposomes were composed of HSPC:Chol:mPEG (2:1:0.1) or HSPC:Chol:mPEG:Mal-PEG (2:1:0.08:0.02). Panels C and D: Liposomes were composed of SM:Chol:mPEG (55:40:5) or SM:Chol:mPEG:Mal-PEG (55:40:4:1). Data are expressed as pmoles PL / 1 million cells. Each point is an average of 3 replicates ± S.D. from one representative experiment.

4.4.2 *In vivo* survival studies

The therapeutic effectiveness of DXR-loaded immunoliposomes targeted via either αCD19 or αCD20 was evaluated individually or in combination in SCID mice bearing Namalwa cells (Table 4.1). Mice treated with DXR-containing liposomes targeted via either αCD19 or αCD20 had significantly longer survival times than mice that received no treatment (control) ($P<0.01$). DXR-HSPC-SL or free DXR were not therapeutically better than control groups ($P>0.05$). These results suggest that antibody-mediated delivery of liposomal drugs to antigens expressed on the surface of B-cells can increase the therapeutic effectiveness of anticancer drugs. Free DXR is ineffective as it has large volume of distribution and hence low plasma drug levels are achieved. On the other hand, non-targeted liposomes containing DXR can maintain high levels of entrapped (i.e., non-bioavailable) drug in circulation for long periods of time as the release rate of DXR from liposomes is slow (Chapter 2). However, non-targeted liposomes are not bound to and internalized by the target B-cells and so the entrapped drug is not delivered to these cells in a very efficient manner. This makes it unlikely that therapeutically relevant intracellular concentrations of drug are achieved.

As observed in chapter 3, mice treated with DXR-HSPC-SIL[αCD19] increased the survival of mice to a significantly greater extent compared to DXR-HSPC-SIL[αCD20] ($P<0.001$), DXR-HSPC-SL ($P<0.001$) or free DXR ($P<0.001$). No significant difference was observed between mice treated with DXR-HSPC-SIL[αCD20] and free DXR ($P>0.05$). Mice treated with DXR-HSPC-SIL[αCD20]

had survival times that were marginally different from DXR-HSPC-SL ($P<0.05$). These results can be explained by the observations reported in chapter 3, i.e., DXR-loaded immunoliposomes targeted via αCD19 are rapidly internalized into Namalwa cells in contrast to immunoliposomes targeted via αCD20, which are not internalized. Receptor-mediated intracellular delivery of DXR-HSPC-SIL[αCD19] and subsequent release of drugs inside the cells can lead to high intracellular drug concentrations. In contrast, DXR-HSPC-SIL[αCD20] binds to the target cells and releases drug to the extracellular medium where it can rapidly redistribute *in vivo*.

Another explanation for improved results seen with DXR-HSPC-SIL[αCD19] over DXR-HSPC-SIL[αCD20], may lie in the more homogeneous distribution of the CD19 epitope on the surface of Namalwa cells compared to the CD20 epitope (coefficient of variation: for CD20 = 78, CD19 = 45; unstained cells = 44). DXR-HSPC-SIL[αCD20] may have been ineffective against cells which had low or no expression of CD20. In contrast, the high effectiveness of DXR-HSPC-SIL[αCD19] could have been due to a homogeneous expression of the CD19 epitope on the target cells.

In this study, the combination group of DXR-HSPC-SIL[αCD19] and DXR-HSPC-SIL[αCD20], was more effective than DXR-HSPC-SIL[αCD20] alone ($P<0.0005$), but did not significantly improve the therapeutic effectiveness over that seen with DXR-HSPC-SIL[αCD19] alone ($P>0.05$) since DXR-HSPC-SIL[αCD20] alone had little or no therapeutic effect. However, mice injected with a combination

of DXR-HSPC-SIL[αCD19] and DXR-HSPC-SIL[αCD20] had significantly improved survival time over mice injected with a combination of free mAbs ($P<0.005$) or a combination of drug-free liposomes ($P<0.0005$).

Mice injected with free αCD19 or αCD20 had significantly longer survival times than untreated controls ($P<0.01$). We suggest that the cytotoxic effects of free αCD19 or αCD20 occur through Fc-mediated complement-dependent cytotoxicity (CDC) and/or Ab-dependent cell-mediated cytotoxicity (ADCC) rather than signaling mechanisms due to antigen-antibody interactions. This is because drug-free liposomes conjugated to Fab'fragments of αCD19 or αCD20, did not have any therapeutic effects in this model (ref. Results in chapter 2 and P. Sapra personal observation). However, more studies are warranted to clarify the mechanism of action of free mAbs. It was interesting to observe that combinations of free mAbs were significantly better than individual mAbs ($P<0.0001$) which could be due to the higher total binding of the two populations of mAbs on cell surface, i.e., higher apparent receptor density, possibly leading to increases in signal transduction mechanisms.

Injection of mice with drug-free liposomes conjugated to either αCD19 or αCD20 did not improve the survival times of mice compared to untreated controls, unlike comparable amounts of free αCD19 or αCD20. As suggested in chapter 3, drug-free immunoliposomes, in spite of the multivalent display of mAbs at the liposomes surface, may be less effective than similar concentration of free mAbs

Table 4.1 Survival times of SCID mice after immunoliposomal DXR treatments. SCID mice (5-7/group) were injected i.v. with 5 x 10^6 Namalwa cells in 0.2 ml PBS. After 24 h they were injected i.v. in the tail vein with a single bolus dose of 3 mg/kg as free DXR or liposomal DXR. Liposomes were composed of HSPC:Chol:mPEG (2:1:0.1) or HSPC:Chol:mPEG:Mal-PEG (2:1:0.08:0.02). DXR-loaded liposomes targeted with mAbs had 76 μg αCD19 /μmol PL or 70 μg αCD20 /μmol PL (40 mAb/liposome or 37 mAb/liposomes), respectively; i.e., each mouse received 15 μg αCD19 or 13 μg αCD20 conjugated to the DXR-containing immunoliposomes. Hence, the same amounts of free mAbs were administered per mouse, and empty immunoliposomes also contained comparable doses of Ab and PL. Empty liposomes had 36 mAb/liposome or 33 mAb/liposomes of αCD19 or αCD20, respectively. The combination groups of free mAbs, empty or DXR-loaded liposomes had both components in equal parts. The combination of DXR-loaded liposomes was dosed at a total DXR dose of 3 mg/kg, and of free Abs at a total dose of 14 μg per mouse.

Group	Mean survival time ± S.D.	% increase life span	Long-term survivors (>150 days)
Control (saline)	27.6 ± 0.5		0/5
free DXR	31.3 ± 2.7	13	0/5
DXR-HSPC-SL	28.6 ± 1.0	4	0/5
HSPC-SIL[αCD20]	30.5 ± 1.0	11	0/6
HSPC-SIL[αCD19]	31.5 ± 2.4	14	0/6
HSPC-SIL[αCD20] + HSPC-SIL[αCD19]	33.2 ± 2.0	20	0/6
αCD20	34.3 ± 1.1	24	0/6
αCD19	34.8 ± 1.0	26	0/6
αCD20 + αCD19	40.7 ± 2.0	47	0/6
DXR-HSPC-SL + αCD20	33.0 ± 1.3	20	0/6
DXR-HSPC-SL + αCD19	39.5 ± 1.0	43	0/6
DXR-HSPC-SIL[αCD20]	34.3 ± 4.2	24	0/7
DXR-HSPC-SIL[αCD19]	45.7 ± 4.7	66	0/7
DXR-HSPC-SIL[αCD20] + DXR-HSPC-SIL[αCD19]	48.6 ± 4.4	76	0/7

Table 4.2 Statistical comparison of results of the in vivo survival study reported in Table 4.1

Comparisons were done using one-way analysis of variance with InStat software (GraphPad software, Version 3.0, San Diego, CA). The Tukey post-test was used to compare means. Comparisons were made for all experimental groups but only groups that were statistically significant are given in the Table.

Comparison	*P* value
Control vs HSPC-SIL[αCD20] + HSPC-SIL[αCD19]	*P*<0.05
Control vs αCD20	*P*<0.01
Control vs αCD19	*P*<0.01
Control vs αCD20 + αCD19	*P*<0.001
Control vs DXR-HSPC-SL + αCD19	*P*<0.001
Control vs DXR-HSPC-SIL[αCD20]	*P*<0.01
Control vs DXR-HSPC-SIL[αCD19]	*P*<0.001
Control vs DXR-HSPC-SIL[αCD20] + DXR-HSPC-SIL[αCD19]	*P*<0.001
free DXR vs αCD20 + αCD19	*P*<0.001
free DXR vs DXR-HSPC-SL + αCD19	*P*<0.001
free DXR vs DXR-HSPC-SIL[αCD19]	*P*<0.001
free DXR vs DXR-HSPC-SIL[αCD20] + DXR-HSPC-SIL[αCD20]	*P*<0.001
DXR-HSPC-SL vs αCD20	*P*<0.05
DXR-HSPC-SL vs αCD19	*P*<0.05
DXR-HSPC-SL vs αCD20 + αCD19	*P*<0.001
DXR-HSPC-SL vs DXR-HSPC-SL + αCD19	*P*<0.001
DXR-HSPC-SL vs DXR-HSPC-SIL[αCD20]	*P*<0.05
DXR-HSPC-SL vs DXR-HSPC-SIL[αCD19]	*P*<0.001
DXR-HSPC-SL vs DXR-HSPC-SIL[αCD19] + DXR-HSPC-SIL[αCD19]	*P*<0.001
HSPC-SIL[αCD20] vs αCD20 + αCD19	*P*<0.001
HSPC-SIL[αCD20] vs DXR-HSPC-SL + αCD19	*P*<0.001
HSPC-SIL[αCD20] vs DXR-HSPC- SIL[αCD19]	*P*<0.001
HSPC-SIL[αCD20] vs DXR-HSPC- SIL[αCD20] + DXR-HSPC-SIL[αCD19]	*P*<0.001
HSPC-SIL[αCD19] vs αCD20 + αCD19	*P*<0.001
HSPC-SIL[αCD19] vs DXR-HSPC-SL + αCD19	*P*<0.001
HSPC-SIL[αCD19] vs DXR-HSPC-SIL[αCD19]	*P*<0.001
HSPC-SIL[αCD19] vs DXR-HSPC-SIL[αCD20] + DXR-HSPC-SIL[αCD19]	*P*<0.001
HSPC-SIL[αCD20] + HSPC-SIL[αCD20] vs αCD20 + αCD19	*P*<0.001

HSPC-SIL[αCD20] + HSPC-SIL[αCD20] vs DXR-HSPC-SL + αCD19	$P<0.01$
HSPC-SIL[αCD20] + HSPC-SIL[αCD20] vs DXR-HSPC-SIL[αCD19]	$P<0.001$
HSPC-SIL[αCD20] + HSPC-SIL[αCD20] vs DXR-HSPC-SIL[αCD20] + DXR-HSPC-SIL[αCD19]	$P<0.001$
αCD20 vs αCD20 + αCD19	$P<0.01$
αCD20 vs DXR-HSPC-SIL[αCD20]	$P<0.001$
αCD20 vs DXR-HSPC-SIL[αCD20] + DXR-HSPC-SIL[αCD19]	$P<0.001$
αCD19 vs αCD20 + αCD19	$P<0.05$
αCD19 vs DXR-HSPC-SIL[αCD19]	$P<0.001$
αCD19 vs DXR-HSPC-SIL[αCD20] + DXR-HSPC-SIL[αCD19]	$P<0.001$
αCD20 + αCD19 vs DXR-HSPC-SL + αCD20	$P<0.001$
αCD20 + αCD19 vs DXR-HSPC-SIL[αCD20]	$P<0.01$
αCD20 + αCD19 vs DXR-HSPC-SIL[αCD20] + DXR-HSPC-SIL[αCD19]	$P<0.001$
DXR-HSPC-SL + αCD20 vs DXR-HSPC-SL + αCD19	$P<0.01$
DXR-HSPC-SL + αCD20 vs DXR-HSPC-SIL[αCD19]	$P<0.001$
DXR-HSPC-SL+ αCD20 vs DXR-HSPC-SIL[αCD20] + DXR-HSPC-SIL[αCD19]	$P<0.001$
DXR-HSPC-SL + αCD19 vs DXR-HSPC-SIL[αCD20]	$P<0.05$
DXR-HSPC-SL + αCD19 vs DXR-HSPC-SIL[αCD19]	$P<0.01$
DXR-HSPC-SL + αCD19 vs DXR-HSPC-SIL[αCD20] + DXR-HSPC-SIL[αCD19]	$P<0.001$
DXR-HSPC-SIL[αCD20] vs DXR-HSPC-SIL[αCD19]	$P<0.001$
DXR-HSPC-SIL[αCD20] vs DXR-HSPC-SIL[αCD19] + DXR-HSPC-SIL[αCD19]	$P<0.001$

because the orientation of the bound Abs with respect to the liposome surface might shield the Fc segment and hinder its activity. Alternatively, different cellular processing pathways for the free mAbs vs. the immunoliposomes may account for the different effects of each. Also, free mAbs in combination resulted in significantly improved survival times compared to drug-free immunoliposomes in combination ($P<0.0001$).

DXR-HSPC-SL had synergistic cytotoxicic effects with free αCD19. This combination was more therapeutically effective than control treatments, free DXR or DXR-HSPC-SL ($P<0.001$). DXR-HSPC-SIL[αCD19] was significantly more effective than DXR-HSPC-SL + αCD19 ($P<0.01$). However, more experiments needs to be performed to confirm if this statistical significance also has biological significance. The combination of DXR-HSPC-SL and free αCD20 was not therapeutically better than control treatments, free DXR or DXR-HSPC-SL ($P>0.05$). DXR-HSPC-SIL[αCD20] was also not better than the the combination of DXR-HSPC-SL and free αCD20.

We performed a separate study to evaluate the therapeutic effects of VCR-containing liposomes conjugated to either αCD19 or αCD20, used individually or in combination (Table 4.2). The most interesting observation was that treatment with VCR-SM-SIL[αCD20] increased the survival of mice to a significantly greater extent than either VCR-SM-SL or free VCR ($P<0.005$) and was not significantly different from VCR-SM-SIL[αCD19] ($P>0.05$). Also, five out of seven mice injected with the combination of VCR-SM-SIL[αCD19] and VCR-SM-SIL[αCD20] were long-term

survivors (>150 days) and the remaining two mice had significantly improved life span.

These results suggest internalization of immunoliposomes does not appear to be a requirement for improved therapeutic efficacy for liposomes containing VCR. In this model, treatment of the tumor-bearing mice with free VCR resulted in a significant increase in survival relative to untreated controls ($P<0.005$), but this was not observed for free DXR relative to controls. Free DXR has little or no effect in this lymphoma model. An explanation for the improved therapeutics of VCR-SM-SIL[αCD20] relative to DXR-HSPC-SIL[αCD20] may lie in the faster rate of release from liposomes of VCR relative to DXR, as shown in Chapter 2. Free VCR is more potent than free DXR against the Namalwa cell line, and the faster release of the drug from VCR-SM-SIL[αCD20] at the cell surface appears to lead to higher cytotoxic levels of drug being delivered internally relative to DXR-HSPC-SIL[αCD20]. The requirement for Ab-based therapies, in general, to be internalized for biological activity still remains unclear. Previous studies have reported that Vinca-alkaloid immunonjugates do not require internalization for therapeutic activity (267, 268). The authors proposed that cytotoxicity of these immunoconjugates might be due to the release of free drug from the conjugate at tumor cell periphery, followed by intracellular transport. On the other hand, studies have shown that adriamycin conjugates linked to internalizing Abs, have significantly improved therapeutics over adriamycin conjugates linked to non-internalizing Abs (αCD20) (269).

Table 4.3 Survival times of SCID mice after immunoliposomal VCR treatments. SCID mice (6-7/group) were injected i.v. with 5 x 10^6 Namalwa cells in 0.2 ml PBS. After 24 h they were injected i.v. in the tail vein with a single bolus dose of 0.66 mg/kg as free VCR or liposomal VCR. Liposomes were composed of SM:Chol:mPEG (55:40:5) or SM:Chol:mPEG:Mal-PEG (55:40:4:1). Liposomes targeted with mAbs had 66 μg αCD19 /μmol PL or 52 μg αCD20 /μmol PL (34 mAb/liposome or 27 mAb/liposomes respectively). The combination group had VCR-SM-SIL[αCD19] and VCR-SM-SIL[αCD20] (total dose = 0.66 mg/kg) in equal parts.

Group	Mean survival time ± S.D.	% increase life span	Long-term survivors (>150 days)
Control (saline)	25.4 ± 0.5		0/6
free VCR	38.7 ± 4.0	53	0/6
VCR-SM-SL	31.9 ± 3.0	26	0/7
VCR-SM-SL + αCD20	44.7 ± 5.9	76	0/6
VCR-SM-SL + αCD19	62.3 ± 8.8	145	0/6
VCR-SM-SIL[αCD20]	49.0 ± 4.6	93	2/7
VCR-SM-SIL[αCD19]	66.0 ± 13.1	160	3/7
VCR-SM-SIL[αCD20]+ VCR-SM-SIL[αCD19]	77.0, 91.0	203, 258	5/7

Table 4.4 Statistical comparison of results of the *in vivo* survival study reported in Table 4.3.
Comparisons were done using using Kaplan-Meier plots, using GraphPad Prism software (GraphPad software, Version 3.0, San Diego, CA). Comparisons were made for all experimental groups but only groups that were statistically significant are given in the Table.

Comparison	***P* value**
Control vs free VCR	$P<0.005$
Control vs VCR-SM-SL	$P<0.0005$
Control vs VCR-SM-SL + αCD20	$P<0.005$
Control vs VCR-SM-SL + αCD19	$P<0.005$
Control vs VCR-SM-SIL[αCD20]	$P<0.0005$
Control vs VCR-SM-SIL[αCD19]	$P<0.0005$
Control vs VCR-SM-SIL[αCD20] + VCR-SM-SIL[αCD19]	$P<0.0005$
free VCR vs VCR-SM-SL	$P<0.05$
free VCR vs VCR-SM-SL + αCD20	$P<0.05$
free VCR vs VCR-SM-SL + αCD19	$P<0.001$
free VCR vs VCR-SM-SIL[αCD20]	$P<0.005$
free VCR vs VCR-SM-SIL[αCD19]	$P<0.0001$
free VCR vs VCR-SM-SIL[αCD20] + VCR-SM-SIL[αCD19]	$P<0.0005$
VCR-SM-SL vs VCR-SM-SL + αCD20	$P<0.0005$
VCR-SM-SL vs VCR-SM-SL + αCD19	$P<0.0005$
VCR-SM-SL vs VCR-SM-SIL[αCD20]	$P<0.005$
VCR-SM-SL vs VCR-SM-SIL[αCD19]	$P<0.005$
VCR-SM-SL vs VCR-SM-SIL[αCD20] + VCR-SM-SIL[αCD19]	$P<0.0005$
VCR-SM-SL + αCD20 vs VCR-SM-SL + αCD19	$P<0.01$
VCR-SM-SL + αCD20 vs VCR-SM-SIL[αCD20]	$P<0.01$
VCR-SM-SL + αCD20 vs VCR-SM-SIL[αCD19]	$P<0.0005$
VCR-SM-SL + αCD20 vs VCR-SM-SIL[αCD20] + VCR-SM-SIL[αCD19]	$P<0.0005$
VCR-SM-SL + αCD19 vs VCR-SM-SIL[αCD19]	$P<0.01$
VCR-SM-SL + αCD19 vs VCR-SM-SIL[αCD20] + VCR-SM-SIL[αCD19]	$P<0.0005$

In another study, Ab-drug conjugates composed of αCD20 (Rituxan®) and monomethyl auristatin (MMAE) demonstrated significantly improved therapeutics over those made of DXR and Rituxan (270). MMAE is a derivative of synthetic analogue of dolastatin 10, which belong to the antimitotic class of chemotherapeutics, similar to VCR. Our results are in accordance with these results and lead us to hypothesize that antimitotic drugs may be an exception to the general rule that immunoliposomes require internalization for improved therapeutics. In chapter 3, we demonstrated improved therapeutics of internalizing (DXR-HSPC-SIL[αCD19]) over non-internalizing formulations (DXR-HSPC-SIL[αCD20]) in the Namalwa model (234). We therefore conclude that the requirement for internalization for therapeutic activity of immunotherapeutics like immunotoxins, drug-Ab immunoconjugates and immunoliposomal drugs can vary with the nature of the drug and the release rate of the drug from the liposomes.

As observed for DXR-containing liposomes, VCR-containing liposomes also have synergistic cytototoxic effects with signaling mAbs. Therapy with the combination of VCR-SM-SL and αCD20 or with VCR-SM-SL and αCD19 was significantly better than controls ($P< 0.005$), therapy with free VCR ($P<0.05$) or VCR-SM-SL ($P<0.005$). Therapy with either immunoliposomal VCR (i.e., VCR-SM-SIL[αCD19] or VCR-SM-SIL[αCD20]) was significantly better than the combination of VCR-SM-SL and free Abs ($P<0.01$).

In this study, there was a tendency for a higher cure rate in mice treated with a combination of VCR-SM-SIL[αCD19] and VCR-SM-SIL[αCD20], although this did

not reach statistical signifcance($P>0.05$). The high cure rate was probably due to some additive effect of the individual therapies.

This study demonstrates for the first time that immunoliposomal anticancer drugs, used in combination, can result in improved therapeutics, when the appropriate drug and drug release rate are chosen. Further studies, using combinations of immunoliposomal drugs, are hence warranted.

CHAPTER 4A (Addendum to Chapter 4)

Evaluation of a combination regimen of immunoliposomal DXR targeted to two internalizing (CD19 and CD22) epitopes

4A.1 Rationale

In chapters 3 and 4 we showed that, because αCD20-targeted liposomal DXR by itself did not significantly improve the therapeutic outcomes in xenograft models of human B-lymphoma (due to lack of internalization into Namalwa cells), there was no therapeutic advantage to the combination anti-CD19- and anti-CD20-targeted DXR-loaded liposomes. A set of experiments was therefore performed to evaluate the effect of a combination regimen of DXR-loaded liposomes targeted to two internalizing epitopes (CD19 and CD22).

4A.2 Materials and Methods

The mAb, αCD22 (IgG_1) was kindly provided by Dr. E. Vitetta, University of Texas Southwestern Medical Center, Dallas, TX. The CD22 antigen is rapidly internalized and is expressed on the surface of most B-cell malignancies . Liposomes were made as described in chapter 4. *In vitro* cell association and *in vivo* survival studies were performed as described in chapter 4. In cell association experiments, combinations of HSPC-SIL[αCD19] and HSPC-SIL[αCD22] were mixed at a 1:1 ratio, before incubating with the Namalwa cells. In therapeutic experiments where combinations of either two drug-loaded immunoliposomal formulations, two free mAbs or two empty immunoliposomal formulations were used, the total dose administered was composed of equal parts of each component.

4A.3 Results and Discussion

4A.3.1 *In vitro* cell association

The levels of cellular association of either HSPC-SIL[αCD19] or HSPC-SIL[αCD22] with Namalwa cells were significantly higher than seen for SLs (non-targeted) at either 37°C or 4°C (Figure 4A.1A). The levels of cellular association of 1:1 combinations of HSPC-SIL[αCD19] and HSPC-SIL[αCD22] were higher than those seen for either of the individual immunoliposome formulations at all PL concentrations. This increase appeared to be sub-additive i.e., the cell association of combinations of HSPC-SIL[αCD19] and HSPC-SIL[αCD22] was less than the sum of the cell association of individual liposomes (Figure 4A.1B.). For example, the cell association of 1.6 mM of the combination of SIL[αCD19] and SIL[αCD22] was less than the sum of cell association of 1.6 mM SIL[αCD19] and 1.6 mM SIL[αCD22]. As both SIL[αCD19] and SIL[αCD22] bind to and internalize into Namalwa cells via receptor-mediated endocytosis, we speculate that there exists competition between the two immunoliposomes for internalization into the cells. In chapter 4, immunoliposomes were targeted to an internalizing (CD19) and a non-internalizing receptor (CD20), where there are less chances of cross talk. Another speculation would be that on the surface of B-cells, CD19 receptor is more in proximity to CD22 than CD20. Hence there are higher chances of competition for receptor sites between SIL[αCD19] and SIL[αCD22] than between SIL[αCD19] and SIL[αCD20]. However, more experiments are required prior to commenting on these speculations.

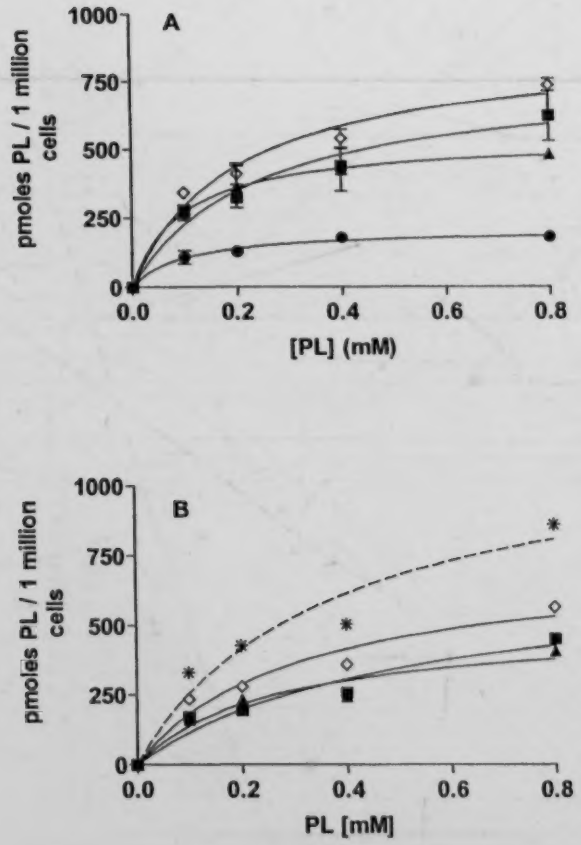

Figure 4A.1 ***In vitro*** **cellular association of liposomes with Namalwa cells as a function of concentration at 37°C.**

Non targeted liposomes HSPC-SL(●); Targeted HSPC-SIL[αCD19] (▲); Targeted HSPC-SIL[αCD22] (■); Targeted combination of HSPC-SIL[αCD19] + HSPC-SIL[αCD22] (1:1) (◇). Liposomes were composed of HSPC:Chol:mPEG (2:1:0.1) or HSPC:Chol: mPEG:Mal-PEG (2:1:0.08:0.02). Liposomes were labeled with [^{3}H]CHE and incubated with 1 million Namalwa cells after which the cells were washed with cold PBS to remove the unbound liposomes. The concentration of mAbs on HSPC-SILs was 103 μg αCD19/μmol PL or 80 μg αCD22/μmol PL. Data are expressed as pmoles PL/10^6 cells. Each point is an average of 3 replicates ± S.D. from one experiment. **(A)**: Total cell association; **(B)**: Specific cell association with Namalwa cells. (*) represents the calculated sum of cell association of SIL[αCD19] and SIL[αCD22].

4A.3.2 *In vivo* survival

Table 4A.1 gives the mean survival times for tumor-bearing mice inoculated with Namalwa cells and treated with immunoliposomal formulations of DXR targeted via αCD19 (DXR-HSPC-SIL[αCD19]) or via αCD22 (DXR-HSPC-SIL[αCD22]), individually, or in combination. An unexpected finding was that DXR-HSPC-SIL[αCD22] was not therapeutically better than either non-targeted liposomes (DXR-HSPC-SL) or free DXR ($P>0.05$). DXR-HSPC-SIL[αCD19] had significantly better therapeutic outcomes than DXR-HSPC-SIL[αCD22] ($P<0.001$). The combination group of DXR-HSPC-SIL[αCD19] and DXR-HSPC-SIL[αCD22] was therapeutically more efficacious than DXR-HSPC-SIL[αCD22] ($P<0.05$), but not better than DXR-HSPC-SIL[αCD19] ($P>0.05$). The reason for the lack of therapeutic efficacy of DXR-HSPC-SIL[αCD22] in this experiment remains to be determined, however some reasons suggest themselves.

αCD22, used in this experiment had been in our laboratory for almost 3 years. The biological properties of αCD22 could have been altered due to long period of storage. An SDS-PAGE analysis was performed before starting the experiment, which showed that αCD22 had not physically degraded, but this does not comment on the biological activity of αCD22. Previous experiments performed by a former graduate student in our laboratory, showed that DXR-HSPC-SIL[αCD22] had therapeutic activity comparable to DXR-HSPC-SIL[αCD19] in the Namalwa model (D. Lopes, unpublished observations).

Table 4A.1 Survival times of SCID mice after immunoliposomal DXR treatments.

SCID mice (5-7/group) were injected i.v. with 5 x 10^6 Namalwa cells in 0.2 ml PBS. After 24 h they were injected i.v. in the tail vein with a single bolus dose of 3 mg/kg as free DXR or liposomal DXR. Liposomes were composed of HSPC:Chol:mPEG (2:1:0.1) or HSPC:Chol:mPEG:Mal-PEG (2:1:0.08:0.02) . Liposomes targeted with mAbs had 49 μg αCD19 /μmol PL or 69 μg αCD22 /μmol PL (26 mAb/liposome or 36 mAb/liposomes), respectively; i.e., each mouse received 11 μg αCD19 or 15 μg αCD22 conjugated to the DXR-containing immunoliposomes. Hence, the same amounts of free mAbs were administered per mouse, and empty immunoliposomes also contained comparable doses of Ab and PL. Empty liposomes had 26 mAb/liposome or 40 mAb/liposomes of αCD19 or αCD22, respectively. The combination groups of free mAbs, empty or DXR-loaded liposomes had both of the components in equal parts. The combination of DXR-loaded liposomes was dosed at a total DXR dose of 3 mg/kg and that of free Abs at a total dose of 13 μg per mouse.

Group	Mean survival time ± S.D	% increase life span	Long-term survivors (> 150 days)
Control (saline)	26.2 ± 1.1		0/5
free DXR	29.2 ± 1.3	11	0/5
DXR-HSPC-SL	27.6 ± 2.3	5	0/5
HSPC-SIL[αCD22]	30.7 ± 3.3	17	0/6
HSPC-SIL[αCD19]	33.7 ± 2.8	29	0/6
HSPC-SIL[αCD22] + HSPC-SIL[αCD19]	34.8 ± 1.2	32	0/6
αCD22	35.3 ± 2.3	35	0/6
αCD19	37.8 ± 4.9	44	0/6
αCD22 + αCD19	34.2 ± 1.6	31	0/6
DXR-HSPC-SL + αCD22	36.2 ± 1.6	38	0/6
DXR-HSPC-SL + αCD19	39.8 ± 1.4	52	0/6
DXR-HSPC-SIL[αCD22]	31.6 ± 3.4	21	0/7
DXR-HSPC-SIL[αCD19]	45.0 ± 7.8	72	0/7
DXR-HSPC-SIL[αCD22] + DXR-HSPC-SIL[αCD19]	39.8 ± 5.3	52	0/7

Table 4A.2 Immunophenotyping of Namalwa cell line using single color flow cytometry.

Namalwa cells (1×10^6) were first stained with 10 μg primary mAb followed by 20 μl of an appropriate dilution of FITC-conjugated secondary mAb. Cell associated fluorescence was analyzed on a Becton-Dickinson FACScan using Lysis II software (Beckton Dickinson, San Jose, CA). Background MFI=15-18

Cell surface epitope	Mean Fluorescence intensity (MFI)	% population of gated cells expressing the epitope
CD19	175	99.9
CD20	259	99.1
CD22	30.2	83.9

Therefore future studies should aim at determining the efficacy of DXR-HSPC-SIL[αCD22] using a fresh source of αCD22 in this model. It would also be desirable to compare the combination therapy using VCR instead of DXR.

Another possible explanation for the lack of therapeutic efficacy of DXR-HSPC-SIL[αCD22] lies in the low levels of expression of CD22 on Namalwa cells. Immunophenotyping of Namalwa cells demonstrated that this cell line had a higher expression of CD19 than CD22 (Table 4A.2). Receptor density on target cells seems to be important for determining the efficacy of targeted therapeutics. However, this does not explain why the levels of binding of each immunoliposomal population was approximately the same (Figure 4A.1).

A previous study showed that Namalwa cells which have 3- to 8-fold lower receptor density of CD19 or CD22 respectively, on their surface than Daudi cells, were more than 50 times less susceptible than Daudi cells to immunotoxins against CD19 or CD22 (271). Anti-HER2-targeted liposomal DXR showed improved therapeutic efficacy over non-targeted liposomal DXR in a metastatic model of breast cancer only when cells had 10^5 HER2 receptors per cell (28). Therefore, density of target epiotpe on the surface of malignant cells seems to be an important determinant of therapeutic efficacy of targeted therapeutics. The evaluation of therapeutic efficacy of DXR-HSPC-SIL[αCD22] against a cell line having high levels of CD22 expression (e.g., Daudi) is hence warranted.

CHAPTER 5

CONCLUSIONS AND FUTURE DIRECTIONS

5.1 Summarizing discussion and future directions

Despite several recent advances, cancer chemotherapy is still limited by the lack of specificity to cancer cells, resulting in toxicities to normal cells, and poor therpeutic responses. The toxic side effects often limit optimal dosing of anticancer drugs, leading to disease relapse and the development of drug resistance. Further, the quality of life for patients is severely compromised as a result of these side effects. The goal of anticancer drug discovery and development is to identify therapeutics that have high therapeutic effectiveness with minimal side effects.

One possible approach to improve the selective toxicity of anticancer drugs is by targeting anticancer drugs via monoclonal antibodies (mAbs) or ligands, against antigens or receptors that are expressed on the cancer cells. In this regard, a number of mAb-based therapies like immunotoxins, radioimmunotherapeutics, mAb-drug conjugates and immunoliposomes have received considerable attention. Recent progress in mAb-based therapies is a result of new antibody (Ab) engineering technologies that yielded chimeric or fully human Abs with reduced immunogenicity. The success of Rituxan®, an anti-CD20 mAb, has fueled the enthusiasm of pharmaceutical companies for developing mAbs or mAb-based therapies. In fact, 20% of all biopharmaceuticals, either currently approved or in clinical trials, are mAbs or mAb-based therapies, making this the second largest category of biopharmaceutical products.

Although other mAb-based therapies have gained clinical approval, immunoliposomal anticancer drugs have yet to receive this stage for the treatment of

cancer. In order to produce a clinically viable immunoliposomal formulation, optimization of all components of the immunoliposomal delivery system is required. In this thesis, we tried to answer some of the unresolved questions in the immunoliposomal field, such as: whether whole Abs or Ab fragments are more desirable, which surface epitope, with what characteristics (e.g. internalizing vs. non-internalizing) is the best one to target, and what type of drugs are most suited for immunoliposmal drug delivery. Furthermore, we evaluated if immunoliposomal drugs are therapeutically more effective in combination regimens than when given individually. Liposomal doxorubicin (DXR) or vincristine (VCR) were targeted via whole mAbs or Fab' fragments to the internalizing epitopes (CD19, CD22) or the non-internalizing epitope (CD20), that are expressed on the surface of B-cells.

In chapter 2, we showed that immunoliposomal DXR or VCR, targeted via whole anti-CD19 (αCD19) or via its Fab' fragments (Fab'CD19), had significantly better therapeutic effects in xenografts of human B-cell lymphoma than drug-loaded mAb-free controls or free drugs. It was also shown that DXR-loaded liposomes coupled to Fab' fragments had better therapeutic responses than those coupled to whole mAbs. This was likely because liposomes coupled to Fab' fragments had significantly increased circulation times over liposomes coupled to whole mAbs, which allowed Fab'-coupled liposomes more time to localize to the target cells. The longer circulation times imparted by coupling Fab' fragments instead of whole mAbs to the liposome surface did not significantly improve the therapeutic effectiveness for VCR-containing immunoliposomes. This was probably due to the faster leakage rate

from liposomes of VCR compared to DXR. Therefore, we speculate that Fab' fragments are preferred targeting agents over whole mAbs for immunoliposomes that have slow release rates (DXR), as opposed to those that have faster leakage rates (VCR). However, our speculations are based on the comparison of only two immunoliposomal drugs with different drug leakage rates. Future experiments should compare immunoliposomal formulations of anticancer drugs having a spectrum of different leakage rates to refine these results. We further hypothesize that liposomes coupled to Fab' fragments or even smaller fragments (scFv), will be more suited than whole mAbs for clinical applications since they may both reduce the immune response to murine Abs because they lack the immunogenic Fc portion of the Ab molecule.

In chapter 2, we also observed that immunoliposomes containing a schedule-dependent anticancer drug (VCR) had improved therapeutic outcomes over immunoliposomes containing a schedule-independent drug (DXR). This was in spite of the fact that mice were dosed at 1/3 of the maximum tolerated dose (MTD) for VCR, while DXR was given at the MTD. These results suggest that schedule-dependent drugs such as VCR may represent a rational choice to be developed as liposomal or immunoliposomal drugs because liposomes can help to maintain a sustained exposure of cancer cells to therapeutic drug levels relative to administration of free drugs, which will allow more cells to be exposed to drug at times when they are susceptible to drug effects. Further testing will be needed to verify that this hypothesis applies to other schedule-dependent drugs besides VCR. Future

experiments should compare immunoliposomal formulations of other schedule-dependent drugs such as vinorelbine, topotecan, 5-fluorouracil or methotrexate with schedule-independent drugs such as daunorubicin or cisplatin. The improved therapeutic results observed for VCR-containing liposomes over DXR-containing liposomes could be due to several factors, some of which include: drug-related properties such as mechanisms of resistance, physical and chemical properties of drugs, different release rates of the drugs from liposomes and different routes and rates of intracellular drug delivery.

In our research, some animals were cured at an immunoliposomal VCR dose of 0.66 mg/kg (MTD is 2 mg/kg), but no cures could be obtained for immunoliposomal DXR even at its MTD. Future studies should be performed at higher doses of VCR to investigate the possibility of complete remissions at higher doses

Treatment of xenograft models of human B-cell lymphoma with immunoliposomal drugs resulted in significantly greater increases in survival rates than treatment with free mAbs, drug-free liposomes or combinations of non-targeted liposomes and free mAbs. This indicates that the majority of the observed therapeutic effect was due to specific targeting of the immunoliposomes, rather than to signaling properties of the mAbs, although free whole mAbs and drug-free liposomes conjugated to whole mAbs (but not Fab'fragments) had therapeutic effects that may be due to antibody-dependent cell-mediated cytotoxicity (ADCC) and complement-mediated cytotoxicity (CDC) mechanisms.

Non-targeted liposomal formulations of DXR or VCR had synergistic cytotoxic effects with free mAbs. Although, immunoliposomal drugs resulted in significantly improved therapeutic effects compared with combinations of non-targeted liposomal drugs and signaling free mAbs, it needs to be determined if the cost-benefit ratio for the development of immunoliposomes is at least comparable to that for therapeutic doses of free mAbs combined with non-targeted liposomal drugs. Several clinical trials have demonstrated superior response of combinations of free drugs and mAbs compared with those achieved with either treatment alone (90, 93). In such a scenario, we need to see if immunoliposomal drugs can offer a less toxic, more effective and economic alternative to conventional therapies.

A recent study demonstrated that the homodimerization of mAbs converts them into strong signaling therapeutics (184). We could not demonstrate these effects by the multivalent display of whole mAbs or Fab' fragments on the surface of liposomes, at least at the Ab densities employed in our experiments. However, it is possible that signaling mechanisms will be facilitated by increasing the density of whole mAbs or Fab' fragments on the liposome surface, i.e., by decreasing the intermolecular distance between them.

High mAb densities on the liposome surface should increase the mAb avidity for the antigen. A concern with increasing the density of whole mAbs at the liposome surface is that it has been shown to lead to a decrease in circulation half-lives of the immunoliposomes (58). As the pharmacokinetics of Fab'-coupled liposomes appears

not to be compromised by high fragment densities, further studies should evaluate the effects of high Fab' density on the therapeutic efficacy of immunoliposomes.

Chapters 3 and 4 examine the effect of targeting to different B-cell epitopes, individually and in combination. It is generally accepted in the field of immunoliposomes that targeting of immunoliposomal drugs to internalizing epitopes is necessary for good therapeutic responses. Ideally, liposomes should retain encapsulated drugs until the liposomes reach the target cells and then they should release the drug so that it becomes bioavailable (drug entrapped in liposomes is not bioavailable). Our results showed that immunoliposomes having slow release rates of DXR had improved therapeutic effects when they were targeted to the internalizing epitope, CD19. Internalizing epitopes facilitate the delivery of the drug liposome package inside the cells via receptor-mediated endocytosis. Intracellular breakdown of the liposomes leads to release of the drugs, but this process appears to be slower than desired (108). In support of the use of internalizing epitopes, a recent study has demonstrated that a Stealth® liposomal formulation of cisplatin that lacked efficacy in pilot clinical studies (due to extremely slow drug leakage rates from the liposomes), when converted into an immunoliposome and targeted to an internalizing epitope, gave good therapeutic results (272).

Immunoliposomal VCR, with its faster release rates, had equivalent therapeutic effects when targeted to either internalizing or non-internalizing epitopes. The mechanism underlyng this effect is not currently understood. However it appears that drugs having faster release rates from the liposomes may be able to achieve

cytotoxic concentrations within the cell either by internalization or by drug release at the cell periphery. However, it remains to be seen whether our conclusions in regard to leakage rates have applications to a wider range of drugs that act by different mechanisms of action, or only to the two drugs examined in this thesis.

Although drug release rates can be manipulated to some extent by changing the lipid compositions of liposomes, in reality, control over drug release rates is not always easy to achieve for some immunoliposomal anticancer drugs. At the two extremes, liposomes with extremely fast rates of drug release may release their contents in the blood prior to reaching the target cells; liposomes with very slow drug release rates may retain the contents even after localizing to the target cells, resulting in low bioavailability of the drug. We believe that an important reason for the high therapeutic efficacy seen with VCR-containing immunoliposomes in this thesis was that the drug release rate may have been close to optimal. The $t_{1/2}$ (time for 50% of the drug to be released from liposomes) of VCR-containing immunoliposomes was of the order of 7-15 h *in vitro* and *in vivo*, which would have allowed liposomes to bind to the malignant B-cells before they released their drug.

In chapter 3, empty liposomes targeted with a non-internalizing mAb, anti-CD20 (αCD20) were not very effective in treating mice bearing Namalwa cells, even though αCD20 is reported to be a strong signaling mAb (186, 187, 196-198). However, it needs to be pointed out that in these studies, each mouse received around 10-15 μg of αCD20-conjugated to immunoliposomes. To obtain therapeutic efficacy, other researchers have injected mg quantities of mAbs into mice, so the amount of

mAb attached to the liposomes may not have been sufficient to effect a response (184, 186, 187).

In chapters 4 and 4A, we show that combination regimens of immunoliposomal drugs worked well for certain combinations of target eptiopes and drugs but not for others. When injected with a combination of VCR-loaded immunoliposomes targeted to both CD19 and CD20, a higher percentage of cures (over 70%) was obtained than for either type of immunoliposome given alone, suggesting that some additivity is occuring. Since DXR-loaded immunoliposomes targeted to CD20 alone had no improved effect over non-targeted liposomes, combinations of DXR-loaded immunoliposomes targeted to both CD19 and CD20 did not improve the therapeutic effects over liposomes targeted to CD19 alone.

Unexpectedly, in our model, targeting of immunoliposomal DXR to two internalizing epitopes (CD19 and CD22), did not improve the therapeutic outcome compared to targeting of DXR-loaded liposomes to CD19 alone. As described in chapter 4A, the biological activity of αCD22, might have been compromised due to long period of storage, even though αCD22 still retained good binding activity. Further studies using a fresh batch of αCD22 are warranted. Immunotoxin combinations directed against CD19 and CD22 have demonstrated improved therapeutics in animal xenografts compared to single immunotoxin therapy (99, 265, 273), and this combination is presently in clinical trials (274). Therefore we recommend that immunoliposomal anticancer drug combinations against CD19 and CD22 be reevaluated in the Namalwa model or evaluated in another model of B-

lymphoma (e.g., Daudi), where expression of CD22 is documented to be much higher than that in Namalwa cells (271). Although the relationship of antigen density to therapeutic efficacy is still not clear, evidence is now accumulating that indicates that high receptor densities may be important for effective targeted therapies (28, 271). One way to increase the total number of target epitopes on the cell surface is to target to more than one epitope. More research on rational combinations of immunoliposomal drugs, targeted to epitopes that are internalized and expressed at high densities on target cells, is hence warranted.

5.2 Clinical applications of immunoliposomal anticancer drugs

5.2.1 Immunoliposomal anticancer drugs in the treatment of hematological malignancies

This thesis evaluated the applicability of immunoliposomal DXR and VCR, for the treatment of B-cell lymphoma, a hematological malignancy in murine xenograft models. Despite recent advances in the treatment of B-cell lymphomas, standard chemotherapeutic regimens are only effective in patients with low-grade B-cell lymphomas. For patients with intermediate and aggressive B-cell lymphomas, conventional chemotherapy or hematopoietic stem cell transplantation is generally ineffective and disease relapse eventually occurs. Although patients may respond to alternative chemotherapy or radiotherapy, the potential for long-term curative therapy in these relapsed patients is low. Furthermore, conventional chemotherapeutics are associated with severe side effects. Therefore, new therapeutic strategies with high efficacies and lower toxicities are needed.

We postulate that hematological malignancies are excellent targets for immunoliposomal anticancer drugs because in comparison to solid tumors, cells are more readily accessible to systemically administered immunoliposomes. In our studies, immunoliposomal drugs were targeted to lineage-restricted antigens (CD19, CD20 and CD22) that have little or no expression on stem cells (B-cell progenitors). Therefore, stem cells are expected to replace the normal lymphocytes killed during therapy. Further, CD19 and CD20 are expressed on more than 90 % of B-cell malignancies, and therefore immunoliposomal formulations of DXR or VCR developed in this thesis will be suited for a wide variety of B-cell lymphomas. For example, liposomal drugs targeted to CD19 or CD20 could be used for most of the non-Hodgkin's lymphomas such as chronic lymphocytic leukemia, precursor B-cell lymphoblastic lymphoma, follicular lymphoma or Burkitt's lymphoma. High levels of expression of the CD22 antigen is seen on fewer types of B-cell neoplasms than the CD19 or the CD20 antigen (271), which makes it a less attractive target.

The results presented in this thesis suggest that immunoliposomal VCR or DXR targeted to CD19 or CD20 may have important clinical applications. We obtained long-term survivors with immunoliposomal formulations of the high potency, schedule-dependent drug, VCR, targeted to either CD19 or CD20, or to both, in combination. A classical (non-PEGylated) liposomal formulation of VCR (Onco-TCS) is presently undergoing clinical trials at Inex Pharmaceuticals, Vancouver, B.C. (237, 238). Inex Pharmaceuticals chose a non-PEGylated formulation of VCR since they were concerned that insertion of PEG on VCR

liposomes would increase the leakage of VCR from the liposomes to unacceptable levels (by an as yet unknown mechanism) (252). This is not so much of a concern for targeted liposomes, where the binding of the immunoliposomes to cells results in fast uptake of the drug. Results presented in this thesis show that coupling mAbs to the PEG terminus did not further increase the leakage of VCR from the liposomes, but it significantly improved the therapeutic outcomes. The improvement was likely because the targeted liposomal formulations of VCR could deliver the drug to the target cells before most of the drug is released from liposomes. Hence, liposomal formulations of VCR targeted to B cell epitopes (e.g., CD19, CD20) may represent a rational choice for clinical development.

The therapeutic effectiveness of DXR-loaded liposomes could be increased by targeting the liposomes via Fab' fragments instead of whole mAbs and targeting to internalizing epitopes instead of non-internalizing epitopes. Stealth® formulations of DXR (Doxil®/Caelyx® and Myocet®) and another anthracycline drug, daunorubicin (Daunosome®) have already received clinical approval. The effectiveness of Stealth® immunoliposomal formulations of DXR has previously been evaluated in a number of animal models. We speculate that Stealth® immunoliposomal formulations of DXR or other anthracyline drugs targeted via small Ab fragments (Fab' or single chain Fv) to internalizing epitopes (e.g., CD19, CD22) is also a logical strategy to treat B-cell malignancies. In fact a Stealth® immunoliposomal formulation of DXR targeted via scFv against the human epidermal growth factor (HER2), has received approval for clinical trials for the treatment of breast cancer (28).

We evaluated the applicability of immunoliposomal drugs targeted to B-cell surface epitopes (CD19, CD20 and CD22). It is reasonable to suggest that the insights gained from these studies can be applied for targeting liposomal anticancer drugs to other hematological malignancies. For example, immunoliposomal anticancer drugs (e.g. immunoliposomal DXR or VCR) can have therapeutic potential for the treatment of multiple myeloma. Multiple myeloma is a cancer characterized by terminally differentiated malignant B-cells that have low levels of B-cell differentiation antigens such as CD19, CD20 or CD22. However, they have a strong expression of CD38. Liposomal anticancer drugs targeted via anti-CD38, should be an effective strategy for the treatment of multiple myeloma. Other examples could be targeting liposomal anticancer drugs to CD33, a leukocyte differentiation antigen for the treatment of acute myeloid leukemia (AML), or targeting to CD52, a cytoadhesion molecule for the treatment of B-cell chronic lymphocytic leukemia (B-CLL).

5.2.2 Immunoliposomal anticancer drugs targeted to solid tumors

Immunoliposomal anticancer drugs can also be used for the treatment of solid tumors, by targeting them to tumor-associated or tumor-specific antigens. Some targets that are being explored include HER2 for the treatment of breast cancer, MUC1 for the treatment of breast and bladder cancer, or CEA for the treatment of ovarian cancer. A review of literature and our experience lead us to believe that for solid tumors, immunoliposomes would probably be more suited for the treatment of

CANADIAN THESIS
THESES CANADIENNES

SAPRA, Puja
ANTIBODY-TARGETED LIPOSOMAL ANTICANCER DRUGS FOR THE ...

ISBN 0-612-88043-5
NQ-88043

residual, micrometastatic disease, following primary therapy of solid tumors by surgery and/or radiation (2, 233).

An attractive strategy for the treatment of solid tumors is the targeting of immunoliposomal cytotoxic drugs to the neovasculature of solid tumors, where immunoliposomes would have easy access. Targeting of mAb-based therapies against the tumor vasculature is currently an area of considerable interest (275-279). Directing therapy to antigens selectively expressed on the vascular endothelium, as opposed to directing them against tumor-associated antigens, is expected to reduce the impact of physical barriers that impede the penetration and uniform distribution of mAbs throughout the tumor, e.g., heterogeneous blood flow and elevated interstitial pressure (280, 281). In a recent study, it was shown that drug-loaded liposomes, targeted using peptides specific for tumor angiogenic vasculature, resulted in a significant suppression of tumor growth compared to non-targeted liposomes or free drugs (147). The authors also outlined some additional advantages of anti-neovascular therapy, including the occurrence of little or no drug resistance and the potential for effectiveness against essentially all types of solid tumors (147, 282). A number of receptors specifically expressed on tumor vascular endothelium have now been identified and these can be exploited for liposome-based anticancer drug delivery (reviewed in (277, 278)).

5.2.3 Combination therapies with immunoliposomal drugs

With rare exceptions, chemotherapy is provided as a combination of drugs or therapeutics in order to achieve the maximum therapeutic results. The rationale for

the use of multiple agents takes into consideration heterogeneity within tumor cell populations and differences in tumor cell sensitivity to individual drug classes. Combination chemotherapy generally includes drugs or therapeutics with different mechanisms of action and non-overlapping side effects in order to attain maximum therapeutic benefit.

Liposomal anticancer drugs targeted via signaling Abs is an interesting strategy for combination therapy because it combines the therapeutic benefits of the encapsulated drug and the signaling Ab. Although liposomal or immunoliposomal drugs may be active as single agents, it is likely that their major role will be in combination therapy regimens. Combination strategies with immunoliposomes may include either targeting different liposomal drugs to the same epitope, or targeting the same liposomal drug to different epitopes or targeting different liposomal drugs to different epitopes. By using any of these combinations, we are basically combining the benefits of multiple anticancer therapeutics, which work via different mechanisms of action and have non-overlapping side effects. For example, in clinic, if we treat patients having B-cell malignancies with immunoliposomal DXR targeted to CD19 and immunoliposomal VCR targeted to CD20, we combine the therapeutic benefits of DXR, VCR, anti-CD19 and anti-CD20. In a previous study, combination therapy with low doses of Stealth® formulations of both DXR and VCR was shown to be more effective in the treatment of MC2 mammary tumors than higher doses of either liposomal drug alone (283, 284). Overall, immunoliposomal anticancer drugs, which

combine the therapeutic effects of chemotherapeutic drugs and signaling antibodies are an attractive, less toxic option for the treatment of B-cell malignancies.

Immunoliposomal anticancer drugs can also be targeted to multiple epitopes using bispecific or multispecific Abs. Considerable research has focused on bispecific Abs, and bispecific anti-CD16/CD30 and anti-CD3/CD19 Abs have undergone PhaseI/II trials (285, 286). Targeting of immunoliposomes to multiple epitopes may help enhance tumor-specific cytotoxicity and decrease problems of multidrug resistance and relapse.

It is expected that future clinical studies try to maximize tumor cell kill by combining various traditional and targeted therapies in an effort to eliminate large tumor masses, metastatic diseases, dormant cells, antigen negative cells. For example, liposomal VCR has been substituted for the free drug Oncovin® in clinical trials using the CHOP + Rituxan® regimen. One can envision that immunoliposomal anticancer drugs (e.g., liposomal VCR targeted via anti-CD20) could also be evaluated in place of free drugs and free mAbs within an established combination regimen such as CHOP + Rituxan®. Immunoliposomal drugs can also be tried in combination with other mAb-based therapies like immunotoxins, Ab-drug conjugates and radioimmunotherapeutics.

5.2.4 Immunoliposomes in the treatment of multidrug resistance

Multidrug resistance can severely limit the effectiveness of chemotherapeutic agents. A variety of multidrug resistant (MDR) transporters such as P-glycoprotein (Pgp) localize in the cell membrane and extrude a variety of chemotherapeutic agents

such as VCR or DXR from the tumor cells. The delivery of immunoliposomes by receptor-mediated internalization provides an alternative route of entry for drugs into cells, which may allow immunoliposomal anticancer drugs to bypass the activity of MDR transporters.

5.3 Barriers and solutions to the clinical approval of immunoliposomes

Problems with immunogenicity are still a barrier to the clinical approval of ligand-targeted therapeutics. In this regard, the immunoliposomal field should benefit from recent advances in Ab engineering and molecular biology, which make it possible to engineer small chimeric or humanized Ab fragments (123, 124) that should lead to further reductions in human anti-mouse antibody (HAMA) responses in patients. Fully human mAbs, generated from transgenic mice that express the human H- and L-chain gene repertoire (287) might prove to be even more acceptable targeting agents for immunoliposomes. Although the development of humanized and fully human Abs can help resolve immunological concerns, immunogenic responses to liposomes coupled to humanized or fully human antibodies may still occur, but this remains to be determined.

From a pharmaceutical standpoint, ligand-targeted liposomes (LTLs) or immunoliposomes will have to meet the quality criteria as defined for pharmaceutical products. Issues like shelf stability, sterilization and scale-up of production require extra consideration for complex delivery systems like immunoliposomes. Another concern that can hinder the development of LTLs in the clinic is the impracticality of manufacturing a wide array of LTLs. In the post-genomic era we can envision

chemotherapy tailored to a specific patient's disease. LTLs can be made from ligands and drugs selected from a library that is based on the patient's receptor status and tumor sensitivity, respectively. Given the number of ligands and drugs available, it will be difficult to construct patient-selective LTLs by conventional ligand coupling techniques. The development of a combinatorial approach that allows a variety of LTLs to be produced by post-inserting ligands on preformed liposomes is an attractive strategy and warrants further investigation (74, 80).

5.4 Future directions in the field of immunoliposomal drugs

This thesis points to the necessity of careful selection of targeting ligands and epitopes. The immunoliposomal field should benefit from recent advances made in molecular biology, like phage display technology, which can help in the identification of internalizing ligands or mAbs with different affinities (109-111). Currently it is not clear whether mAbs with high affinity or low affinity are preferable. There are arguments in favor of either one. For example, it is thought that low affinity mAbs may be able to penetrate solid tumors with more ease than those with high affinities (131, 146). Phage display technology can also be used to select tumor-associated antigens by using a subtractive panning approach, by selecting mAbs that react against tumor cells but not against the normal cells (288).

Internalization of immunoliposomes leading to intercellular delivery of the liposomal drug packages, will lead to improved therapeutic effects only if the majority of the drug reaches to its site of action (e.g., nucleus or mitochondria) within the cell as free drug, i.e., the drug has to be bioavailable. In this regard, more

sophisticated systems to control (or titrate) the rate of drug release from immunoliposomes are needed to ensure high levels of bioavailable drug following internalization. pH-sensitive phospholipids, peptides and polymers associated with liposomes are all being explored as a means of triggering (or controlling) drug release (reviewed in (138)).

Clinical applications in humans may require repeated administration of liposomes to achieve maximum benefit. Considering this, extensive basic research needs to be performed to have a better appreciation of the effects of the dose schedule and dose intensity for multiple dosing of immunoliposomal drugs.

5.5 Conclusions

In conclusion, we have identified a number of factors, including internalization of the immunoliposomes, their circulation half-lives, drug release rates, cellular density of target epitopes, and properties of the encapsulated drug, that should be taken into consideration for designing effective immunoliposomal anticancer drugs. For DXR-containing immunoliposomes optimal strategies might involve manipulating the drug release rate to more rapidly achieve high levels of bioavailable drug intracellularly, targeting the liposomes via Fab' or scFv fragments, and targeting to internalizing epitopes. For immunoliposomes containing the high potency, schedule-dependent drug, VCR, targeting via either whole Abs or Fab' fragments and targeting to either internalizing or non-internalizing epitopes appears to be equally effective, although Fab' or smaller fragments will likely have an advantage in reducing immunogenicity. Immunoliposomes containing VCR appear to give

better therapeutic results than DXR-containing immunoliposomes and targeting of VCR-containing liposomes to multiple epitopes gave the best therapeutic results in our xenograft models. The results presented in this thesis demonstrate that selective targeting of liposomal VCR and/or DXR to various B-cell epitopes improves the selective toxicity of these anticancer drugs and hence is an effective strategy for treating B-cell malignancies. The insights gained from these studies will help in designing better immunoliposomal anticancer drugs. It is reasonable to suggest that with further refinement, immunoliposomal anticancer drugs will soon garner acceptance by the clinical medical community.

REFERENCES

1. Linenberger, M. L., Maloney, D. G., and Bernstein, I. D. Antibody-directed therapies for hematological malignancies. Trends Mol. Med., *8:* 69-76, 2002.

2. Allen, T. M. Ligand-targeted therapeutics in anticancer therapy. Nature Rev.Cancer, *2:* in 750-763, 2002.

3. Milenic, D. E. Monoclonal antibody-based therapy strategies: providing options for the cancer patient. Curr. Pharm. Des., *8:* 1749-1764, 2002.

4. Chabner, B. A., Allegra, C. J., Curt, G. A., and Calabresi, P. Antineoplatic agents. In: J. G. Hardman, E. Limbird, P. B. Molinoff, R. W. Ruddon, and A. G. Gilman (eds.), Goodman and Gilman's the pharmacological basis of therapeutics, 9 edition, pp. 1233-1288: McGraw Hill, 1996.

5. Bangham, A. D., Standish, M. M., and Watkins, J. C. Diffusion of univalent ions across the lamellae of swollen phospholipids. J. Mol. Biol., *13:* 238-252, 1965.

6. Gregoriadis, G. and Ryman, B. E. Liposomes as carriers of enzymes or drugs: a new approach to the treatment of storage diseases. Biochem. J., *124:* 58P, 1971.

7. Allen, T. M. and Chonn, A. Large unilamellar liposomes with low uptake into the reticuloendothelial system. FEBS Lett., *223:* 42-46, 1987.

8. Gabizon, A. and Papahadjopoulos, D. Liposome formulations with prolonged circulation time in blood and enhanced uptake by tumors. Proc. Natl. Acad. Sci. U S A, *85:* 6949, 1988.

9. Papahadjopoulos, D. and Gabizon, A. Liposomes designed to avoid the reticuloendothelial system. Prog. Clin. Biol. Res., *343*: 85-93, 1990.

10. Allen, T. M. and Hansen, C. B. Pharmacokinetics of Stealth versus conventional liposomes: effect of dose. Biochim. Biophys. Acta, *1068:* 133-141, 1991.

11. Allen, T. M. and Stuart, D. Liposome pharmacokinetics: classical, sterically stabilized, cationic liposomes and immunoliposomes, pp.63-97 New York: Marcel Dekker, Inc., 1998.

12. Matsumura, Y. and Maeda, H. A new concept for macromolecular therapeutics in cancer chemotherapy; mechanism of tumoritropic accumulation of proteins and the antitumor agent SMANCS. Cancer Res., *6:* 6387-6392, 1987.

13. Jain, R. K. Transport of molecules across tumor vasculature. Cancer Metastasis Rev., *6(4)* 559-593, 1987.

14. Huang, S. K., Martin, F. J., Jay, G., Vogel, J., Papahadjopoulos, D., and Friend, D. S. Extravasation and transcytosis of liposomes in Kaposi's sarcoma-like dermal lesions of transgenic mice bearing the HIV tat gene. Am. J. Pathol., *143:* 10-14, 1993.

15. Yuan, F., Leunig, M., Huang, S. K., Berk, D. A., Papahadjopoulos, D., and Jain, R. K. Microvascular permeability and interstitial penetration of sterically stabilized (Stealth) liposomes in a human tumor xenograft. Cancer Res., *54:* 3352-3356, 1994.

16. Hobbs, S., Monsky, W. L., Yuan, F., Roberts, W. G., Griffith, L., Torchillin, V. P., and Jain, R. K. Regulation of transport pathways in tumor vessels: role of tumor type and microenvironment. Proc. Natl. Acad. Sci. USA, *95:* 4607-4612, 1998.

17. Jain, R. K. Physiological barriers to delivery of monoclonal antibodies and other macromolecules in tumors. Cancer Res., *50:* 814s-819s, 1990.

18. Northfelt, D. W., Martin, F. J., Working, P., Volberding, P. A., Russell, J., Newman, M., Amantea, M. A., and Kaplan, L. D. Doxorubicin encapsulated in liposomes containing surface-bound polyethylene glycol: pharmacokinetics, tumour localization, and safety in patients with AIDS-related Kaposi's sarcoma. J. Clin. Pharmacol., *36:* 55-63, 1996.

19. Woodle, M. C. and Storm, G. (eds.) Long-circulating Liposomes: Old Drugs New Therapeutics, pp. 1-206. Georgetown, TX: Landes Bioscience, 1998.

20. Allen, T. M. Drug delivery. In: E. Cooper (ed.), PharmaTech, pp. 154-160. London: World Markets Research Centre, 2000.

21. Harrington, K. J. Liposomal cancer chemotherapy: current clinical applications and future prospects. Expert Opin. Investig. Drugs., *10(6):* 1045-1061, 2001.

22. Lee, R. J. and Low, P. S. Folate-mediated tumor cell targeting of liposome-entrapped doxorubicin in vitro. Biochim. Biophys. Acta, *1233:* 134-144, 1995.

23. Wang, S., Lee, R. J., Cauchon, G., Gorenstein, D. G., and Low, P. S. Delivery of antisense oligodeoxyribonucleotides against the human epidermal growth factor

receptor into cultured KB cells with liposomes conjugated to folate via polyethylene glycol. Proc. Natl. Acad. Sci. USA., *92:* 3318-3322, 1995.

24. Lopes de Menezes, D. E., Pilarski, L. M., and Allen, T. M. In vitro and in vivo targeting of immunoliposomal doxorubicin to human B-cell lymphoma. Cancer Res., *58:* 3320-3330, 1998.

25. Gabizon, A., Horowitz, A. T., Goren, D., Tzemach, D., Mandelbaum-Shavit, F., Qazen, M. M., and Zalipsky, S. Targeting folate receptor with folate linked to extremities of poly(ethylene glycol)-grafted liposomes: in vitro studies. Bioconjugate Chem., *10:* 289-298, 1999.

26. Goren, D., Horowitz, A. T., Tzemack, D., Tarshish, M., Zalipsky, S., and Gabizon, A. Nuclear delivery of doxorubicin via folate-targeted liposomes with bypass of multidrug-resistance efflux pump. Clin. Cancer Res., *6:* 1949-1957, 2000.

27. Sugano, M., Egilmez, N. K., Yokota, S. J., Chen, F. A., Harding, J., Huang, S. K., and Bankert, R. B. Antibody targeting of doxorubicin-loaded liposomes suppresses the growth and metastatic spread of established human lung tumor xenografts in severe combined immunodeficient mice. Cancer Res., *60:* 6942-6949, 2000.

28. Park, J. W., Hong, K., Kirpotin, D. B., Colbern, G., Shalaby, R., Baselga, J., Shao, Y., Nielsen, U. B., Marks, J. D., Moore, D., Papahadjopoulos, D., and Benz, C. C. Anti-HER2 immunoliposomes: Enhanced efficacy attributable to targeted delivery. Clin. Cancer Res., *8:* 1172-1181, 2002.

29. Pan, X. Q., Zheng, X., Shi, G., Wang, H., Ratnam, M., and Lee, R. J. Strategy for the treatment of acute myelogenous leukemia based on folate receptor -targeted liposomal doxorubicin combined with receptor induction using all-trans retinoic acid. Blood, *100:* 594-602, 2002.

30. Iinuma, H., Maruyama, K., Okinaga, K., Sasaki, K., Sekine, T., Ishida, O., Ogiwara, N., Johkura, K., and Yonemura, Y. Intracellular targeting therapy of cisplatin-encapsulated transferrin-polyethylene glycol liposome on peritoneal dissemination of gastric cancer. Int. J. Cancer, *99:* 130-137, 2002.

31. Reddy, J. A., Abburi, C., Hofland, H., Howard, S. J., Vlahov, I., Wils, P., and Leamon, C. P. Folate-targeted, cationic liposome-mediated gene transfer into disseminated peritoneal tumors. Gene Ther., *9*: 1542-1550, 2002.

32. Pastorino, F., Brignole, C., Marimpietri, D., Sapra, P., Moase, E., Allen, T. M., and Ponzoni, M. Doxorubicin-loaded Fab' fragments of anti-disialoganglioside immunoliposomes selectively inhibit the growth and dissemination of human neuroblastoma in nude mice. Cancer Res., *63:* 86-92, 2003.

33. Woodle, M. C. and Papahadjopoulos, D. Liposome preparation and size characterization. Meth. Enzymol., *171:* 193-217, 1989.

34. Szoka, F. and Papahadjopoulos, D. Procedure for preparation of liposomes with large internal aqueous space and high capture by reverse-phase evaporation. Proc. Natl. Acad. Sci. USA, *75:* 4194-4198, 1978.

35. Hope, M. J., Bally, M. B., Mayer, L. D., Janoff, A. S., and Cullis, P. R. Generation of multilamellar and unilamellar phospholipid vesicles. Chem. Phys. Lipids, *40:* 89-96, 1986.

36. Phillipot, J. R. and Liautard, J. P. A very mild method allowing the encapsulation of very high amounts of macromolecules into very large (1000 nm) unilamellar liposomes. In: G. Gregoriadis (ed.), Liposome technology: liposome preparation and related techniques, Vol. 1, pp. 81-98. Boca Raton, FL.: CRC Press, 1993.

37. Batzri, S. and Korn, E. D. Single bilayer liposomes prepared without sonication. Biochim. Biophys. Acta, *16:* 1015-1019, 1973.

38. Kirby, C. and Gregoriadis, G. Dehydration-rehydration vesicles (DRV): a new method for high yield drug entrapment in liposomes. Biotechnology, *2:* 979-984, 1984.

39. Olson, F., Hunt, C. A., Szoka, F. C., Vail, W. J., and Papahadjopoulos, D. Preparation of liposomes of defined size distribution by extrusion through polycarbonate membranes. Biochim. Biophys. Acta, *557:* 9-23, 1979.

40. Mayer, L. D., Hope, M. J., Cullis, P. R., and Janoff, A. S. Solute distributions and trapping efficiencies observed in freeze-thawed multilamellar vesicles. Biochim. Biophys. Acta, *817:* 193-196, 1985.

41. Huang, C. H. Studies on phosphatidylcholine vesicles: formation and physical characteristics. Biochemistry, *8:* 344-352, 1969.

42. Talsma, H., Ozer, A. Y., Van Bloois, L., and Crommelin, D. J. A. The size reduction of liposomes with high pressure homogenizer (microfluidizer). Characterization of prepared dispersion and comparison of conventional methods. Drug Dev. Ind. Pharm., *15:* 197-207, 1989.

43. Barenholz, Y., Amselem, S., and Lichtenberg, D. A new method for the preparation of phospholipid vesicles (liposomes) French Press. FEBS Lett., *99:* 210-213, 1979.

44. Mayer, L. D., Hope, M. J., and Cullis, P. R. Vesicles of variable sizes produced by a rapid extrusion procedure. Biochim. Biophys. Acta, *858:* 161-168, 1986.

45. Defrise-Quertain, F., Chatelain, P., Delmelle, M., and Ruysschaert, J. Model studies for drug entrapment and liposome stability. In: G. Gregoriadis (ed.), Liposome Technology, Vol. 2, pp. 1-17. Boca Raton, FL: CRC Press, Inc., 1984.

46. Drummond, D. C., Meyer, O., Hong, K. L., Kirpotin, D. B., and Papahadjopoulos, D. Optimizing liposomes for delivery of chemotherapeutic agents to solid tumors. Pharmacol. Rev., *51:* 691-743, 1999.

47. Ginevra, F., Biffanti, S., Pagnan, A., Biolo, R., Reddi, E., and Jori, G. Delivery of the tumour photosensitizer zinc(II)-phthalocyanine to serum proteins by different liposomes: studies in vitro and in vivo. Cancer Lett., *49:* 59-65, 1990.

48. Lopes de Menezes, D. E. Targeting of immunoliposomal doxorubicin. Pharmacology, pp. 1-280. Edmonton: University of Alberta, 1998.

49. Mayer, L. D., Bally, M. B., Hope, M. J., and Cullis, P. R. Techniques for encapsulating bioactive agents into liposomes. Chem. Phys. Lipids, *40:* 333-345, 1986.

50. Bolotin, E. M., Cohen, R., Bar, L. K., Emanuel, S. N., Lasic, D. D., and Barenholz, Y. Ammonium sulphate gradients for efficient and stable remote loading of amphipathic weak bases into liposomes and ligandosomes. J. Liposome Res., *4:* 455-479, 1994.

51. Boman, N. L., Masin, D., Mayer, L. D., Cullis, P. R., and Bally, M. B. Liposomal vincristine which exhibits increased drug retention and increased circulation longevity cures mice bearing P388 tumors. Cancer Res., *54:* 2830-2833, 1994.

52. Nichols, J. W. and Deamer, D. W. Catecholamine uptake and concentration by liposomes maintaining pH gradients. Biochim. Biophys. Acta, *455:* 269-271, 1976.

53. Mayer, L. D., Bally, M. B., Hope, M. J., and Cullis, P. R. Uptake of antineoplastic agents into large unilamellar vesicles in response to a membrane potential. Biochim. Biophys. Acta, *816:* 294-302, 1985.

54. Mayer, L. D., Bally, M. B., Loughrey, H., Masin, D., and Cullis, P. R. Liposomal vincristine preparations which exhibit decreased drug toxicity and increased activity against murine L1210 and P388 tumors. Cancer Res., *50:* 575-579, 1990.

55. Madden, T. D., Harrigan, P. R., Tai, L. C., Bally, M. B., Mayer, L. D., Redelmeier, T. E., Loughrey, H. C., Tilcock, C. P., Reinish, L. W., and Cullis, P. R. The accumulation of drugs within large unilamellar vesicles exhibiting a proton gradient: a survey. Chem. Phys. Lipids, *53:* 37-46, 1990.

56. Haran, G., Cohen, R., Bar, L. K., and Barenholz, Y. Transmembrane ammonium sulfate gradients in liposomes produce efficient and stable entrapment of amphipathic weak bases. Biochim. Biophys. Acta, *1151:* 201-215, 1993.

57. Lasic, D. D., Frederik, P. M., Stuart, M. C., Barenholz, Y., and McIntosh, T. J. Gelation of liposome interior. A novel method for drug encapsulation. FEBS Lett., *312:* 255-258, 1992.

58. Allen, T. M., Brandeis, E., Hansen, C. B., Kao, G. Y., and Zalipsky, S. A new strategy for attachment of antibodies to sterically stabilized liposomes resulting in efficient targeting to cancer cells. Biochim. Biophys. Acta, *1237:* 99-108, 1995.

59. Hansen, C. B., Kao, G. Y., Moase, E. H., Zalipsky, S., and Allen, T. M. Attachment of antibodies to sterically stabilized liposomes: evaluation, comparison and optimization of coupling procedures. Biochim. Biophys. Acta, *1239:* 133-144, 1995.

60. Kirpotin, D., Park, J. W., Hong, K., Zalipsky, S., Li, W.-L., Carter, P., Benz, C. C., and Papahadjopoulos, D. Sterically stabilized anti-HER2 immunoliposomes: design and targeting to human breast cancer cells in vitro. Biochemistry, *36:* 66-75, 1997.

61. Allen, T. M., Hansen, C. B., and Zalipsky, S. Antibody-targeted Stealth® liposomes. In: D. D. Lasic and F. Martin (eds.), Stealth Liposomes, pp. 193-202. Boca Raton, FL: CRC Press, Inc., 1995.

62. Allen, T. M., Hansen, C. B., and Stuart, D. D. Targeted sterically stabilized liposomal drug delivery. In: D. D. Lasic and D. Papahadjopoulos (eds.), Medical Applications of Liposomes, pp. 297-323. Amsterdam: Elsevier Science Publishers, 1998.

63. Aragnol, D. and Leserman, L. Immune clearance of liposomes inhibited by an anti-Fc receptor antibody in vivo. Proc. Natl. Acad. Sci. U S A, *83:* 2699-2703, 1986.

64. Debs, R. J., Heath, T. D., and Papahadjopoulos, D. Targeting of anti-Thy 1.1 monoclonal antibody conjugated liposomes in Thy 1.1 mice after intravenous administration. Biochim. Biophys. Acta, *901:* 183-190, 1987.

65. Derksen, J. T. P., Morselt, H. W. M., and Scherphof, G. L. Uptake and processing of immunoglobulin-coated liposomes by subpopulations of rat liver macrophages. Biochim. Biophys. Acta, *917:* 127-136, 1988.

66. Klibanov, A. L., Maruyama, K., Beckerleg, A. M., Torchilin, V. P., and Huang, L. Activity of amphipathic poly(ethyleneglycol) 5000 to prolong the circulation time of liposomes depends on the liposome size and is unfavorable for immunoliposome binding to target. Biochim. Biophys. Acta, *1062:* 142-148, 1991.

67. Maruyama, K., Takizawa, T., Takahashi, N., Tagawa, T., Nagaike, K., and Iwatsuru, M. Targeting efficiency of PEG-immunoliposome-conjugated antibodies at PEG terminals. Adv. Drug Del. Rev., *24:* 235-242, 1997.

68. Blume, G. and Cevc , G. Molecular mechanism of the lipid vesicle longevity in vivo. Biochim. Biophys. Acta, *1146:* 157-168, 1993.

69. Maruyama, K., Takizawa, T., Yuda, T., Kennel, S. J., Huang, L., and Iwatsuru, M. Targetability of novel immunoliposomes modified with amphipathic poly(ethylene glycol)s conjugated at their distal terminals to monoclonal antibodies. Biochim. Biophys. Acta, *1234:* 74-80, 1995.

70. Allen, T. M., Hansen, C. B., and Zalipsky, S. Antibody-targeted Stealth® liposomes, p. 193-202. Boca Raton, FL: CRC Press, Inc., 1995.

71. Allen, T. M., Agrawal, A. K., Ahmad, I., Hansen, C. B., and Zalipsky, S. Antibody-mediated targeting of long-circulating (Stealth®) liposomes. J. Liposome Res., *4:* 1-25, 1994.

72. Zalipsky, S. Synthesis of end-group functionalised polyethylene glycol-lipid conjugates for preparation of polymer-grafted liposomes. Bioconjugate Chem., *4:* 296-299, 1993.

73. Iden, D. L. A novel method to prepare ligand-targeted liposomes. Pharmacology, pp. 152. Edmonton: University of Alberta, 2001.

74. Iden, D. L. and Allen, T. M. In vitro and in vivo comparison of immunoliposomes made by conventional coupling techniques with those made by a new post-insertion technique. Biochim. Biophys. Acta, *1513:* 207-216, 2001.

75. Martin, F. J., Hubbell, W. l., and Papahadjopoulos, D. Immunospecific targeting of liposomes to cells: a novel and efficient method for covalent attachment of Fab' fragments via disulfide bonds. Biochemistry, *20:* 4229-4238, 1981.

76. Martin, F. J. and Papahadjopoulos, D. Irreversible coupling of immunoglobulin fragments to preformed vesicles. An improved method for liposome targeting. J. Biol. Chem., *257:* 286-288, 1982.

77. Zalipsky, S. Synthesis of end-group functionalized polyethylene glycol-lipid conjugates for preparation of polymer-grafted liposomes. Bioconjugate Chem., *4:* 296-299, 1993.

78. Torchilin, V. P., Levchenko, T. S., Lukyanov, A. N., Khaw, B. A., Klibanov, A. L., Rammohan, R., Samokhin, G. P., and Whiteman, K. R. p-Nitrophenylcarbonyl-PEG-PE-liposomes: fast and simple attachment of specific ligands, including monoclonal antibodies, to distal ends of PEG chains via p-nitrophenylcarbonyl groups. Biochim. Biophys. Acta, *1511:* 397-411, 2001.

79. Bendas, G., Krause, A., Bakowsky, U., Vogel, J., and Rothe, U. Targetability of novel immunoliposomes prepared by a new antibody conjugation technique. Int. J. Pharmaceutics, *181:* 79-93, 1999.

80. Ishida, T., Iden, D. L., and Allen, T. M. A combinatorial approach to producing sterically stabilized (Stealth) immunoliposomal drugs. FEBS Lett., *460:* 129-133, 1999.

81. Allen, T. M., Sapra, P., and Moase, E. Use of the post-insertion method for the formation of ligand-coupled liposomes. Cell. Mol. Biol. Lett., *7:* 889-894, 2002.

82. Moreira, J. N., Ishida, T., Gaspar, R., and Allen, T. M. Use of the post-insertion technique to insert peptide ligands into pre-formed Stealth liposomes with retention of binding activity and cytotoxicity. Pharm. Res., *19:* 265-269, 2002.

83. Ahmad, I., Longenecker, M., Samuel, J., and Allen, T. M. Antibody-targeted delivery of doxorubicin entrapped in sterically stabilized liposomes can eradicate lung cancer in mice. Cancer Res., *53:* 1484-1488, 1993.

84. Park, J. W., Hong, K., Kirpotin, D. B., Meyer, O., Papahadjopoulos, D., and Benz, C. C. Anti-HER2 immunoliposomes for targeted therapy of human tumors. Cancer Lett., *118:* 153-160, 1997.

85. Carter, P. Improving the efficacy of antibody-based cancer therapies. Nature Rev. Cancer, *1:* 118-129, 2001.

86. Drummond, D. C., Hong, K., Park, J. W., Benz, C. C., and Kirpotin, D. B. Liposome targeting to tumors using vitamin and growth factor receptors. Vitam. Horm., *60:* 285-332, 2001.

87. Baselga, J., Norton, L., Albanell, J., Kim, Y. M., and Mendelsohn, J. Recombinant humanized anti-HER2 antibody (Herceptin) enhances the antitumor activity of paclitaxel and doxorubicin against HER2/neu overexpressing human breast cancer xenografts. Cancer Res., *58:* 2825-2831, 1998.

88. Demidem, A., Lam, T., Alas, S., Hariharan, K., Hanna, N., and Bonavida, B. Chimeric anti-CD20 (IDEC-C2B8) monoclonal antibody sensitizes a B cell lymphoma cell line to cell killing by cytotoxic drugs. Cancer Biother. Radiopharm., *12:* 177-186, 1997.

89. Slamon, D. J., Leyland-Jones, B., Shak, S., Fuchs, H., Paton, V., Bajamonde, A., Fleming, T., Eiermann, W., Wolter, J., Pegram, M., Baselga, J., and Norton, L.

Use of chemotherapy plus a monoclonal antibody against HER2 for metastatic breast cancer that overexpresses HER2. N. Engl. J. Med., *344:* 783-792, 2001.

90. Coiffier, B., Lepage, E., Briere, J., Herbrecht, R., Tilly, H., Bouabdallah, R., Morel, P., Van Den Neste, E., Salles, G., Gaulard, P., Reyes, F., and Gisselbrecht, C. CHOP chemotherapy plus Rituximab compared with CHOP alone in elderly patients with diffuse large B-cell lymphoma. N. Eng. J. Med., *346:* 235-242, 2002.

91. McLaughlin, P., Grillo-Lopez, A. J., Link, B. K., Levy, R., Czuczman, M. S., Williams, M. E., Heyman, M. R., Bence-Bruckler, I., White, C. A., Cabanillas, F., Jain, V., Ho, A. D., Lister, J., Wey, K., Shen, D., and Dallaire, B. K. Rituximab chimeric anti-CD20 monoclonal antibody therapy for relapsed indolent lymphoma: half of patients respond to a four-dose treatment program. J. Clin. Oncol., *16:* 2825-2833, 1998.

92. Czuczman, M. S., Grillo-Lopez, A. J., White, C. A., Saleh, M., Gordon, L., LoBuglio, A. F., Jonas, C., Klippenstein, D., Dallaire, B., and Varns, C. Treatment of patients with low-grade B-cell lymphoma with the combination of chimeric anti-CD20 monoclonal antibody and CHOP chemotherapy. J. Clin. Oncol., *17:* 268-276, 1999.

93. Pietras, R. J., Fendly, B. M., Chazin, V. R., and Pergram, M. D. Antibody to HER-2/neu receptor blocks DNA repair after cisplatin in human breast and ovarian cancer cells. Oncogene, *9:* 1829-1838, 1994.

94. Ghetie, M. A., Picker, L. J., Richardson, J. A., Tucker, K., Uhr, J. W., and Vitetta, E. S. Anti-CD19 inhibits the growth of human B-cell tumor lines in vitro and

of Daudi cells in SCID mice by inducing cell cycle arrest. Blood, *83:* 1329-1336, 1994.

95. Ghetie, M.-A., Ghetie, V., and Vitetta, E. S. Anti-CD19 antibodies inhibit the function of the P-gp pump in multidrug-resistant B lymphoma cells. Clin. Cancer Res., *5:* 3920-3927, 1999.

96. Bradbury, L. E., Kansas, G. S., Levy, S., Evans, R. L., and Tedder, T. F. The CD19/CD21 signal transducing complex of human B-lymphocytes includes the target of antiproliferative antibody-1 and leu-13 molecules. J. Immunol., *149:* 2841-2850, 1992.

97. Dubowchik, G. M. and Walker, M. A. Receptor-mediated and enzyme-dependent targeting of cytotoxic anticancer drugs. Pharm. Therap., *83:* 67-123, 1999.

98. Kuby, J. Immunology, 3 edition, p. 1-664: W.H. Freeman and company, 1997.

99. Flavell, D. J., Noss, A., Pulford, K. A. F., Ling, N., and Flavell, S. U. Systemic therapy with 3BIT, a triple combination cocktail of anti-CD19, -CD22, and -CD38-saporin immunotoxins, is curative of human B-cell lymphoma in severe combined immunodeficient mice. Cancer Res., *57:* 4824-4829, 1997.

100. Regimbald, L. H., Pilarski, L. M., Longenecker, B. M., Reddish, M. A., Zimmermann, G., and Hugh, J. C. The breast mucin MUC1 as a novel adhesion ligand for endothelial intercellular adhesion molecule 1 in breast cancer. Cancer Res., *56:* 4244-4249, 1996.

101. van Hof, A. C., Molthoff, C. F. M., Davies, Q., Perkins, A. C., Verheijen, R. H. M., Kenemans, P., Hollander, W. D., Wilhelm, A. J., and Baker, T. S.

Biodistribution of 111Indium-labeled engineered human antibody CTMO1 in ovarian cancer patients: influence of protein dose. Cancer Res., *56:* 5179-5185, 1996.

102. Huang, A., Kennel, S. J., and Huang, L. Interactions of immunoliposomes with target cells. J. Biol. Chem., *258:* 14034-14040, 1983.

103. Allen, T. M. Long-circulating (sterically stabilized) liposomes for targeted drug delivery. Trends Pharmacol. Sci., *15:* 215-220, 1994.

104. Goren, D., Horowitz, A. T., Zalipsky, S., Woodle, M. C., Yarden, Y., and Gabizon, A. Targeting of stealth liposomes to erB-2 (Her/2) receptor: in vitro and in vivo studies. Br. J. Cancer, *74:* 1749-1756, 1996.

105. Vingerhoeds, M. H., Steerenberg, P. A., Hendriks, J. J. G. W., Kekker, L. C., van Hoesel, Q. G. C. M., Crommelin, D. J. A., and Storm, G. Immunoliposome-mediated targeting of doxorubicin to human ovarian carcinoma in vitro and in vivo. Br. J. Cancer, *74:* 1023-1029, 1996.

106. Straubinger, R. M., Hong, K., Friend, D. S., and Papahadjopoulos, D. Endocytosis of liposomes and intracellular fate of encapsulated molecules: encounter with a low pH compartment after internalization in coated vesicles. Cell, *32:* 1069-1079, 1983.

107. Park, J. W., Hong, K., Carter, P., Asgari, H., Guo, L. Y., Keller, G. A., Wirth, C., Shalaby, R., Kotts, C., Wood, W. I., Papahadjopoulos, D., and Benz, C. C. Development of anti-p185^{HER2} immunoliposomes for cancer therapy. Proc. Natl. Acad. Sci. USA, *92:* 1327-1331, 1995.

108. Lopes de Menezes, D. E., Kirchmeier, M. J., Gagne, J.-F., Pilarski, L. M., and Allen, T. M. Cellular trafficking and cytotoxicity of anti-CD19-targeted liposomal doxorubicin in B lymphoma cells. J. Liposome Res., *9:* 199-228, 1999.

109. Nielsen, U. B. and Marks, J. D. Internalizing antibodies and targeted cancer therapy: direct selection from phage display libraries. Pharm. Sci. Technol. Today, *3:* 282-291, 2000.

110. Poul, M. A., Becerril, B., Nielsen, U. B., Morisson, P., and Marks, J. D. Selection of tumor-specific internalizing human antibodies from phage libraries. J. Mol. Biol., *301:* 1149-1161, 2000.

111. Nielsen, U. B., Kirpotin, D. B., Pickering, E. M., Hong, K., Park, J. W., Shalaby, M. R., Shao, Y., Benz, C. C., and Marks, J. D. Therapeutic efficacy of anti-ErbB2 immunoliposomes targeted by a phage antibody selected for cellular endocytosis. Biochim. Biophys. Acta, *1591:* 109-118, 2002.

112. Maruyama, K., Takahashi, N., Tagawa, T., Nagaike, K., and Iwatsuru, M. Immunoliposomes bearing polyethyleneglycol-coupled Fab' fragment show prolonged circulation time and high extravasation into targeted solid tumors in vivo. FEBS Lett., *413:* 177-180, 1997.

113. Baxter, L. T., Zhu, H., Mackensen, D. G., and Jain, R. K. Physiologically based pharmacokinetic model for specific and nonspecific monclonal antibodies and fragments in normal tissues and human tumor xenografts in nude mice. Cancer Res., *54:* 1517-1528, 1994.

114. Wang, S. and Low, P. S. Folate-mediated targeting of antineoplastic drugs, imaging agents, and nucleic acids to cancer cells. J Control Rel., *53:* 39-48, 1998.

115. Reddy, J. A. and Low, P. S. Folate-mediated targeting of therapeutic and imaging agents to cancers. Crit. Rev. Ther. Drug Carrier Syst., *15:* 587-627, 1998.

116. Singh, M. Transferrin as a targeting ligand for liposomes and anticancer drugs. Curr. Pharm. Design, *5:* 443-451, 1999.

117. Kohler, G. and Milstein, C. Continuous cultures of fused cells secreting antibody of predetermined specificity. Nature (London), *256:* 495-497, 1975.

118. Schroff, R. W., Foon, K. A., Beatty, S. M., Oldham, R. K., and Morgan, A. C. Human anti-mouse immunoglobulin responses in patients receiving monoclonal antibody therapy. Cancer Res., *48:* 879-885, 1985.

119. Shawler, D. L., Bartholomew, R. M., Smith, L. M., and Dillman, R. O. Human immune response to multiple injections of murine monoclonal IgG. J. Immunology, *135:* 1530-1535, 1985.

120. Maruyama, K., Holmber, E., Kennel, S. J., Klibanov, A., Torchilin, V., and Huang, L. Characterization of in vivo immunoliposome targeting to pulmonary endothelium. J. Pharm. Sci., *79:* 978-984, 1990.

121. Phillips, N. C. and Emili, A. Immunogenicity of immunoliposomes. Immunol. Lett., *30:* 291-296, 1991.

122. Harding, J. A., Engbers, C. M., Newman, M. S., Goldstein, N. I., and Zalipsky, S. Immunogenicity and pharmacokinetic attributes of poly(ethyleneglycol)-grafted immunoliposomes. Biochim. Biophys. Acta, *1327:* 181-192, 1997.

123. Morrison, S. L., Johnson, M. J., Herzenberg, L. A., and Oi, V. T. Chimeric human antibody molecules: mouse antigen-binding domains with human constant region domains. Proc Natl Acad Sci U S A, *81:* 6851-6855, 1984.

124. Winter, G. and Harris, W. J. Humanized antibodies. Trends Pharmacol. Sci., *14:* 139-143, 1993.

125. Winter, G., Griffiths, A. D., Hawkins, R. E., and Hoogenboom, H. R. Making antibodies by phage display technology. Annu. Rev. Immunol., *12:* 433-455, 1994.

126. Fishwild, D. M., O'Donnell, S. L., Bengoechea, T., Hudson, D. V., Harding, F., Bernhard, S. L., Jones, D., Kay, R. M., Higgins, K. M., Schramm, S. R., and Lonberg, N. High-avidity human IgG kappa monoclonal antibodies from a novel strain of minilocus transgenic mice. Nat. Biotechnol., *14*: 845-851, 1996.

127. Brekke, O. H. and Sandlie, I. Therapeutic antibodies for human diseases at the dawn of the twenty-first century. Nature Rev. Cancer, *2:* 52-62, 2003.

128. Scheinberg, D. A., Sgouros, G., and Junghans, R. P. Antibody-based immunotherapies for cancer. In: B. A. Chabner and D. L. Longo (eds.), Cancer chemotherapy and biotherapy, 3 edition, pp. 850-890: Lippincott Williams and Wilkins, 2001.

129. Allen, T. M., Sapra, P., Moase, E., Moreira, J. N., and Iden, D. L. Adventures in targeting. J. Liposome Res., *121:* 5-12, 2002.

130. Koning, G., G.A., Morselt, H. W. M., Gorter, A., Allen, T. M., Zalipsky, S., Kamps, J. A. A. M., and Scherphof, G. L. Pharmacokinetics of differently designed

immunoliposome formulations in rats with or without hepatic colon concer metastases. Phamaceut. Res., *18:* 1291-1298, 2001.

131. Weinstein, J. N. and van Osdol, W. Early intervention in cancer using monoclonal antibodies and other biological ligands: micropharmacology and the "binding site barrier". Cancer Res., *52:* 2747-2751, 1992.

132. Kirpotin, D., Hong, K., Mullah, N., Papahadjopoulos, D., and Zalipsky, S. Liposomes with detachable polymer coating: destabilization and fusion of dioleoylphosphatidylethanolamine vesicles triggered by cleavage of surface-grafted poly(ethylene glycol). FEBS Lett., *388:* 115-118, 1996.

133. Vogel, K., Wang, S., Lee, R. J., Chmielewski, J., and Low, P. S. Peptide mediated release of folate targeted liposome contents from endosomal compartments. J. Am. Chem. Soc., *118:* 1581-1586, 1996.

134. Bailey, A., Monck, M. A., and Cullis, P. R. pH-induced destabilization of lipid bilayers by a lipopeptide derived from influenza hemagglutinin. Biochim. Biophys. Acta, *1324:* 232-244, 1997.

135. Connor, J. and Huang, L. pH-sensitive immunoliposomes as an efficient and target-specific carrier for antitumor drugs. Cancer Res., *46:* 3431-3435, 1986.

136. Kono, K., Zenitani, K., and Takagishi, T. Novel pH-sensitive liposomes: liposomes bearing a poly(ethylene glycol) derivative with carboxyl groups. Biochim. Biophys. Acta, *1193:* 1-9, 1994.

137. Zignani, M., Drummond, D. C., Meyer, O., Hong, K., and Leroux, J.-C. In vitro characterization of a novel polymeric-based pH-sensitive liposome system. Biochim. Biophys. Acta, *1463:* 383-394, 2000.

138. Drummond, D. C., Zignani, M., and Leroux, J. Current status of pH-sensitive liposomes in drug delivery. Prog. Lipid Res., *39:* 409-460, 2000.

139. Stohrerm, M., Boucher, Y., Stangassinger, M., and Jain, R. K. Oncotic pressure in solid tumors is elevated. Cancer Res., *60:* 4251-4255, 2000.

140. Huang, S. K., Lee, K. D., Hong, K., Friend, D. S., and Papahadjopoulos, D. Microscopic localization of sterically stabilized liposomes in colon carcinoma-bearing mice. Cancer Res., *52:* 5135-5143, 1992.

141. Scherphof, G. L., Kamps, J. A. A. M., and Koning, G. A. In vivo targeting of surface-modified liposomes to metastatically growing colon carcinoma cells and sinusoidal endothelial cells in the rat liver. J. Liposome Res., *7:* 419-432, 1997.

142. Lopes de Menezes, D. E., Pilarski, L. M., Belch, A. R., and Allen, T. M. Selective targeting of immunoliposomal doxorubicin against human multiple myeloma in vitro and ex vivo. Biochim. Biophys. Acta, *1466:* 205-220, 2000.

143. Moase, E., Qi, W., Ishida, T., Gabos, Z., Longenecker, B. M., Zimmermann, G. L., Ding, L., Krantz, M., and Allen, T. M. Anti-MUC-1 immunoliposomal doxorubicin in the treatment of murine models of metastatic breast cancer. Biochim. Biophys. Acta, *1510:* 43-55, 2001.

144. Moreira, J. N., Gaspar, R., and Allen, T. M. Targeting Stealth liposomes in a murine model of human small cell lung cancer. Biochim. Biophys. Acta, *1515:* 167-176, 2001.

145. Koning, G. A., Morselt, J. M. W., Velinova, M. J., Donga, J., Gorter, A., Allen, T. M., Zalipsky, S., Kamps, J. A. A. M., and Scherphof, G. L. Selective transfer of a lipophilic prodrug of 5-fluorodeoxyuridine (FUdR) from immunoliposomes to colon cancer cells. Biochim. Biophys. Acta, *1420:* 153-167, 1999.

146. Park, J. W., Kirpotin, D. B., Hong, K., Shalaby, R., Shao, Y., Nielsen, U. B., Marks, J. D., Papahadjopoulos, D., and Benz, C. C. Tumor targeting using anti-Her2 immunoliposomes. J. Control. Rel., *74:* 95-113, 2001.

147. Asai, T., K., S., K., M., K., K., Watanabe, H., Ogino, K., Taki, T., S., S., A., M., and Oku, N. Anti-neovascular therapy for liposomal DPP-CNDAC targeted to angiogenic blood vessels. FEBS Lett., *520(1-3),* 167-170, 2002.

148. Park, J. W., Hong, K., Kirpotin, D. B., Papahadjopoulos, D., and Benz, C. C. Immunoliposomes for cancer treatment. Adv. Pharmacol., *40:* 399-435, 1997.

149. Pagnan, G., Montaldo, P. G., Pastorino, F., Chiesa, L., Raffaghello, L., Kirchmeier, M., Allen, T. M., and Ponzoni, M. GD_2 -mediated melanoma cell targeting and cytotoxicity of liposome-entrapped fenretinide. Int. J. Cancer, *81:* 268-274, 1999.

150. Allen, T. M., Ahmad, I., Lopes de Menezes, D. E., and Moase, E. H. Immunoliposome-mediated targeting of anti-cancer drugs in vivo. Biochem. Soc. Trans., *23:* 1073-1079, 1995.

151. Pilarski, L. M. and Jensen, G. S. Monoclonal circulating B cells in multiple myeloma: a continuously differentiating, possible invasive, population as defined by expression of CD45 isoforms and adhesion molecules. Hematol. Oncol. Clin. North America, *6:* 297-322, 1992.

152. Pilarski, L. M., Masellis-Smith, A., Szczepek, A., Mant, M., J., and Belch, A. R. Circulating clonotypic B cells in the biology of myeloma: speculations on the origins of multiple myeloma. Leuk. Lymphoma, *18:* 179-187, 1995.

153. Pilarski, L. M. and Belch, A. R. Intrinsic expression of the multidrug transporter, P-glycoprotein 170, in multiple myeloma: implications for treatment. Leuk. Lymphoma, *17:* 367-374, 1995.

154. Szczepek, A. J., Bergsagel, P. L., Axelsson, L., Brown, C. B., Belch, A. R., and Pilarski, L. M. $CD34^+$ cells in the blood of patients with multiple myeloma express CD19 and IgH mRNA and have patient-specific IgH VDJ rearrangements. Blood, *89:* 1824-1833, 1997.

155. Szczepek, A. J., Seeberger, K., Wizniak, J., Mant, M. J., Belch, A. R., and Pilarski, L. M. A high frequency of circulating B cells share clonotypic IgH VDJ rearrangements with autologous bone marrow plasma cells in multiple myeloma, as measured by single cell and in situ RT-PCR. Blood, *90:* 2844-2855, 1998.

156. Tseng, Y. L., Hong, R. L., Tao, M. H., and Chang, F. H. Sterically stabilized anti-idiotype immunoliposomes improve the therapeutic efricacy of doxorubicin in a murine B-cell lymphoma model. Int. J. Cancer, *80:* 723-730, 1999.

157. Maruyama, K. In vivo targeting by liposomes. Biol. Pharm. Bull., *23:* 791-799, 2000.

158. Matsuo, H., Wakasugi, M., Takanaga, H., Ohtani, H., Naito, M., Tsuruo, T., and Sawada, Y. Possibility of the reversal of multidrug resistance and the avoidance of side effects by liposomes modified with MRK-16, a monoclonal antibody to P-glycoprotein. J. Control. Rel., *77:* 77-86, 2001.

159. Koning, G., Gorter, A., Scherphof, G., and Kamps, J. Antiproliferative effect of immunoliposomes containing 5-fluorodeoxyuridine-dipalmitate on colon cancer cells. Br. J. Cancer, *80:* 1718-1725, 1999.

160. Kessner, S., Krause, A., Rothe, U., and Bendas, G. Investigation of the cellular uptake of E-selectin-targeted immunoliposomes by activated human endothelial cells. Biochim. Biophys. Acta, *1514:* 177-190, 2001.

161. Nam, S. M., Kim, H. S., Ahn, W. S., and Park, Y. S. Sterically stabilized anti-G_{M3}, anti-Le^x immunoliposomes: targeting to B16BL6, HRT-18 cells. Oncol. Res., *11:* 9-16, 1999.

162. Dagar, S., Sekosan, M., Lee, B. S., Rubinstein, I., and Onyuksel, H. VIP receptors as molecular targets of breast cancer: implications for targeted imaging and drug delivery. J. Control. Rel., *74:* 129-134, 2001.

163. Jaafari, M. R. and Foldvari, M. P0 protein mediated targeting of liposomes to melanoma cells with high level of ICAM-1 expression. J. Drug Target., *7:* 101-112, 1999.

164. Medina, O. P., Soderlund, T., Laakkonen, L. J., Tuominen, E. K. J., Koivunen, E., and Kinnunen, P. K. J. Binding of novel peptide inhibitors of type IV collagenases to phospholipid membranes and use in liposome targeting to tumor cells in vitro. Cancer Res., *61:* 3978-3985, 2001.

165. Lee, R. J. and Low, P. S. Delivery of liposomes into cultured KB cells via folate receptor-mediated endocytosis. J. Biol. Chem., *269:* 3198-3204, 1994.

166. Ni, S., Stephenson, S.M. and Lee, R. J. Folate receptor targeted delivery of liposomal daunorubicin into tumor cells. Anticancer Res., *22:* 2131-2135, 2002.

167. Ishida, O., Maruyama, K., Tanahashi, H., Iwatsuru, M., Sasaki, K., Eriguchi, M., and Yanagie, H. Liposomes bearing polyethyleneglycol-coupled transferrin with intracellular targeting property to the solid tumors in vivo. Pharm. Res., *18:* 1042-1048, 2001.

168. Eavarone, D. A., Yu, X., and Bellamkonda, R. V. Targeted drug delivery to C6 glioma by transferrin-coupled liposomes. Journal of Biomedical Materials Research, 51: 10-14, 1999.

169. Eliaz, R. E. and Szoka, F. C. J. Liposome-encapsulated doxorubicin targeted to CD44: a strategy to kill CD44-overexpressing tumor cells. Cancer Res., *61:* 2592-2601, 2001.

170. Suzuki, S., Inoue, K., Hongoh, A., Hashmoto, Y., and Yamazoe, Y. Modulation of doxorubicin resistance in a doxorubicin-resistant human leukaemia cell by an immunoliposome targeting transferrin receptor. Br. J. Cancer, *76:* 83-89, 1997.

171. Lee, R. J. and Low, P. S. Folate-targeted liposomes for drug delivery. J. Liposome Res., *7:* 455-466, 1997.

172. Derycke, A. S. L. and De Witte, P. A. M. Transferrin-mediated targeting of hypericin embedded in sterically stabilized PEG-liposomes. Int. J. Oncol., *20:* 181-187, 2002.

173. Pan, X. Q., Wang, H., and Lee, R. J. Boron delivery to a murine lung carcinoma using folate receptor-targeted liposomes. Anticancer Res., *22:* 1629-1633, 2002.

174. Dalla-Favera, R. and Gaidano, G. Molecular biology of lymhomas. In: J. DeVita, V.T., S. Hellman, and S. A. Rosenberg (eds.), Cancer Principles and Practice of Oncology, 6 edition, pp. 2215-2234. Philadelphia: Lippincott Williams and Wilkins, 2001.

175. DeVita, J., V.T. and Canellos, G. P. The Lymphomas. Semin. Hematol., *36:* 84-94, 1999.

176. Harris, N. L., Jaffe, E. S., Stein, H., Banks, P. M., Chan, J. K., Cleary, M. L., Delsol, G., De Wolf-Peeters, C., Falini, B., and Gatter, K. C. A revised European-American classification of lymphoid neoplasms: a proposal from the International Lymphoma Study Group. Blood, *84:* 1361-1392, 1994.

177. Jaffe, E. S., Harris, N. L., Diebold, J., and Muller-Hermelink, H. K. World Health Organization classification of neoplastic diseases of the hematopoietic and lymphoid tissues. A progress report. Am. J. Clin. Pathol., *111:* S8-12, 1999.

178. Tedder, T. F., Zhou, L.-J., and Engel, P. The CD19/CD21signal transduction complex of B lymphocytes. Immunol. Today, *15:* 437-442, 1994.

179. Krop, I., Shaffer, A. L., Fearon, D. T., and Schlissel, M. S. The signaling activity of murine CD19 is regulated during cell development. J. Immunol, *157:* 48-56, 1996.

180. Uckun, F. M., Jaszcz, W., Ambrus, J. L., Fauci, A. S., Gajl-Peczalska, K., Song, S. W., Wick, M. R., Myers, D. E., Waddick, K., and Ledbetter, J. A. Detailed studies on expression and function of CD19 surface determinant by using B43 monoclonal antibody and the clinical potential of anti-CD19 immunotoxins. Blood, *71:* 13-29, 1988.

181. Press, O. W., Farr, A. G., Borroz, K. I., Andersen, S. K., and Martin, P. J. Endocytosis and degradation of monoclonal antibodies targeting human B-cell malignancies. Cancer Res., *49:* 4906-4912, 1989.

182. Matsumoto, A. K., Kopicky-Burd, J., Carter, R. H., Tuveson, D. A., Tedder, T. F., and Fearon, D. T. Intersection of the complement and immune systems: a signal transduction complex of the B lymphocyte-containing complement receptor type 2 and CD19. J. Exp. Med., *173:* 55-64, 1991.

183. Tedder, T. F., Inaoki, M., and Sato, S. The CD19-CD21 complex regulates signal transduction thresholds governing humoral immunity and autoimmunity. Immunity, *6:* 107-118, 1997.

184. Ghetie, M.-A., Bright, H., and Vitetta, E. S. Homodimers but not monomers of Rituxan (chimeric anti-CD20) induce apoptosis in human B-lymphoma cells and synergize with a chemotherapeutic agent and an immunotoxin. Blood, *97:* 1392-1398, 2001.

185. Maloney, D. G., Liles, T. M., Czerwinski, D. K., Waldichuk, C., Rosenberg, J., Grillo-Lopez, A., and Levy, R. Phase I clinical trial using escalating single-dose infusion of chimeric anti-CD20 monoclonal antibody (IDEC-C2B8) in patients with recurrent B-cell lymphoma. Blood, *84,* 1994.

186. Reff, M. E., Carner, K., Chambers, K. S., Chinn, P. C., Leonard, J. E., Raab, R., Newman, R. A., Hanna, N., and Anderson, D. R. Depletion of B cells in vivo by a chimeric mouse human monoclonal antibody to CD20. Blood, *83:* 435-445, 1994.

187. Maloney, D. G., Smith, B., and Appelbaum, F. R. The anti-tumor effect of monoclonal anti-CD20 antibody (mAb) therapy includes direct anti-proliferative activity and induction of apoptosis in CD20 positive non-Hodgkin's lymphoma (NHL) cell lines. Blood., *88 (suppl 1):* 673A, 1996.

188. Press, O. W., Appelbaum, F., Ledbetter, J. A., Martin, P. J., Zarling, J., Kidd, P., and Thomas, E. D. Monoclonal antibody IF5 (anti-CD20) serotherapy of human B cell lymphomas. Blood, *69:* 584-591, 1987.

189. Tedder, T. F. and Engel, P. CD20: a regulator of cell-cycle progression of B lymphocytes. Immunol. Today, *15:* 450-454, 1994.

190. Vangeepuram, N., Ong, G. L., and Mattes, M. J. Processing of antibodies bound to B-cell lymphomas and lymphoblastoid cell lines. Cancer, *80:* 2425-2430, 1997.

191. Tedder, T. F., Boyd, A. W., Freedman, A. S., Nadler, L. M., and Schlossman, S. F. The B cell surface molecule B1 is functionally linked with B cell activation and differentiation. J. Immunol., *135:* 973-979, 1985.

192. Golay, J. T., Clark, E. A., and Beverley, P. C. The CD20 (Bp35) antigen is involved in activation of B cells from the G0 to the G1 phase of the cell cycle. J. Immunol., *135:* 3795-3801, 1985.

193. Kansas, G. S. and Tedder, T. F. Transmembrane signals generated through MHC class II, CD19, CD20, CD39, and CD40 antigens induce LFA-1-dependent and -independent adhesion in human B cells through a tyrosine kinase-dependent pathway. J. Immunol., *147:* 4094-4102, 1991.

194. Bubien, J. K., Zhou, L. J., Bell, P. D., Frizzell, R. A., and Tedder, T. F. Transfection of the CD20 cell surface molecule into ectopic cell types generates a Ca2+ conductance found constitutively in B lymphocytes. J. Cell Biol., *121:* 1121-1132, 1993.

195. Grillo-Lopez, A. J. Rituximab: an insider's historical perspective. Semin. Oncol., *27:* 9-16, 2000.

196. Shan, D., Ledbetter, J. A., and Press, O. W. Signaling events involved in anti-CD20-induced apoptosis of malignant human B cells. Cancer Immunol. Immunother., *48:* 673-683, 2000.

197. Golay, J., Zaffaroni, L., Vaccari, T., Lazzari, M., Borleri, G. M., Bernasconi, S., Tedesco, F., Rambaldi, A., and Introna, M. Biologic response of B lymphoma cells to anti-CD20 monoclonal antibody rituximab in vitro: CD55 and CD59 regulate complement-mediated cell lysis. Blood, *95:* 3900-3908, 2000.

198. Pedersen, I. M., Buhl, A. M., Klausen, P., Geisler, C. H., and Jurlander, J. The chimeric anti-CD20 antibody rituximab induces apoptosis in B-cell chronic lymphocytic leukemia cells through a p38 mitogen activated protein-kinase-dependent mechanism. Blood, *99:* 1314-1319, 2002.

199. Chow, K. U., Sommerlad, W. D., Boehrer, S., Schneider, B., Seipelt, G., Rummel, M. J., Hoelzer, D., Mitrou, P. S., and Weidmann, E. Anti-CD20 antibody (IDEC-C2B8, rituximab) enhances efficacy of cytotoxic drugs on neoplastic lymphocytes in vitro: role of cytokines, complement, and caspases. Haematologica, *87:* 33-43, 2002.

200. Boue, D. R. and Lebien, T. W. Structural characterization of the human B lymphocyte-restricted differentiation antigen CD22. Comparison with CD21 (complement receptor type 2/Epstein-Barr virus receptor). J. Immunol., *140:* 192-199, 1988.

201. Bofill, M., Janossy, G., Janossa, M., Burford, G. D., Seymour, G. J., Wernet, P., and Kelemen, E. Human B cell development. II. Subpopulations in the human fetus. J. Immunol., *134:* 1531-1538, 1985.

202. Schwartz-Albiez, R., Dorken, B., Monner, D. A., and Moldenhauer, G. CD22 antigen: biosynthesis, glycosylation and surface expression of a B lymphocyte protein involved in B cell activation and adhesion. Int. Immunol., *3:* 623-633, 1991.

203. Dorken, B., Moldenhauer, G., Pezzutto, A., Schwartz, R., Feller, A., Kiesel, S., and Nadler, L. M. HD39 (B3), a B lineage-restricted antigen whose cell surface expression is limited to resting and activated human B lymphocytes. J. Immunol., *136:* 4470-4479, 1986.

204. Pezzutto, A., Rabinovitch, P. S., Dorken, B., Moldenhauer, G., and Clark, E. A. Role of the CD22 human B cell antigen in B cell triggering by anti-immunoglobulin. J. Immunol., *140:* 1791-1795, 1988.

205. Peaker, C. J. and Neuberger, M. S. Association of CD22 with the B cell antigen receptor. Eur. J. Immunol., *6:* 1358-1363, 1993.

206. Shih, L. B., Lu, H. H., Xuan, H., and Goldenberg, D. M. Internalization and intracellular processing of an anti-B-cell lymphoma monoclonal antibody, LL2. Int. J. Cancer, *56:* 538-545, 1994.

207. Shan, D. and Press, O. W. Constitutive endocytosis and degradation of CD22 by human B cells. J. Immunol., *154:* 4466-4475, 1995.

208. Leonard, J. P. and Link, B. K. Immunotherapy of non-Hodgkin's lymphoma with hLL2 (epratuzumab, an anti-CD22 monoclonal antibody) and Hu1D10 (apolizumab). Semin. Oncol., *29, Suppl 2:* 81-86, 2002.

209. Vitetta, E. S., Stone, E., Amlot, P., Fay, J., May, R., Till, M., Newman, J., Clark, P., Collins, R., Cunningham, D., Ghetie, V., Uhr, J. W., and Thorpe, P. E. Phase I immunotoxin trial in patients with B-cell lymphoma. Cancer Res., *51:* 4052, 1991.

210. Multani, P. S., O'Day, S., Nadler, L. M., and Grossbard, M. L. Phase II clinical trial of bolus infusion anti-B4 blocked ricin immunoconjugate in patients with relapsed B-cell non-Hodgkin's lymphoma. Clin. Cancer Res., *4:* 2599-2604, 1998.

211. Vose, J. M., Colcher, D., Gobar, L., Bierman, P. J., Augustine, S., Tempero, M., Leichner, P., Lynch, J. C., Goldenberg, D., and Armitage, J. O. Phase I/II trial of multiple dose 131Iodine-MAb LL2 (CD22) in patients with recurrent non-Hodgkin's lymphoma. Leuk Lymphoma, *38(1-2):* 91-101, 2000.

212. Wei, B. R., Ghetie, M. A., and Vitetta, E. S. The combined use of an immunotoxin and a radioimmunoconjugate to treat disseminated human B-cell lymphoma in immunodeficient mice. Clin. Cancer Res., *6:* 631-642, 2000.

213. Schindler, J., Sausville, E. A., Messmann, R., Uhr, J. W., and Vitetta, E. S. The toxicity of deglycosylated ricin A chain-containing immunotoxins in patients with non-Hodgkin's lymphoma is exacerbated by prior radiotherapy: a retrospective analysis of patients in five clinical trials. Clin. Cancer Res., *7:* 255-258, 2001.

214. Owellen, R. J., Owens, A. H. J., and Donigian, D. W. The binding of vincristine, vinblastine and colchicine to tubulin. Biochem. Biophys. Res. Commun., *47:* 685-691, 1972.

215. Owellen, R. J., Hartke, C. A., Dickerson, R. M., and Hains, F. O. Inhibition of tubulin-microtubule polymerization by drugs of the Vinca alkaloid class. Cancer Res, *36:* 1499-1502, 1976.

216. Zhou, X. J. and Rahman, R. Preclinical and clinical pharmacology of vinca alkaloids. Drugs, *44:* 1-16, 1992.

217. Sandler, S. G., Tobin, W., and Henderson, E. S. Vincristine-induced neuropathy. A clinical study of fifty leukemic patients. Neurology, *19:* 367-374, 1969.

218. Weiden, P. L. and Wright, S. E. Vincristine neurotoxicity. N. Engl. J. Med., *286:* 1369-1370, 1972.

219. Miller, B. R. Neurotoxicity and vincristine. JAMA, 253: 2045, 1985.

220. Rowinsky, E. K. and Donehower, R. C. Antimicrotubule agents. In: B. A. Chabner and D. L. Longo (eds.), Cancer Chemotherapy and Biotherapy, 3 edition, pp. 329-372: Lippincott Williams & Wilkins, 2001.

221. Kaufman, I. A., Kung, F. H., Koenig, H. M., and Giammona, S. T. Overdosage with vincristine. J. Pediatr., *89:* 671-674, 1976.

222. Rowinsky, E. K. and Donehower, R. C. The clinical pharmacology and use of antimicrotubule agents in cancer chemotherapeutics. Pharmacol. Ther. *52(1)*: 35-84, 1991.

223. Owellen, R. J., Root, M. A., and Hains, F. O. Pharmacokinetics of vindesine and vincristine in humans. Cancer Res, *37:* 2603-2607, 1977.

224. Nelson, R. L., Dyke, R. W., and Root, M. A. Comparative pharmacokinetics of vindesine, vincristine and vinblastine in patients with cancer. Cancer Treat. Rev., *7:* 17-24, 1980.

225. Nelson, R. L. The comparative clinical pharmacology and pharmacokinetics of vindesine, vincristine, and vinblastine in human patients with cancer. Med. Pediatr. Oncol., *10:* 115-127, 1982.

226. Jackson, D. V., Jr. and Bender, R. A. Cytotoxic thresholds of vincristine in a murine and a human leukemia cell line in vitro. Cancer Res., *39:* 4346-4349, 1979.

227. Doroshow, J. H. Anthracyclines and Antracenediones. In: B. A. Chabner and D. L. Longo (eds.), Cancer chemotherapy & biotherapy: priniciples and practice, 3 edition, pp. 500-537. Philidelphia: Lippincott Williams & Wilkins, 2001.

228. Gewirtz, D. A. A critical evaluation of the mechanisms of action proposed for the antitumor effects of the anthracycline antibiotics adriamycin and daunorubicin, Biochemical pharmacology. Biochem. Pharmacol., *57:* 727-741, 1999.

229. Hortobagyi, G. N. Anthracyclines in the treatment of cancer. An overview. Drugs, *54:* 1-7, 1997.

230. Allen, T. M., Newman, M. S., Woodle, M. C., Mayhew, E., and Uster, P. S. Pharmacokinetics and anti-tumor activity of vincristine encapsulated in sterically stabilized liposomes. Int. J. Cancer, *62:* 199-204, 1995.

231. Ahmad, I. and Allen, T. M. Antibody-mediated specific binding and cytotoxicity of liposome-entrapped doxorubicin to lung cancer cells in vitro. Cancer Res., *52:* 4817-4820, 1992.

232. Moreira, J. N., Hansen, C. B., Gaspar, R., and Allen, T. M. A growth factor antagonist as a targeting agent for sterically stabilized liposomes in human small cell lung cancer. Biochim. Biophys. Acta, *1514:* 303-317, 2001.

233. Allen, T. M. and Moase, E. H. Therapeutic opportunities for targeted liposomal drug delivery. Adv. Drug Del. Rev., *21:* 117-133, 1996.

234. Sapra, P. and Allen, T. M. Internalizing antibodies are necessary for improved therapeutic efficacy of antibody-targeted liposomal drugs. Cancer Res., *62:* 7190-7194, 2002.

235. Phillips, N. C. and Dahman, J. Immunogenicity of immunoliposomes: reactivity against species-specific IgG and liposomal phospholipids. Immunol. Lett., *45:* 149-152, 1995.

236. Papahadjopoulos, D., Allen, T. M., Gabizon, A., Mayhew, E., Matthay, K., Huang, S. K., Lee, K. D., Woodle, M. C., Lasic, D. D., Redemann, C., and Martin, F. J. Sterically stabilized liposomes: improvements in pharmacokinetics and antitumor therapeutic efficacy. Proc. Natl. Acad. Sci. USA, *88:* 11460-11464, 1991.

237. Gelmon, K. A., Tolcher, A., Diab, A. R., Bally, M. B., Embree, L., Hudon, N., Dedhar, C., Ayers, D., Eisen, A., Melosky, B., Burge, C., P., L., and Mayer, L. D. Phase I study of liposomal vincristine. J. Clin. Oncol., *17:* 697-705, 1999.

238. Sarris, A. H., Hagemeister, F., Romanguera, J., Rodriguez, M. A., McLaughlin, P., Tsimberidou, A. M., Medeiros, L. J., Samuels, B., Pate, O., Oholendt, M., Kantarjian, H., Burge, C., and Cabanillas, F. Liposomal vinicristine in relapsed non-Hodgkin's lymphomas: early results of an ongoing phase II trial. Ann. Oncol., *11:* 69-72, 2000.

239. Northfelt, D. W., Dezube, B. J., Thommes, J. A., Levine, R., Von Roenn, J. H., Dosik, G. M., Rios, A., Krown, S. E., DuMond, C., and Mamelok, R. D. Efficacy of pegylated-liposomal doxorubicin in the treatment of AIDS-related Kaposi's sarcoma after failure of standard chemotherapy. J. Clin. Oncol., *15:* 653-659, 1997.

240. Muggia, F., Hainsworth, J. D., Jeffers, S., Miller, P., Groshen, S., Tan, M., Roman, L., Uziely, B., Muderspach, L., Garcia, A., Burnett, A., Greco, F. A., Morrow, C. P., Paradiso, L. J., and Liang, L.-J. Phase II study of liposomal doxorubicin in refractory ovarian cancer: antitumor activity and toxicity modification by liposomal encapsulation. J. Clin. Oncol., *15:* 987-993, 1997.

241. Safra, T., Muggia, F., Jeffers, S., Tsao-Wei, D. D., Groshen, S., Lyass, O., Henderson, R., Berry, G., and Gabizon, A. Pegylated liposomal doxorubicin (Doxil): reduced clinical cardiotoxicity in patients reaching or exceeding cumulative doses of 500 mg/m2. Ann. Oncol., *11:* 1029-1033, 2000.

242. Allen, T. M., Hansen, C. B., Martin, F., Redemann, C., and Yau-Young, A. Liposomes containing synthetic lipid derivatives of poly(ethylene glycol) show prolonged circulation half-lives in vivo. Biochim. Biophys. Acta, *1066:* 29-36, 1991.

243. Sommerman, E. F., Pritchard, P. H., and Cullis, P. R. ^{125}I labelled inulin: a convenient marker for deposition of liposomal contents in vivo. Biochem. Biophys. Res. Commun., *122:* 319-324, 1984.

244. Bartlett, G. R. Phosphorus assay in column chromatography. J. Biol. Chem., *234:* 466-468, 1959.

245. Zola, H., Macardle, P. J., Bradford, T., Weedon, H., Yasui, H., and Kurosawa, Y. Preparation and characterization of a chimeric CD19 monoclonal antibody. Immunol. Cell Biol., *69:* 411-422, 1991.

246. Yamaguchi, Y., Kim, H., Kato, K., Masuda, K., Shimada, I., and Arata, Y. Proteolytic fragmentation with high specificity of mouse immunoglobulin G. J. Immunol. Methods, 181: 259-267, 1995.

247. Allen, T. M., Hansen, C. B., and Lopes de Menezes, D. E. Pharmacokinetics of long circulating liposomes. Adv. Drug Del. Rev., *16:* 267-284, 1995.

248. Allen, T. M. Liposomes in the therapy of infectious diseases and cancer. In: UCLA Symposium on Molecular and Cellular Biology, New York, 1988, pp. 405-415.

249. Harasym, T. O., P.R., C., and Balley, M. B. Intratumor distribution of doxorubicin following i.v. administration of drug encapsulated in egg phosphaticdylcholine/cholesterol liposomes. Cancer Chemother.Pharmacol., *40:* 309-317, 1997.

250. Parr, M. J., Masin, D., Cullis, P. R., and Bally, M. B. Accumulation of liposomal lipid and encapsulated doxorubicin in murine Lewis lung carcinoma: the

lack of beneficial effects by coating liposomes with poly(ethylene glycol). J. Pharmacol. Exp. Ther., *280:* 1319-1327, 1997.

251. Webb, M. S., Logan, P., Kanter, P. M., St.-Onge, G., Gelmon, K., Harasym, T., Mayer, L. D., and Bally, M. B. Preclinical pharmacology, toxicology and efficacy of sphingomyelin/cholesterol liposomal vincristine for therapeutic treatment of cancer. Cancer Chemother. Pharmacol., *42:* 461-470, 1998.

252. Webb, M. S., Harasym, T. O., Masin, D., Bally, M. B., and Mayer, L. D. Sphingomyelin cholesterol liposomes significantly enhance the pharmacokinetic and therapeutic properties of vincristine in murine and human tumour models. Br. J. Cancer, *72:* 896-904, 1995.

253. van Oosterhout, Y. V. J. M., van den Herik-Oudijk, I. E., Wessels, H. M. C., de Witte, T., van de Winkel, J. G. J., and Preijers, F. W. M. B. Effect of isotype on internalization and cytotoxicity of CD19-ricin A immunotoxins. Cancer Res., *54:* 3527-3532, 1994.

254. Ishida, T., Kirchmeier, M. J., Moase, E. H., Zalipsky, S., and Allen, T. M. Targeted delivery and triggered release of liposomal doxorubicin enhances cytotoxicity against human B lymphoma cells. Biochim. Biophys. Acta, *1515:* 144-158, 2001.

255. Kirchmeier, M. J., Ishida, T., Chevrette, J., and Allen, T. M. Correlations between the rate of intracellular release of endocytosed liposomal doxorubicin and cytotoxicity as determined by a new assay. J. Liposome Res., *11:* 15-29, 2001.

256. Mayer, L. D., Nayar, R., Thies, R. L., Boman, N. L., Cullis, P. R., and Bally, M. B. Identification of vesicle properties that enhance the antitumour activity of liposomal vincristine against murine L1210 leukemia. Cancer Chemother. Pharmacol., *33:* 17-24, 1993.

257. Jackson, D. V., Jr., Jobson, V. W., Homesley, H. D., Welander, C., E.A., H., Pavy, M. D., Votaw, M. L., Richards, F. I., and Muss, H. B. Vincristine infusion in refractory gynecologic malignancies. Gynecol. Oncol., *25:* 212-216, 1986.

258. Jackson, D. V., White, D. R., Spurr, C., L., Hire, E. A., Pavy, M. D., Robertson, M., Legos, H. C., and McMahan, R. A. Moderate-dose vincristine infusion in refractory breast cancer. Am. J. Clin. Oncol., *9:* 376-378, 1986.

259. Mastrobattista, E., Koning, G., and Storm, G. Immunoliposomes for the targeted delivery of antitumor drugs. Adv. Drug Deliv. Rev., *40:* 103-127, 1999.

260. Nemecek, E. R. and Matthews, D. C. Antibody-based therapy of human leukemia. Curr. Opin. Hematol., *9:* 316-321, 2002.

261. Levy, R. and Miller, R. A. Therapy of lymphoma directed at idiotypes. J. Natl Cancer Inst Monogr, *10,* 61-68, 1990.

262. Engert, A., Gottstein, C., Bohlen, H., Winkler, U., Schon, G., Manske, O., Schnell, R., Diehl, V., and Thorpe, P. Cocktails of Ricin A-chain immunotoxins against different antigens on hodgkin and sternberg-reed calls have superior antitumor effects against H-RS cells in vitro and solid hodgkin tumors in mice. Int. J. Cancer, *63:* 304-309, 1995.

263. Flavell, D. J., Boehm, D. A., Emery, L., Noss, A., Ramsay, A., and Flavell, S. U. Therapy of human B-cell lymphoma bearing SCID mice is more effective with anti-CD19- and anti-CD38-saporin immunotoxins used in combination than with either immunotoxin used alone. Int. J. Cancer, *62:* 337-344, 1995.

264. Flavell, D. J., Boehm, D. A., Noss, A., Warnes, S. L., and Flavell, S. U. Therapy of human T-cell acute lymphoblastic leukaemia with a combination of anti-CD7 and anti-CD38-saporin immunotoxins is significantly better than therapy with each individual immunotoxin. Br. J. Cancer, *84:* 571-578, 2001.

265. Ghetie, M.-A., Podar, E. M., Gordan, B. E., Pantazis, P., Uhr, J. W., and Vitetta, E. S. Combination immunotoxin treatment and chemotherapy in SCID mice with advanced, disseminated daudi lymhoma. Int. J. Cancer, *68:* 93-96, 1996.

266. Ghetie, M.-A., Tucker, K., Richardson, J., Uhr, J. W., and Vitetta, E. S. Eradication of minimal disease in SCID mice with disseminated Daudi Lymhoma using chemotherapy and an immunotoxin cocktail. Blood, *84:* 702-707, 1994.

267. Starling, J. J., Hinson, N. A., Marder, P., Maciak, R. S., and Laguzza, B. C. Rapid internalization of antigen-immunoconjugate complexes is not required for anti-tumor activity of monoclonal antibody-drug conjugates. Antibody, Immunoconjugates and Radiopharmaceuticals, *1:* 311-324, 1988.

268. Starling, J. J., Maciak, R. S., Law, K. L., Hinson, N. A., Briggs, S. L., Laguzza, B. C., and Johnson, D. A. In vivo antitumor activity of monoclonal antibody-vinca alkaloid immunoconjugate directed against a solid tumor membrane

antigen characterized by heterogenous expression and noninternalization of antibody-antigen complexes. Cancer Res., *51:* 2965-2972, 1991.

269. Braslawsky, G. S., Kadow, K., Knipe, J., McGoff, K., Edson, M., and Kaneko, T. Adriamycin(hydrazone)-antibody conjugates require internalization and intracellular acid hydrolysis for antitumor activity. Cancer Immunol. Immunother., *33(6)* 367-374, 1991.

270. Wahl, A. F., Cerveny, C. G., Klussman, K., Chace, K. A., Gordan, K. A., Meyer, D. L., Doronina, S. O., Siegall, C. B., Senter, P. D., Francisco, J. A., and Law, C. L. Anti-cancer activity of high-potency anti-CD20 antibody-drug conjugates. Proc. Am. Assoc for Cancer Res., *44:* 175, 2003.

271. Ghetie, M. A., May, R. D., Till, M., Uhr, J. W., Ghetie, V., Knowles, P. P., Relf, M., Brown, A., Wallace, P. M., and Janossy, G. Evaluation of ricin-A-chain containing immunotoxins directed against CD19 and CD22 antigens on normal and malignant human B cells as potential reagents for in vivo therapy. Cancer Res., *48:* 2610-2617, 1988.

272. Abra, R. M., Bankert, R. B., Chen, F., Egilmez, N. K., Huang, K., Saville, R., Slater, J. L., Sugano, M., and Yokota, S. J. The next generation of liposome delivery systems: recent experience with tumor-targeted, sterically-stabilized immunoliposomes and active-loading gradients. J. Liposome Res., *12:* 1-3, 2002.

273. Herrera, L., Yarbrough, S., Ghetie, V., Aquino, D. B., and Vitetta, E. S. Treatment of SCID/human B cell precursor ALL with anti-CD19 and anti-CD22 immunotoxins. Leukemia, *17:* 334-338, 2003.

274. Messmann, R. A., Vitetta, E. S., Headlee, D., Senderowicz, A. M., Figg, W. D., Schindler, J., Michiel, D. F., Creekmore, S., Steinberg, S. M., Kohler, D., Jaffe, E. S., Stetler-Stevenson, M., Chen, H., Ghetie, V., and Sausville, E. A. A phase I study of combination therapy with immunotoxins IgG-HD37-deglycosylated ricin A chain (dgA) and IgG-RFB4-dgA (Combotox) in patients with refractory CD19(+), CD22(+) B cell lymphoma. Clin. Cancer Res., *6:* 1302-1313, 2000.

275. Burrows, F. J. and Thorpe, P. E. Vascular targeting--a new approach to the therapy of solid tumors. Pharmacol. Ther, *64:* 155-174, 1994.

276. Folkman, J. Angiogenesis in cancer, vascular, rheumatoid and other disease. Nature Med., *1:* 27-31, 1995.

277. Brekken, R. A., Huang, S., King, S. W., and Thorpe, P. E. Vascular endothelial growth factor as a marker of tumor endothelium. Cancer Res., *58:* 1952-1959, 1998.

278. Brekken, R. A. and Thorpe, P. E. Vascular endothelial growth factor and vascular targeting of solid tumors. Anticancer Res., *21:* 4221-4229, 2001.

279. Veenendaal, L. M., Jin, H., Ran, S., Cheung, L., Navone, N., Marks, J. W., Waltenberger, J., Thorpe, P., and Rosenblum, M. G. In vitro and in vivo studies of a VEGF121/rGelonin chimeric fusion toxin targeting the neovasculature of solid tumors. Proc. Natl. Acad. Sci. USA, *99:* 7866-7871, 2002.

280. Jain, R. K. Delivery of molecular and cellular medicine to solid tumors. Adv. Drug Deliv. Rev., *46:*149-168, 2001.

281. Jain, R. K. Delivery of molecular and cellular medicine to solid tumors. J Control Rel., *53:* 49-67, 1998.

282. Oku, N., Asai, T., Watanabe, K., Kuromi, K., Nagatsuka, M., Kurohane, K., Kikkawa, H., Ogino, K., Tanaka, M., Ishikawa, D., Tsukada, H., Momose, M., Nakayama, J., and Taki, T. Anti-neovascular therapy using novel peptides homing to angiogenic vessels. Oncogene, *21:* 2662-2669, 2002.

283. Vaage, J., Donovan, D., Mayhew , E., Uster , P., and Woodle, M. Therapy of mouse mammary carcinomas with vincristine and doxorubicin encapsulated in sterically stabilized liposomes. Int. J. Cancer, *54:* 959-964, 1993.

284. Vaage, J., Vaage , J., Donovan, D., Loftus, T., Uster, P., and Working, P. Prophylaxis and therapy of mouse mammary carcinomas with doxorubicin and vincristine encapsulated in sterically stabilised liposomes. Eur. J. Cancer, *31(A):* 367-372, 1995.

285. Hartmann, F., Renner, C., Jung, W., da Costa, L., Tembrink, S., Held, G., Sek, A., Konig, J., Bauer, S., Kloft, M., and Pfreundschuh, M. Anti-CD16/CD30 bispecific antibody treatment for Hodgkin's disease: role of infusion schedule and costimulation with cytokines. Clin. Cancer Res., *7:* 1873-1881, 2001.

286. Manzke, O., Tesch, H., Lorenzen, J., Diehl, V., and Bohlen, H. Locoregional treatment of low-grade B-cell lymphoma with CD3xCD19 bispecific antibodies and CD28 costimulation. II. Assessment of cellular immune responses. Int. J. Cancer, *91:* 516-522, 2001.

287. Green, L. L., Hardy, M. C., Maynard-Currie, C. E., Tsuda, H., Louie, D. M., Mendez, M. J., Abderrahim, H., Noguchi, M., Smith, D. H., and Zeng, Y. e. a. Antigen-specific human monoclonal antibodies from mice engineered with human Ig heavy and light chain YACs. Nat. Genet., *7:* 13-21, 1994.

288. Ridgway, J. B., Ng, E., Kern, J. A., Lee, J., Brush, J., Goddard, A., and Carter, P. Identification of a human anti-CD55 single-chain Fv by subtractive panning of a phage library using tumor and nontumor cell lines. Cancer Res., *59:* 2718-2723, 1999.